DEFORMATION THEORY ANALYSIS OF A DYNAMICALLY LOADED RIGID - PLASTIC CANTILEVER

F.X. LIEBENBERG

A thesis submitted in partial fulfilment of
the requirements for the Degree of Master of Science in
the Faculty of Engineering at the University of Cape Town

Department of Civil Engineering
UNIVERSITY OF CAPE TOWN

September 1980

DECLARATION OF CANDIDATE

I, Franciscus Xavierius Liebenberg, hereby declare that this thesis is my own work and that it has not been submitted for a degree at another University.

Signed by candidate

September 1980

This research was done with the financial assistance
of the
Council for Scientific and Industrial Research

ACKNOWLEDGEMENTS

I am indebted to:

Professor J.B. Martin - for his guidance and supervision of this research

Dr B.D. Reddy - for help and advice

Mrs S.J. Louw - for typing the manuscript

LIST OF SYMBOLS

α	$= \frac{P\ell}{M_p}$	
β	$= \frac{m\ell}{G}$	
∞		infinity
κ		curvature
θ		hinge rotation at support
θ_c		hinge rotation at centre of beam or at moving hinge
τ		dimensionless time $= \sqrt{\frac{M_p}{G\ell^2}} \cdot t$
ξ	$= \frac{x}{\ell}$	
Δ		change in
$\lvert\ \rvert$		absolute value of
$[\ ]$	$= (\ )^+ - (\ )^-$	
m		mass / unit length
ℓ		length of cantilever
z_o		position of θ_c during acceleration
G		tip mass
V_o		initial tip velocity
p, P		accelerating force
M_p		yield moment

K		kinetic energy
V		potential energy
L	$=$	$K - V$
E_T		total energy
S		shear force
M		moment
L_M		linear momentum
u, v, w		displacement variables
z		position of hinge θ_c along beam
$\bar{u}, \bar{v}, \bar{w}$		dimensionless displacement variables
x		distance along beam from tip
t, t_o, t_1, t_f		time
δJ		variation of J

I N D E X

CHAPTER 1.

INTRODUCTION

1.1 GENERAL BACKGROUND

There are a number of important areas in engineering technology which require an understanding of the behaviour of ductile structures subjected to high intensity short duration loading. The analyses of problems in this class is extremely complex, and two basic approaches have been followed; the first is that of detailed numerical analysis and the second that of making several simplifying assumptions to permit analytical solutions which reveal essential features of the response. The two approaches are complementary. Detailed design must rely on detailed computer analysis, but physical understanding and order of magnitude estimates necessary for computer program verification can only be obtained by making suitable simplifying assumptions.

One of the most common simplifying assumptions is the neglect of linear elastic behaviour. Further simplifications are the assumption of rate independent perfectly plastic behaviour and small deflections. This leads to the now classical simple rigid-plastic dynamic analysis; while it applies directly in only very few actual practical situations, it gives a basic theory to which various elaborations can be added.

Small displacement rigid-plastic theory leads essentially to the study of viscous behaviour in structures, in that stress and strain rate are directly related. While this in itself has several advantages, and the basic theory is now well established (see, for example, Martin 1979), it does mean that several classical results in mechanics, which are concerned with conservative systems, are not applicable.

Further, the simple rigid-plastic theory has led to studies in the formulation of simple and effective approximate solutions. This came about because the simple rigid-plastic theory proved to become quite complex in any but quite straightforward geometries and loading functions. The approximate methods have included bounding methods and the

so-called mode approximation methods (see, for example, Symonds 1979).

Taya and Mura (1974) introduced a new thought into rigid-plastic approximate methods by presenting what was claimed to be an extension of Hamilton's Principle (normally considered to be restricted to conservative systems) to rigid-plastic structural dynamics. A comment by Professor A.R.S. Ponter, however, has led to the present study. Professor Ponter queried whether Taya and Mura had indeed extended Hamilton's Principle; it could equally well be interpreted that in the limited applications which they considered they had replaced the usual non-holonomic viscous rigid-plastic relation by a holonomic deformation theory or non-linear elastic relation. This interpretation can be made because Taya and Mura did not consider any applications in which unloading took place.

In this chapter we shall elaborate on this query put forward by Professor Ponter, and show that indeed, in one of the examples given by Taya and Mura, it appears to be justified. Nevertheless, the query raises the question of whether deformation theory, or a holonomic theory of placticity, can be used profitably in simple rigid-plastic dynamic analysis. This appears to be an unexplored area, and we shall set out to analyse a specific problem, a cantilever with a tip mass on which a transverse impulse is applied, using a holonomic theory, and to draw what conclusions we can from this study.

1.2 THE EXTENSION OF HAMILTON'S PRINCIPLE GIVEN BY TAYA AND MURA

Taya and Mura (1974) considered an extension of Hamilton's Principle to non-conservative systems for the formulation of the equations of motion of dynamically loaded rigid, perfectly plastic structures. A brief summary of their results will be given, with an example of a cantilever beam.

Hamilton's Principle for a conservative system is formulated in terms of a functional J, given by

$$J = \int_{t_0}^{t_1} (T - U)dt , \tag{1.1}$$

where T is the kinetic energy of the system, U is the potential energy and $t_0 \leqq t \leqq t_1$ is the time interval over which motion is considered. Then, quoting from Courant and Hilbert (1953), "the actual motion makes the value of the integral J stationary with respect to all neighbouring virtual motions which lead from the initial to the final position of the system in the same interval of time." The stationary condition is written as

$$\delta J = 0 , \tag{1.2}$$

where variations are taken with respect to generalised coordinates q_i and their rates of change $\dot{q}_i$.

Taya and Mura suggest that, for the non-conservative rigid, perfectly plastic dynamic problems, the stationary condition (1.2) may be replaced by

$$J = \delta\int_{t_0}^{t_1} (T - U)dt = \int_{t_0}^{t_1} \delta E dt , \tag{1.3}$$

where δE is the variation of the energy dissipated in time dt. This modification is justified by energy balance arguments.

It is sufficient for the present purpose to consider the application of the condition given in equation (1.3) to a beam problem in which

displacements are assumed to be small. Consider a rigid, perfectly plastic beam of length ℓ, plastic limit moment M_p and mass per unit length m. Let the transverse displacement be $u(x)$, x being measured along the beam. The curvature is $\kappa = \frac{\delta^2 u}{\delta x^2}$, and the shear strain is zero. A transverse distributed load $p(x)$ also acts on the beam. Equation (1.3) becomes, in this special case,

$$\delta J = \delta \int_{t_1}^{t_1} \int_0^{\ell} \{\tfrac{1}{2} m \dot{u}^2 + pu\} dx dt = \int_{t_0}^{t_1} \int_0^{\ell} M_p \delta\kappa dx dt \ . \tag{1.4}$$

Consider the application of this equation to the specific problem shown in Fig. 1.1. A cantilever beam is uniform, of mass m/unit length, and has a concentrated mass G attached at the tip. A transverse impulsive load is applied, leading to a transverse velocity V_o of the tip at time $t = 0$. Thus the initial conditions can be given formally as

$$\begin{aligned} u(x,0) &= 0 \quad , \quad 0 \leqq x \leqq \ell \ , \\ \dot{u}(x,0) &= 0 \quad , \quad 0 < x \leqq \ell \ , \\ \dot{u}(0,0) &= V_o \ . \end{aligned} \tag{1.5}$$

This problem was first solved by Parkes (1954). The detailed solution, which will be given in Section 1.4, consists of two phases. In the first phase a plastic hinge forms in the beam, moving from the tip to the base, so that the transverse velocity diagram is as shown in Fig. 1.2(a). When the moving plastic hinge reaches the support ($z = \ell$), the beam rotates as a rigid body about the support, with the velocity diagram as shown in Fig. 1.2 (b). The solution depends on the ratio of the mass of the beam to the tip mass, $m\ell/G$; in the limiting case of a massless beam the travelling hinge phase is not present.

In applying equation (1.4) to the problem, Taya and Mura assumed that the velocity and displacement field were of the form shown in Fig. 1.2(b), thus ignoring the travelling hinge phase. They put

$$u(x,t) = w(t).\frac{x}{\ell} \ , \tag{1.6}$$

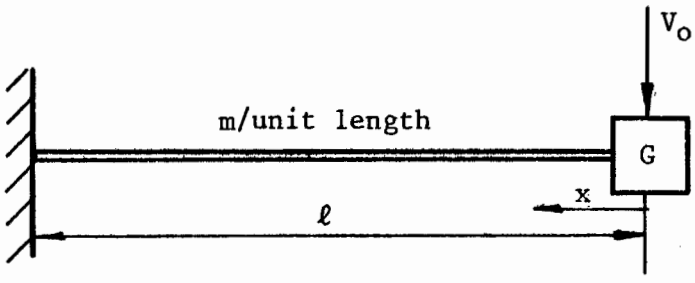

Fig. 1.1 : Cantilever with Tip Mass

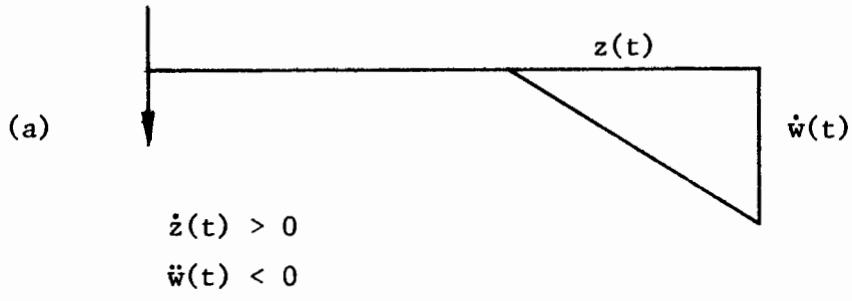

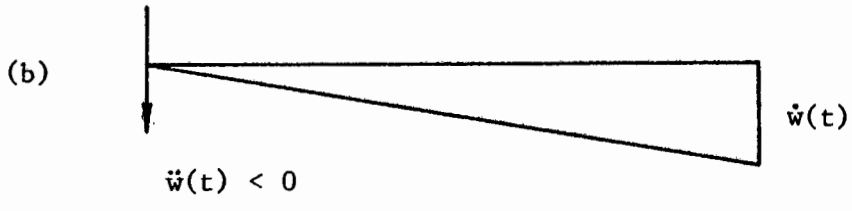

Fig. 1.2 : Velocity Fields

and further assumed that

$$w(t) = \tfrac{1}{2}C_1(t - t_f)^2 + C_2 \ , \tag{1.7}$$

where t_f is the time at which the structure comes to rest, all the initial kinetic energy being absorbed in plastic work. The condition given in equation (1.4) becomes

$$\delta\left\{\int_0^{t_f} \tfrac{1}{2}G\dot{w}^2 dt + \int_0^{t_f}\int_0^{\ell} \tfrac{1}{2}m\dot{u}^2 dx dt\right\} = \int_0^{t_f} M_p \delta\theta dt \ . \tag{1.8}$$

On the right hand side of this equation, θ is the rotation of the hinge at the base $x = 0$, and is thus

$$\theta = \frac{w}{\ell} \ . \tag{1.9}$$

After substituting equations (1.6), (1.7) and (1.9) into (1.8), we have an expression in which the coefficients C_1, C_2 and t_f are not known. However, the initial conditions (1.5) permitted them to put

$$\begin{aligned} w(0) &= 0 \ , \quad \text{i.e.} \quad C_2 = -\tfrac{1}{2}C_1 t_f^{\,2} \ , \\ \dot{w}(0) &= V_o, \quad \text{i.e.} \quad t_f = \frac{V_o}{C_1} \ . \end{aligned} \tag{1.10}$$

The variations of equation (1.8) are thus carried out with respect to the single parameter C_1. This allows the determination of C_1, given by

$$C_1 = \frac{-M_p}{\ell(G + \frac{1}{3}m\ell)} \ . \tag{1.11}$$

It follows from equation (1.10) and (1.5) that

$$t_f = \frac{V_o \ell (G + \frac{1}{3}m\ell)}{M_p} \ , \tag{1.12}$$

and that

$$w_f = w(t_f) = \frac{V_o \ell^2 (G + \frac{1}{3}m\ell)}{2M_p} \ . \tag{1.13}$$

1.3 DISCUSSION OF THE RESULT OF TAYA AND MURA

If we compare the equation generated by Taya and Mura for the cantilever problem with Parke's solution, it is immediately clear that the travelling hinge phase is ignored. It follows from this that Taya and Mura cannot give an exact solution, but at best an approximation.

What is more significant, however, is that the extended Hamilton's principle is applied only in the case where the displacement field can be written as a separable function of space and time, as in equation (1.6). In these situations the curvature rate (or the rotation rate of a hinge) has the same sign throughout the motion, and unloading of the rigid-plastic material does not occur, at least until the structure comes to rest. It follows from this that the equations of motion for this limited class of displacement fields does not involve unloading of the material. If, indeed, we were to alter the material so that while the moment-curvature relation (Fig. 1.4) were identical for loading, it unloaded back along the same curve, there would be no change in the equations of motion.

However, by making this change, we have changed the material from a dissipative material to a non-linear elastic material, and the system from a non-conservative one to a conservative one. The strain energy per unit length of the beam would have the form

$$W = M_p|\kappa| \ , \tag{1.14}$$

and its variation is

$$\delta W = M_p \delta\kappa \ . \tag{1.15}$$

If the strain energy is included in the potential energy U of the system, Hamilton's principle can be applied directly to the system. With

$$U = \int_0^{\ell} \{M_p|\kappa| - pu\}dx \ , \tag{1.16}$$

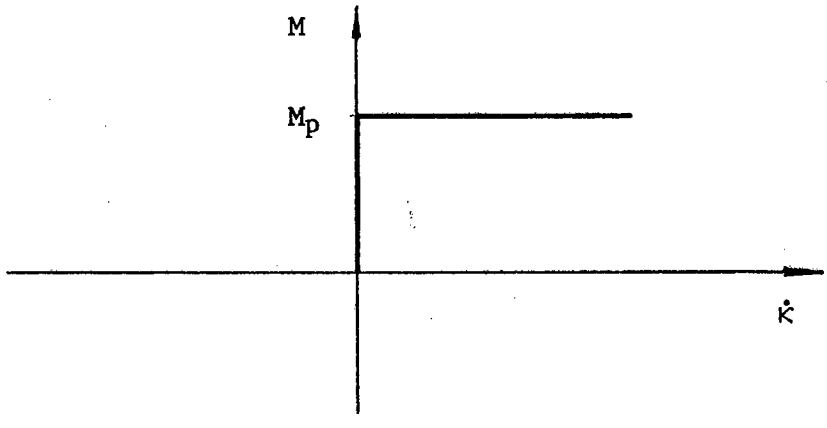

Fig. 1.3 : Non-Holonomic

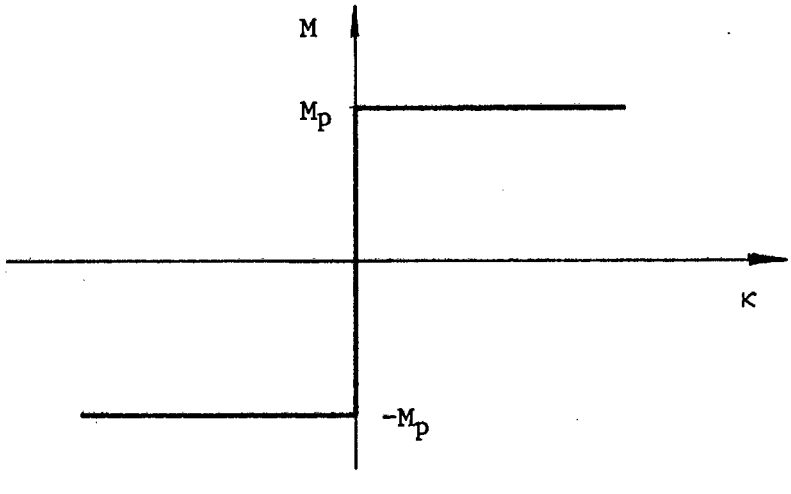

Fig. 1.4 : Holonomic

the appropriate form of the Hamiltonian is

$$\delta J = \delta\int_{t_o}^{t}\int_{0}^{\ell}\{\tfrac{1}{2}m\dot{u}^2 + pu - M_p|\kappa|\}dx = 0 . \qquad (1.17)$$

If equations (1.17) and (1.4) are compared, it is seen that they are essentially identical. This suggests that what Taya and Mura have actually done is the following: rather than extend Hamilton's principle to a non-conservative rigid-plastic system, they have modified the material to make the system conservative, and developed equations of motion for situations where the change in material behaviour has no effect. Without the derivation of the equation of motion for the travelling hinge phase, it must be concluded that an extension of Hamilton's principle has not been demonstrated.

Thus we must accept, in the absence of more convincing evidence, that Taya and Mura are suggesting simply that approximate solutions to rigid-plastic dynamic problems can be set up by using fixed mode displacement fields and treating the rigid-plastic material as non-linear elastic. The first of these elements, the use of separable fields as approximations, is not new (see, for example, Martin and Symonds (1966)). The second element, however, the use of a reversible rigid-plastic material, has not been previously suggested. The combination of fixed mode displacement fields and reversible rigid-plastic behaviour does not provide us with any advance on irreversible behaviour, except insofar as the derivation of the equations of motion may in certain cases be simplified.

The remaining possibility, however, leads to speculation that a useful method of approximation could be established if we adopt reversible behaviour as a basic assumption, without the limitation of fixed mode behaviour. The idea is attractive, at least, because the system becomes conservative and several simplifying concepts associated with conservative systems can be used.

Our object in this thesis will thus be to explore whether it is feasible to approximate the solutions of rigid-plastic dynamic problems by altering the material behaviour so that the material becomes reversible. We shall refer to the conventional rigid-plastic

relation (Fig. 1.3) as non-holonomic, and the reversible or non-linear elastic approximation (Fig. 1.4) as holonomic.

The study will be limited to the problem of a cantilever beam with a concentrated mass at its tip. In Section 1.4 a detailed analysis for the non-holonomic case will be given. In the remaining chapters of the thesis the holonomic problem will be studied with the intent of establishing whether a reasonable approximation of non-holonomic behaviour is attainable, and whether it is attainable with less effort than the non-holonomic case.

1.4 PARKES'S SOLUTION FOR AN IMPULSIVELY LOADED CANTILEVER

Parkes (1954) uses the rigid perfectly plastic, or non-holonomic, material behaviour model, which is shown by the moment-strain rate relationship in Fig. 1.3.

The analysis is carried out for a cantilever of length ℓ , mass m per unit length and a concentrated tip mass of G , shown in Fig. 1.5.

The velocity and acceleration fields and the shear force and bending moment diagrams are shown in Figs. 1.6 (a) - (d) respectively at time t . The transverse velocity $\dot{u}$ and the position of the hinge are defined in equation (1.18) as follows

$$\begin{aligned} \dot{u}(x,t) &= \text{transverse velocity } \dot{u} \text{ at position } x \text{ at time } t \text{ ,} \\ z(t) &= \text{position of hinge at time } t \text{ .} \end{aligned} \tag{1.18}$$

The initial condition, given in equation (1.19), is that the tip mass starts moving instantaneously with velocity V_o , thus

$$\begin{aligned} z(0) &= 0 \text{ ,} \\ \dot{u}(0,0) &= V_o \text{ .} \end{aligned} \tag{1.19}$$

A travelling hinge will form at the tip of the cantilever and move towards the support. The bending moment, shown in Fig. 1.6(d), has a value of M_p at the travelling hinge. Since the bending moment may not exceed M_p , this is a position of maximum bending moment and thus of zero shear force. The section of beam between the hinge and the tip has bending moments which are less than M_p , i.e. no deformation occurs and the section moves as a rigid body about the hinge. The section of beam between the support and the hinge has constant bending moment of M_p and has zero transverse velocity.

The velocity variables are $\dot{w}$ and z , as shown in Fig. 1.5. The velocity field in Fig. (a) is continuous throughout, but there is a discontinuity in the acceleration field at the hinge as shown in Fig. 1.6(b). The transverse velocity of any point between the hinge

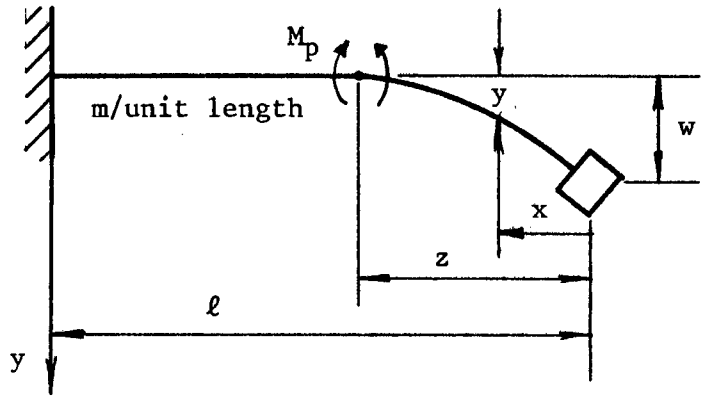

Fig. 1.5 : Cantilever with Tip Mass

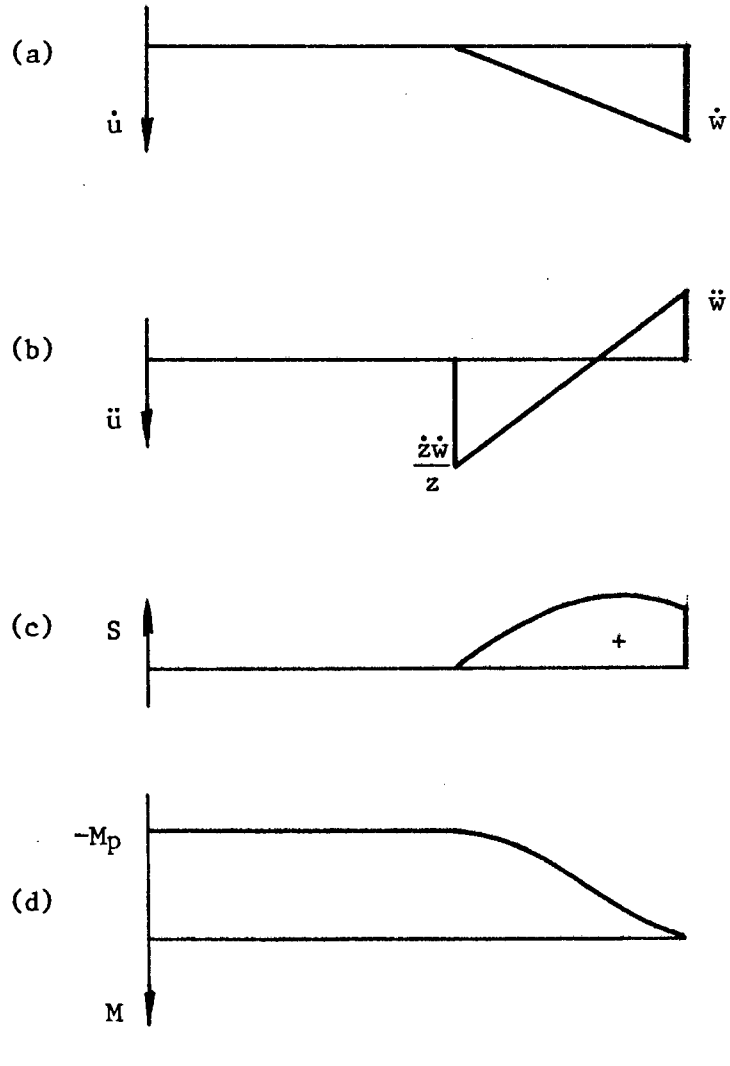

Fig. 1.6

and the tip is given by

$$\dot{u}(x,t) = \left\{\frac{z - x}{z}\right\}\dot{w} ,$$

$$= \left\{1 - \frac{x}{z}\right\}\dot{w} . \qquad (1.20)$$

The acceleration is obtained by differentiating equation (1.20) with respect to time, thus

$$\ddot{u} = \left\{1 - \frac{x}{z}\right\}\ddot{w} + \frac{w}{z^2}\cdot\dot{z}\dot{w} . \qquad (1.21)$$

The discontinuity in acceleration at the hinge, or acceleration just to the right of the hinge since the acceleration to the left of the hinge is zero, is obtained by substituting $x = z$ into equation (1.21); thus

$$[\ddot{u}] = \frac{\dot{z}\dot{w}}{z} . \qquad (1.22)$$

Since the section of beam between the support and the hinge has no shear force acting on it, and thus remains stationary, the dynamic analysis will only be applied to the section between the hinge and the tip. A lateral force balance gives

$$G\ddot{w} + \tfrac{1}{2}mz\left\{\frac{\dot{z}\dot{w}}{z} + \ddot{w}\right\} = 0 . \qquad (1.23)$$

The term $\frac{1}{2}\left\{\frac{\dot{z}\dot{w}}{z} + \ddot{w}\right\}$ is the average acceleration between the hinge and tip. The sum of moments about the tip gives

$$\int_0^z m\ddot{u}x\,dx = M_p . \qquad (1.24)$$

Substituting equation (1.21) into equation (1.24) gives

$$\int_0^z m\left\{\left\{1 - \frac{x}{z}\right\}\ddot{w} + \frac{x}{z^2}\dot{z}\dot{w}\right\}x\,dx = M_p ,$$

and then

$$\tfrac{1}{6}m\ddot{w}z^2 + \tfrac{1}{3}m\dot{z}\dot{w}z = M_p . \qquad (1.25)$$

Equations (1.23) and (1.25) are integrated with respect to time to yield, respectively,

$$G\dot{w} + \tfrac{1}{2}mz\dot{w} = A \ , \tag{1.26}$$

and

$$\tfrac{1}{6}mz^2\dot{w} = M_p t + B \ , \tag{1.27}$$

where A and B are constants that have to be determined from initial conditions (1.19). Substituting equation (1.19) into equations (1.26) and (1.27), we have, respectively,

$$G(V_o) + \tfrac{1}{2}m(0)(V_o) = A \ ,$$

and

$$\tfrac{1}{6}m(0)\ (V_o) = M_p(0) + B \ ,$$

and thus

$$A = GV_o \ , \tag{1.28}$$

and

$$B = 0 \ . \tag{1.29}$$

Back substituting equations (1.28) and (1.29) into equations (1.26) and (1.27) give, respectively,

$$G\dot{w} + \tfrac{1}{2}mz\dot{w} = GV_o \ , \tag{1.30}$$

and

$$\tfrac{1}{6}mz\ \dot{w} = M_p t \ . \tag{1.31}$$

Solving for $\dot{w}$ in equation (1.30) gives

$$\dot{w} = \frac{GV_o}{(G + \frac{1}{2}mz)} \ . \tag{1.32}$$

Substituting equation (1.32) into equation (1.31) and solving for t gives

$$t = \frac{mV_o}{6M_p} \cdot \frac{z^2}{\left(1 + \frac{mz}{2G}\right)} , \tag{1.33}$$

and differentiating with respect to z gives

$$\frac{dt}{dz} = \frac{mVz}{6M_p} \cdot \frac{\left(2 + \frac{mz}{2G}\right)}{\left(1 + \frac{mz}{2G}\right)^2} . \tag{1.34}$$

An expression for the tip velocity is obtained by rearranging equation (1.32) to give

$$\dot{w} = \frac{V_o}{\left(1 + \frac{mz}{2G}\right)} . \tag{1.35}$$

The velocity of a point in the cantilever $\dot{u}(x,t)$ is zero until the travelling hinge reaches it, i.e. $z = x$. For $z > x$ its velocity is given by

$$\dot{y} = \left\{\frac{z - x}{z}\right\}\dot{w} . \tag{1.36}$$

Equation (1.36 remains valid until the travelling hinge reaches the support, i.e. when $z = \ell$. The displacement $y(x)$ when $z = \ell$ is found by integrating equation (1.36) and substituting into it equations (1.34) and (1.35). Thus

$$y(x) = \int_x^{\ell} \dot{y}dt$$

$$= \int_x^{\ell} \left\{\frac{z-x}{z}\right\}\dot{w}\left\{\frac{dt}{dz}\right\}dz$$

$$= \frac{G^2V_o^2}{3mM_p}\left\{\frac{\frac{1}{2}\beta(3\xi-2)}{(1+\frac{1}{2}\beta)} - \frac{\frac{1}{2}\beta\xi}{(1+\frac{1}{2}\beta\xi)} + \frac{\frac{1}{4}\beta^2(1-\xi)}{(1+\frac{1}{2}\beta)^2} + 2\ell n\left\{\frac{1+\frac{1}{2}\beta}{1+\frac{1}{2}\beta\xi}\right\}\right\} , \tag{1.37}$$

where

$$\beta = \frac{m\ell}{G} ,$$

and

$$\xi = \frac{x}{\ell} . \tag{1.38}$$

When the hinge reaches the support it becomes stationary. The whole cantilever is now rotating about the support as a rigid body with an angular velocity given by

$$\frac{\dot{w}}{\ell} = \frac{V_o}{(1 + \frac{1}{2}\beta)\ell} . \tag{1.39}$$

This is obtained by putting $z = \ell$ and substituting equation (1.38) into equation (1.35) and dividing throughout by ℓ. The cantilever will now keep on rotating about the support until all its kinetic energy is dissipated in the hinge. This rotation is given by

$$\theta = \frac{G^2 V_o^2 \frac{1}{2}\beta(\beta + 3)}{3mM_p\ell(1 + \frac{1}{2}\beta)^2} . \tag{1.40}$$

The total displacement $y(x)$ of the cantilever, after deformation has ended, is obtained by adding equation (1.37) to

$$\theta\ell(1 - \xi) . \tag{1.41}$$

This sum is expressed non-dimensionally as

$$\frac{\frac{y M_p}{\ell}}{\frac{1}{2}GV_o} = \frac{1}{3(1 + \frac{1}{2}\beta)} - \frac{\xi}{3(1 + \frac{1}{2}\beta\xi)} + \frac{4}{3\beta}\ell n\left\{\frac{2 + \beta}{2 + \beta\xi}\right\} . \tag{1.42}$$

The tip acceleration $\ddot{w}$ has different values just before and just after the hinge reaches the support. To obtain the tip acceleration just before the hinge reaches the support, equation (1.23), rewritten below,

$$G\ddot{w} + \tfrac{1}{2}mz\left\{\frac{\dot{z}\dot{w}}{z} + \ddot{w}\right\} = 0 ,$$

is rearranged to give

$$\ddot{w}(G + \tfrac{1}{2}mz) = -\tfrac{1}{2}m(\dot{w}\dot{z}) \ . \tag{1.43}$$

Equation (1.24), also rewritten,

$$\tfrac{1}{6}m\ddot{w}z^2 + \tfrac{1}{3}m\dot{z}\dot{w}z = M_p \ ,$$

is similarly rearranged,

$$(\dot{w}\dot{z}) = \frac{3M_p}{mz} - \tfrac{1}{2}\ddot{w}z \ . \tag{1.44}$$

Substituting equation (1.44) into equation (1.43) and solving for $\ddot{w}$ gives

$$\ddot{w} = \frac{-\dfrac{3M_p}{2z}}{(G + \frac{1}{4}mz)} \ . \tag{1.45}$$

Just before the hinge reaches the support, $z = \ell$ and hence

$$\ddot{w} = \frac{-\dfrac{3M_p}{2\ell}}{(G + \frac{1}{4}m\ell)} \ . \tag{1.46}$$

To obtain an expression for the tip acceleration $\ddot{w}$, just after the hinge reaches the support, equation (1.40) in the previous section has to be rewritten. It is simpler to rederive the expression for $\ddot{w}$ from first principles. Taking moments about the hinge

$$-M_p = G\ddot{w}\ell + \int_0^{\ell} m\left(\frac{x}{\ell}\right)\ddot{w}x\,dx$$

$$= G\ddot{w}\ell + \tfrac{1}{3}m\ell\, w \ . \tag{1.47}$$

Hence

$$\ddot{w} = \frac{-\dfrac{M_p}{\ell}}{(G + \frac{1}{3}m\ell)} \ . \tag{1.48}$$

Comparing equations (1.46) and (1.48), it can be seen that when the hinge reaches the support, the tip acceleration $\ddot{w}$ changes

instantaneously from the value given in equation (1.46) to that in equation (1.48). This will be represented by a discontinuity in slope on a velocity-time graph. The acceleration field changes from that shown in Fig. 1.7 (a) to that in Fig. 1.7 (b). The acceleration discontinuity at the support also disappears.

The hinge velocity along the beam $\dot{z}$ is found by inverting equation (1.34), which is rewritten below

$$\frac{dt}{dz} = \frac{mV_o z}{6M_p} \cdot \frac{\left\{2 + \left(\frac{mz}{2G}\right)\right\}}{\left\{1 + \left(\frac{mz}{2G}\right)\right\}^2} .$$

Thus $\dot{z}$ is given by

$$\dot{z}(t) = \frac{dz}{dt} = \frac{6M_p}{mV_o z} \cdot \frac{\left\{1 + \left(\frac{mz}{2G}\right)\right\}^2}{\left\{2 + \left(\frac{mz}{2G}\right)\right\}} . \qquad (1.49)$$

When the hinge reaches the support at time $t = t_1$, $z = \ell$. Substituting this into equation (1.49), we have

$$\dot{z}(t_1) = \frac{6M_p}{mV_o \ell} \cdot \frac{\left\{1 + \left(\frac{m\ell}{2G}\right)\right\}^2}{\left\{2 + \left(\frac{m\ell}{2G}\right)\right\}} . \qquad (1.50)$$

It can be seen from this that the hinge velocity $\dot{z}$ is not zero when the hinge reaches the support. The hinge velocity is infinite at time $t = 0$ {putting $z = 0$ in equation (1.49)} and reduces monotonically until $z = \ell$ when it jumps to zero.

Two characteristic times can be identified in the response. The first is t_1, the time when the hinge reaches the support. From equation (1.33), with $z = \ell$,

$$t_1 = \frac{mV_o \ell^2}{6M_p} \cdot \frac{1}{\left(1 + \frac{m\ell}{2G}\right)} . \qquad (1.51)$$

Note that t_1 is a function of the mass ratio $m\ell/G$. For $m\ell/G \to 0$, i.e. when the beam mass may be neglected by comparison with the tip

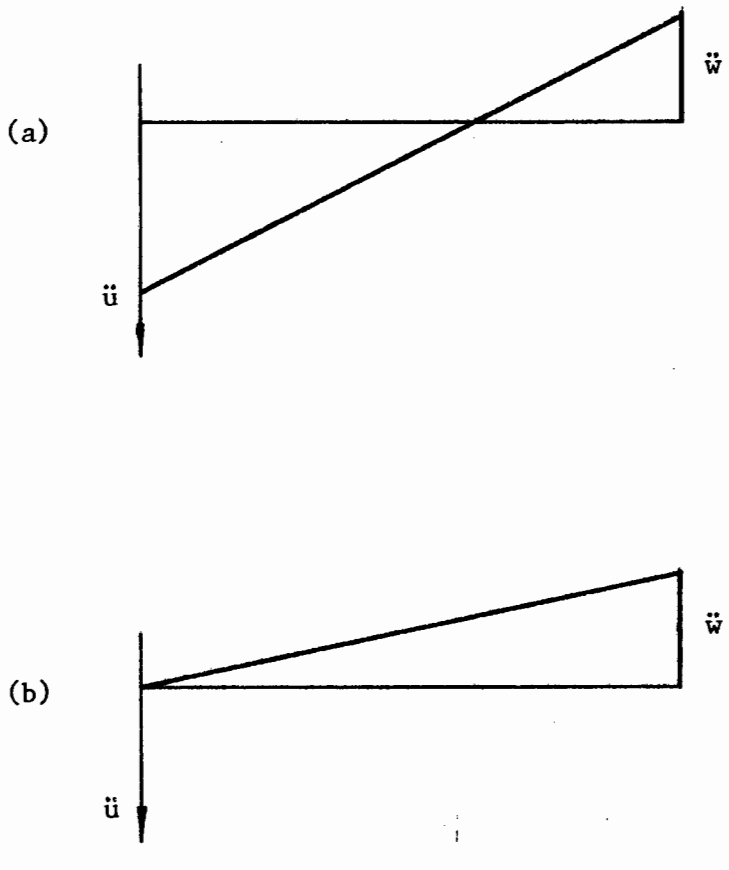

Fig. 1.7 : Acceleration Fields

mass, t, also tends to zero. The time when the beam finally comes to rest, t_f, is given by

$$t_f = \frac{G\ell V_o}{M_p} . \tag{1.52}$$

Note that t_f is independent of the mass ratio.

The response is most conveniently plotted in dimensionless form. The dimensionless time will be given by

$$\tau = \sqrt{\frac{M_p}{G\ell^2}} \cdot t , \tag{1.53}$$

and we put

$$\bar{w} = \frac{w}{\ell} \quad , \quad \dot{\bar{w}} = \frac{d\bar{w}}{d\tau} \quad , \quad \ddot{\bar{w}} = \frac{d^2\bar{w}}{d\tau^2} \quad , \quad \beta = \frac{m\ell}{G} \quad . \tag{1.54}$$

Then equation (1.35) becomes

$$\dot{\bar{w}} = \frac{\bar{V}_o}{\left(1 + \frac{1}{2}\beta\bar{z}\right)} . \tag{1.55}$$

Similarly equation (1.33) becomes

$$\tau = \frac{\bar{V}_o \beta \bar{z}^2}{3(2 + \beta\bar{z})} . \tag{1.56}$$

Equations (1.55) and (1.56) are used to plot the moving hinge part of the response. For the subsequent motion, is rewritten in dimensionless form as

$$\ddot{\bar{w}} = \frac{-1}{\left(1 + \frac{1}{3}\beta\right)} . \tag{1.57}$$

The time of response τ_1 for this phase of the motion is given by

$$\tau_1 = \dot{\bar{w}}\left(1 + \tfrac{1}{3}\beta\right) . \tag{1.58}$$

The total time of response τ_f is given by

$$\tau_f = \bar{V}_o . \tag{1.59}$$

It is convenient to plot $\dot{\bar{w}}/\bar{V}_o$ versus τ/τ_f, as shown in Fig. 1.8.

Fig. 1.8.

Response of Cantilever with Tip Mass

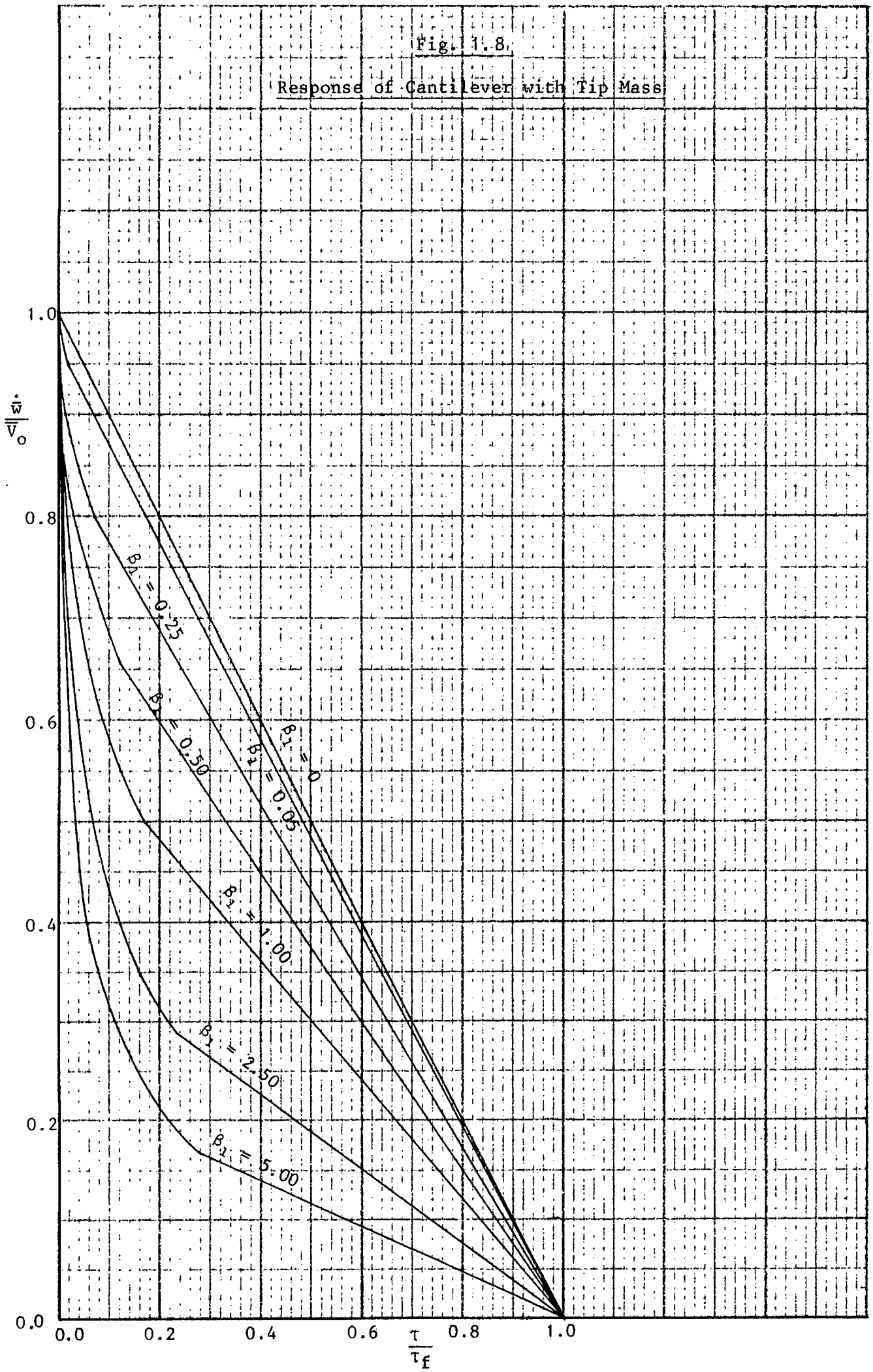

1.5 HOLONOMIC MATERIAL BEHAVIOUR MODEL

The holonomic material model which will be used to approximate the behaviour of a structure undergoing dynamic plastic deformation will be described briefly.

The behaviour is reversible or non-linear elastic as shown by the moment-curvature relationship in Fig. 1.9.

The only type of deformation which will be possible in a cantilever undergoing free dynamic motion is a hinge, or a number of hinges, along the beam with the sections between the hinges remaining undeformed. Deformation takes place only when the moment at that particular position reaches M_p , and a hinge forms.

The strain energy per unit length of structure is given by $M_p|\kappa|$. The strain energy at a particular hinge can similarly be written as $M_p|\theta|$; this is shown as a function of θ in Fig. 1.10. The moment rotation relationship can be recovered from this expression for strain energy, since moment M is given by

$$M = \frac{d}{d\theta}\left\{M_p|\theta|\right\} .$$

Thus

$$M = +M_p \quad \text{if} \quad \theta > 0 ,$$

$$-M_p \leq M \leq M_p \quad \text{if} \quad \theta = 0 ,$$

$$M = -M_p \quad \text{if} \quad \theta < 0 .$$

In the remaining sections of the thesis this holonomic relation will be used to describe the material behaviour of the beam under discussion.

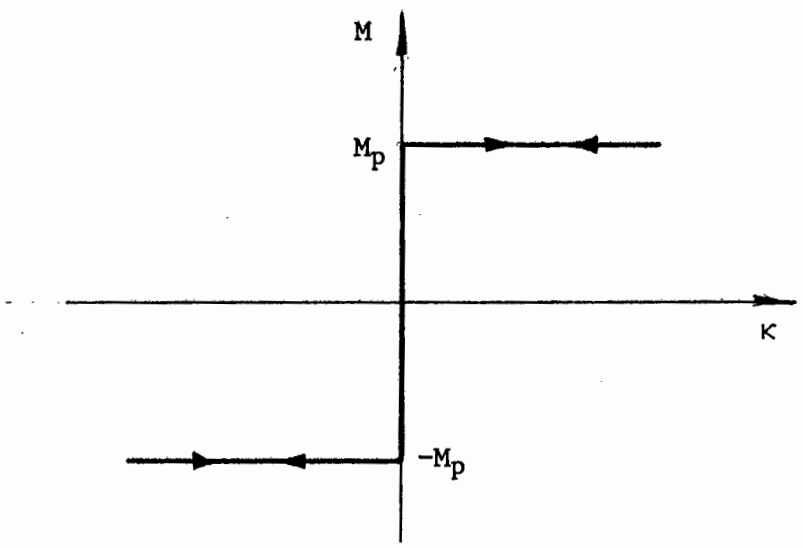

Fig. 1.9 : Moment-Curvature Relationship

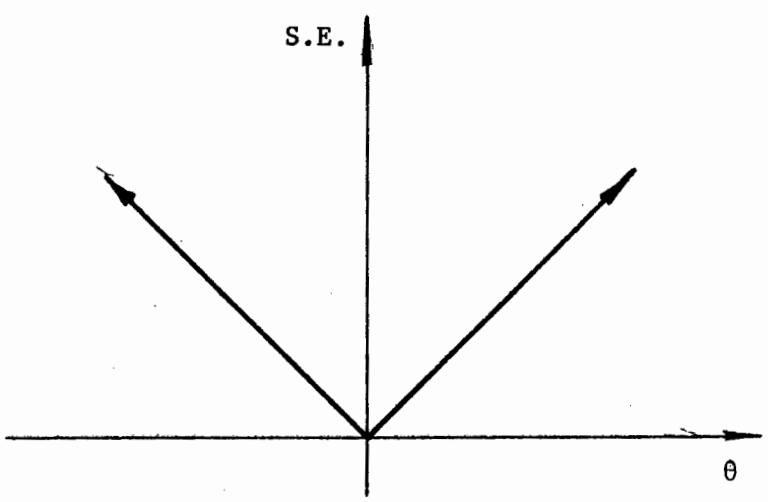

Fig. 1.10 : Strain Energy-Rotation Relationship

CHAPTER 2.

ANALYSIS OF A LUMP MASS MODEL OF THE CANTILEVER

2.1 INTRODUCTION

As a first step towards understanding the response of the holonomic Parkes cantilever, we shall consider a simpler case of a lumped mass cantilever. The problem is simplified in that there will not be any moving hinges or discontinuities of any other kind, and hence the equations of motion will be easier to formulate and solve.

The problem that we shall study is shown in Fig. 2.1. The cantilever is massless, and of span 2ℓ . Equal concentrated masses G are attached at the midpoint and at the tip. It is assumed that the cantilever is subjected to a transverse load P which has a constant value over the time interval $0 \leqq t \leqq t_o$, and then falls to zero. We shall be concerned with the behaviour during the time interval $0 \leqq t \leqq t_o$ and with the subsequent free motion.

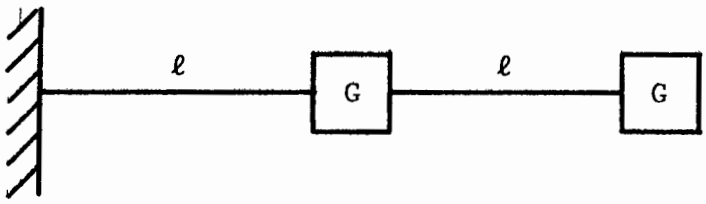

Fig. 2.1 : Lump Mass Model of Cantilever

2.2 NON-HOLONOMIC ANALYSIS OF THE TWO MASS CANTILEVER

In order to provide a comparison between holonomic and non-holonomic analysis, we shall first consider the non-holonomic, or conventional rigid-plastic, analysis of the lump mass model shown in Fig. 2.1.

The response depends on the magnitude of the load P during the load pulse, and three ranges of behaviour can be identified. Each of these ranges will be considered separately.

2.2.1 $P \leq \frac{M_p}{2\ell}$

For this range of P no motion will occur, since the load P is less than the static collapse load.

2.2.2 $\frac{M_p}{2\ell} < P < \frac{3M_p}{\ell}$

For this range of P there will be rotation about a hinge at the support and the cantilever will have velocity and acceleration fields of the shape shown in Fig. 2.2.

Consider the body forces shown in Fig. 2.3. Let the transverse displacements at the tip and the centre mass be denoted by w and w_c respectively. Writing the equations of motion of the masses in Fig. we have

$$P - F = G\ddot{w} \quad , \tag{2.1}$$

$$- F_c = G\ddot{w}_c \quad . \tag{2.2}$$

For the acceleration field shown in Fig.

$$\ddot{w}_c = \tfrac{1}{2}\ddot{w} \quad . \tag{2.3}$$

Equation (2.2) can thus be rewritten as

$$- F_c = G.(\tfrac{1}{2}\ddot{w}) \quad . \tag{2.4}$$

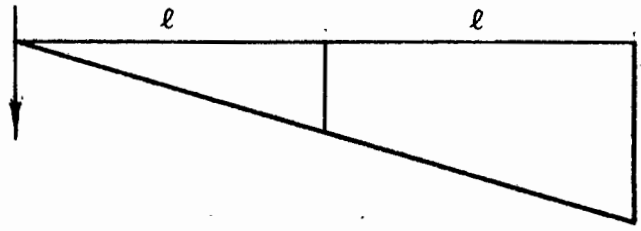

Fig. 2.2 : Velocity and Acceleration Fields

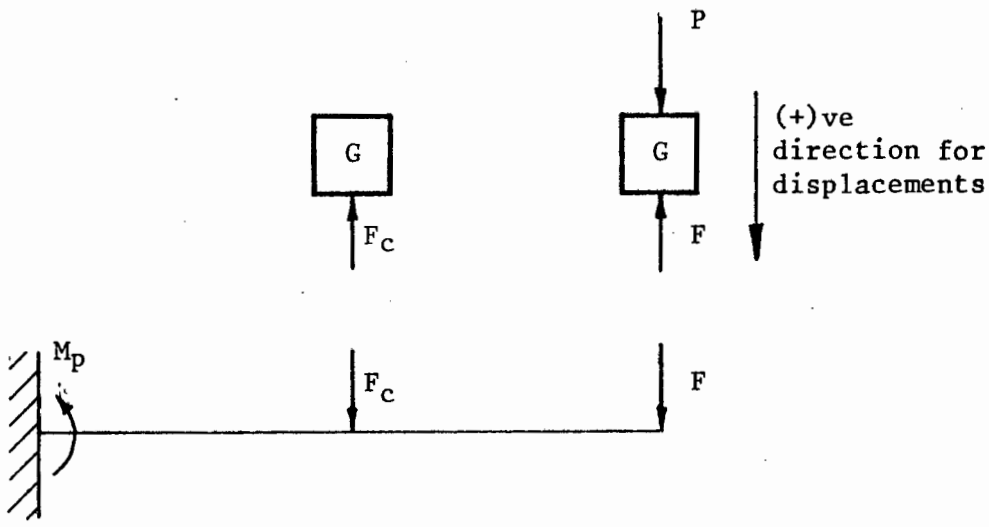

Fig. 2.3 : Body Force Representation

The sum of moments about the support gives

$$F.2\ell + F_c.\ell \Rightarrow M_p \ . \tag{2.5}$$

Equations (2.1) and (2.4) are rearranged to give

$$F = P - G\ddot{w} \ , \tag{2.6}$$

$$F_c = -\tfrac{1}{2}G\ddot{w} \ . \tag{2.7}$$

Equations (2.6) and (2.7) are now substituted into equation (2.5) to give

$$(P - G\ddot{w}).2\ell - (-G\ddot{w}).\ell = M_p \ ,$$

and hence

$$G\ddot{w} = \tfrac{4}{5}\left\{P - \frac{M_p}{2\ell}\right\} \ . \tag{2.8}$$

Equation (2.8) is now back-substituted into equations (2.6) and (2.7) for the forces F and F_c . Thus

$$F = \tfrac{1}{5}P + \tfrac{4}{5}\left\{\frac{M_p}{2\ell}\right\} \ , \tag{2.9}$$

$$F_c = -\tfrac{2}{5}\left\{P - \frac{M_p}{2\ell}\right\} \ . \tag{2.10}$$

Substituting equations (2.9) and (2.10) into equations (2.1) and (2.2) respectively to solve for $\ddot{w}$ and $\ddot{w}_c$ gives

$$\ddot{w} = \tfrac{4}{5}\left\{\frac{P}{G} - \frac{M_p}{2G\ell}\right\} \ , \tag{2.11}$$

$$\ddot{w}_c = \tfrac{2}{5}\left\{\frac{P}{G} - \frac{M_p}{2G\ell}\right\} \ . \tag{2.12}$$

The cantilever will deform with a hinge at the support for a limited range of values of P . The lower limit is the value of P which is just greater than the load which causes static collapse, i.e. for motion to occur

$$P \geq \frac{M_p}{2\ell} \ . \tag{2.13}$$

The upper limit is the value of P for which a hinge forms at the centre of the cantilever. Denoting this bending moment by M, the sum of moments about the centre of the cantilever gives

$$F.\ell = M .$$

The condition that

$$M \leq M_p ,$$

becomes

$$F.\ell \leq M_p . \tag{2.14}$$

Substituting for F in equation (2.14) by using equation (2.9) gives

$$\left\{\tfrac{1}{5}P + \tfrac{4}{5}\left\{\frac{M_p}{2\ell}\right\}\right\}.\ell \leq M_p ,$$

or, simplifying,

$$P \leq \frac{3M_p}{\ell} . \tag{2.15}$$

Thus the range of values of P is found by combining equations (2.13) and (2.15):

$$\frac{M_p}{2\ell} \leq P \leq \frac{3M_p}{\ell} . \tag{2.16}$$

With $P = \frac{3M_p}{2\ell}$, equations (2.11) and (2.12) becomes

$$\ddot{w} = \tfrac{4}{5}\left\{\frac{M_p}{G\ell}\right\} , \tag{2.17}$$

$$\ddot{w}_c = \tfrac{2}{5}\left\{\frac{M_p}{G\ell}\right\} . \tag{2.18}$$

The acceleration phase ends at time $t = t_o$ with the tip velocity of the cantilever equal to $\dot{w}$ and velocity at the centre of the cantilever $\dot{w}_c = \frac{1}{2}\dot{w}$. For the deceleration phase $P = 0$ and

equation (2.6) becomes

$$F = -G\ddot{w} \ . \tag{2.19}$$

Substituting equations (2.19 and (2.7) into equation (2.5) gives

$$(-G\ddot{w}).2\ell + (-\tfrac{1}{2}G\ddot{w}).\ell = M_p \ ,$$

or

$$G\ddot{w} = -\tfrac{2}{5}\left\{\frac{M_p}{\ell}\right\} \ . \tag{2.20}$$

Substituting equation (2.20) into equation (2.19) and (2.7) to solve for forces F and F_c , we have

$$F = \tfrac{2}{5}\left\{\frac{M_p}{\ell}\right\} \ , \tag{2.21}$$

$$F_c = \tfrac{1}{5}\left\{\frac{M_p}{\ell}\right\} \ . \tag{2.22}$$

Substituting equations (2.21) and (2.22) into equations (2.19) and (2.2) respectively to solve for $\ddot{w}$ and $\ddot{w}_c$, we find

$$\ddot{w} = -\tfrac{2}{5}\left\{\frac{M_p}{G\ell}\right\} \ , \tag{2.23}$$

$$\ddot{w}_c = -\tfrac{1}{5}\left\{\frac{M_p}{G\ell}\right\} \ . \tag{2.24}$$

The deceleration continues until the two velocities $\dot{w}$ and $\dot{w}_c$ are zero at time $t = t_o + t_1$. A velocity-time plot for the tip and centre of the cantilever is shown in Fig. 2.4.

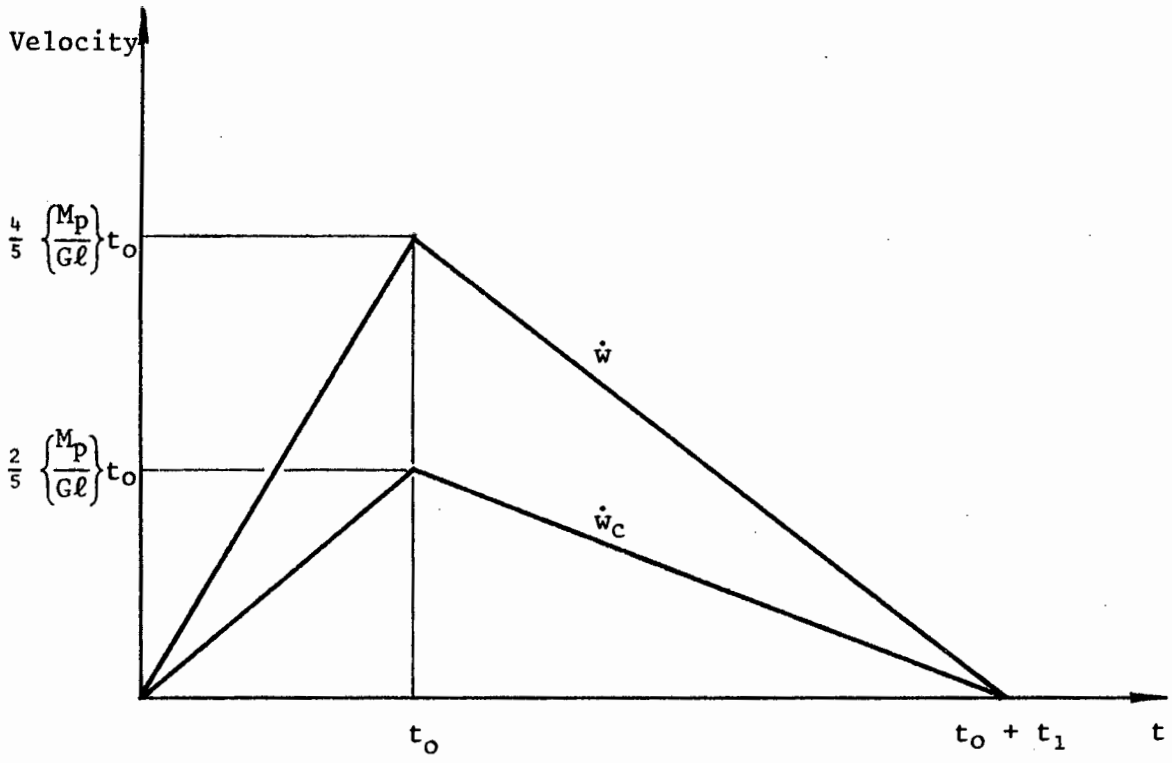

Fig. 2.4 : Velocity-Time Plot for Two Mass Cantilever

2.2.3 $P > \frac{3M_p}{\ell}$

For this range hinges will form at the support and at the centre of the beam. The velocity and acceleration fields will have the shape shown in Fig. 2.5. Consider the body forces shown in Fig. 2.6. The equation of motion of the two masses shown in Fig. 2.6 are

$$P - F = G\ddot{w} \ , \tag{2.25}$$

$$F_c = G\ddot{w}_c \ . \tag{2.26}$$

Moments about the support gives

$$F.2\ell + F_c.\ell = M_p \ , \tag{2.27}$$

and moments to the right of the centre mass gives

$$F.\ell = M_p \ . \tag{2.28}$$

Rearranging equation (2.28) to solve for F ,

$$F = \frac{M_p}{\ell} \ . \tag{2.29}$$

Substituting equation (2.29) into equation (2.27) to solve for F_c we find

$$\left\{\frac{M_p}{\ell}\right\}.2\ell + F_c.\ell = M_p \ ,$$

or

$$F_c = -\frac{M_p}{\ell} \ . \tag{2.30}$$

Backsubstituting equations (2.29) and (2.30) into equations (2.25) and (2.26) respectively, gives

$$G\ddot{w} = P - \frac{M_p}{\ell} \ , \tag{2.31}$$

$$G\ddot{w}_c = \frac{M_p}{\ell} \ . \tag{2.32}$$

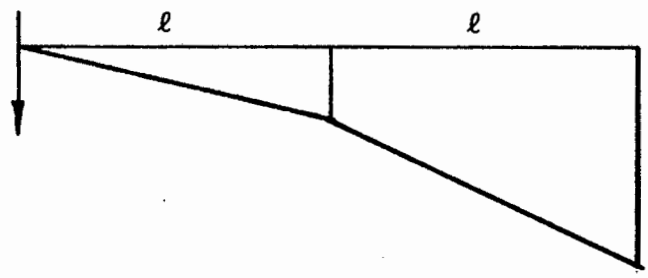

Fig. 2.5 : Velocity and Acceleration Fields

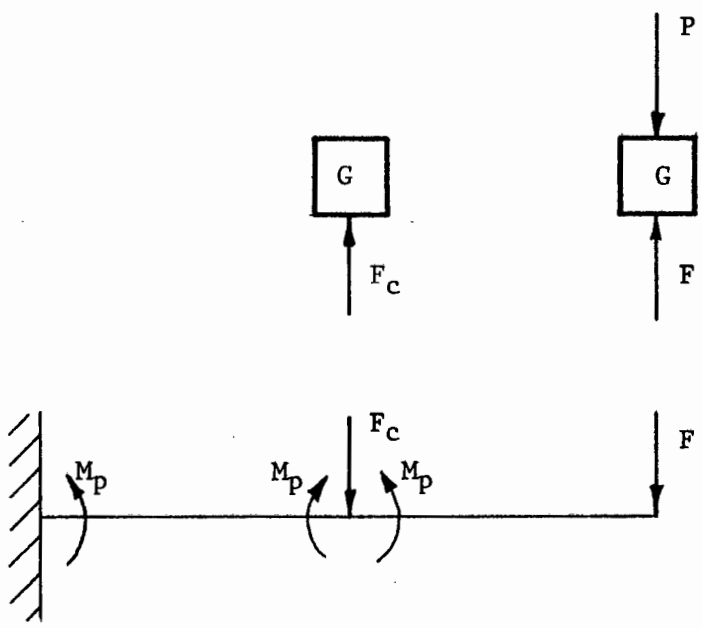

Fig. 2.6 : Body Force Representation for Cantilever

Solving equations (2.31) and (2.32) for the accelerations $\ddot{w}$ and $\ddot{w}_c$ we have

$$\ddot{w} = \frac{P}{G} - \frac{M_p}{G\ell} , \tag{2.33}$$

$$\ddot{w}_c = \frac{M_p}{G\ell} . \tag{2.34}$$

To simplify the solution let us take a specific value of P, say

$$P = 5\left\{\frac{M_p}{\ell}\right\} . \tag{2.35}$$

Substituting equation (2.35) into equation (2.33), we then have

$$\ddot{w} = 4\left\{\frac{M_p}{G\ell}\right\} . \tag{2.36}$$

The motion of the cantilever subjected to the load $P = 5M_p/\ell$ will now be followed. The initial conditions are

$$w(0) = \dot{w}(0) = 0 ,$$

$$w_c(0) = \dot{w}_c(0) = 0 . \tag{2.37}$$

The velocity and displacement are found by integrating the accelerations with respect to time. The accelerations from equations (2.36) and (2.34), are

$$\ddot{w}(t) = 4\left\{\frac{M_p}{G\ell}\right\} , \tag{2.38}$$

$$\ddot{w}_c(t) = \left\{\frac{M_p}{G\ell}\right\} . \tag{2.39}$$

Thus, using initial conditions (2.37),

$$\dot{w}(t) = \int_0^t \ddot{w}(t)dt = 4\left\{\frac{M_p}{G\ell}\right\}t , \tag{2.40}$$

$$\dot{w}_c(t) = \int_0^t \ddot{w}_c(t)dt = \left\{\frac{M_p}{G\ell}\right\}t , \tag{2.41}$$

and

$$w(t) = \int_0^t \dot{w}(t)dt = 2\left\{\frac{M_p}{G\ell}\right\}t^2 , \tag{2.42}$$

$$w_c(t) = \int_0^t \dot{w}_c(t)dt = \tfrac{1}{2}\left\{\frac{M_p}{G\ell}\right\}t^2 . \tag{2.43}$$

At time $t = t_o$, the load $P = 5M_p/\ell$ is removed and the cantilever starts to decelerate. The velocities and displacements at this time are found by substituting $t = t_o$ into equations (2.40), (2.41), (2.42) and (2.43) to give

$$\dot{w}(t_o) = 4\left\{\frac{M_p}{G\ell}\right\}t_o , \qquad w(t_o) = 2\left\{\frac{M_p}{G\ell}\right\}t_o^2 , \tag{2.44}$$

$$\dot{w}_c(t_o) = \left\{\frac{M_p}{G\ell}\right\}t_o , \qquad w_c(t_o) = \tfrac{1}{2}\left\{\frac{M_p}{G\ell}\right\}t_o^2 . \tag{2.45}$$

When the system decelerates, $P = 0$, and equations (2.31) and (2.32) give

$$\ddot{w}(t) = -\frac{M_p}{G\ell} , \tag{2.46}$$

$$w_c(t) = \frac{M_p}{G\ell} . \tag{2.47}$$

It is convenient to restart the time clock at the beginning of each phase. Reinterpreting the initial conditions of equations (2.44) and (2.45), the velocities are

$$\dot{w}(t) = \int_0^t \ddot{w}(t)dt = 4\left\{\frac{M_p}{G\ell}\right\}t_o - \left\{\frac{M_p}{G\ell}\right\}t , \tag{2.48}$$

$$\dot{w}_c(t) = \int_0^t \ddot{w}_c(t)dt = \left\{\frac{M_p}{G\ell}\right\}t_o + \left\{\frac{M_p}{G\ell}\right\}t , \tag{2.49}$$

and the displacements are

$$w(t) = \int_0^t \dot{w}(t)dt = \left\{\frac{M_p}{G\ell}\right\}\left(4t_o t - \tfrac{1}{2}t^2 + 2t_o{}^2\right) , \tag{2.50}$$

$$w_c(t) = \int_0^t \dot{w}(t)dt = \left\{\frac{M_p}{G\ell}\right\}\left(t_o t + \tfrac{1}{2}t + \tfrac{1}{2}t_o{}^2\right) . \tag{2.51}$$

During the acceleration phase, the centre hinge rotation rate increases, while in the deceleration phase the centre hinge rotation rate decreases. This phase ends at time $t = t_1$ when the centre hinge rotation rate becomes zero. The whole cantilever is then moving as a rigid body about the support. Thus at time $t = t_1$,

$$\dot{w}(t_1) = 2\dot{w}_c(t_1) . \tag{2.52}$$

Substituting equations (2.48) and (2.49) into equation (2.52) gives

$$\left(4t_o - t_1\right)\left\{\frac{M_p}{G\ell}\right\} = 2\left(t_o + t_1\right)\left\{\frac{M_p}{G\ell}\right\} ,$$

and hence

$$t_1 = \tfrac{2}{3}t_o . \tag{2.53}$$

The velocities and displacements at time $t = t_1$ are found by substituting equation (2.53) into equations (2.48) to (2.51) to give

$$\dot{w}(t_1) = \tfrac{10}{3}\left\{\frac{M_p}{G\ell}\right\}t_o , \qquad w(t_1) = 4.444\left\{\frac{M_p}{G\ell}\right\}t_o{}^2 , \tag{2.54}$$

$$\dot{w}_c(t_1) = \tfrac{5}{3}\left\{\frac{M_p}{G\ell}\right\}t_o , \qquad w_c(t_1) = 1.389\left\{\frac{M_p}{G\ell}\right\}t_o{}^2 . \tag{2.55}$$

The times t_o and t_1 are the duration of the phases and not the actual time, since each phase starts with time $t = 0$.

The accelerations $\ddot{w}$ and $\ddot{w}_c$ for the final phase are the same as for the cantilever rotating only about the support and are given by

equations (2.23) and (2.24);

$$\ddot{w}(t) = -\frac{2}{5}\left\{\frac{M_p}{G\ell}\right\} ,$$

$$\ddot{w}_c(t) = -\frac{1}{5}\left\{\frac{M_p}{G\ell}\right\} .$$

Reinterpreting the initial conditions (2.54) and (2.55), the velocities are

$$\dot{w}(t) = \int_0^t \ddot{w}(t)dt = \left\{\frac{M_p}{G\ell}\right\}\left(\frac{10}{3}t_o - \frac{2}{5}t\right) , \tag{2.56}$$

$$\dot{w}_c(t) = \int_0^t \ddot{w}_c(t)dt = \left\{\frac{M_p}{G\ell}\right\}\left(\frac{5}{3}t_o - \frac{1}{5}t\right) , \tag{2.57}$$

and the displacements are

$$w(t) = \int_0^t \dot{w}(t)dt = \left\{\frac{M_p}{G\ell}\right\}\left(4.444t_o^2 + 3.333t_o t - 0.200t^2\right) , \tag{2.58}$$

$$w_c(t) = \int_0^t \dot{w}_c(t)dt = \left\{\frac{M_p}{G\ell}\right\}\left(1.389t_o^2 + 1.667t_o t - 0.100t^2\right) . \tag{2.59}$$

This phase, and the motion, ends at time $t = t_2$ when

$$\dot{w} = \dot{w}_c = 0 . \tag{2.60}$$

Substituting equation (2.60) into equation (2.56) we find

$$0 = \left\{\frac{M_p}{G\ell}\right\}\left(\frac{10}{3}t_o - \frac{2}{5}t_2\right) ,$$

or

$$t_2 = \left(\frac{25}{3}\right)t_o . \tag{2.61}$$

Fig. 2.7 is a velocity-time plot for the tip and centre of the cantilever.

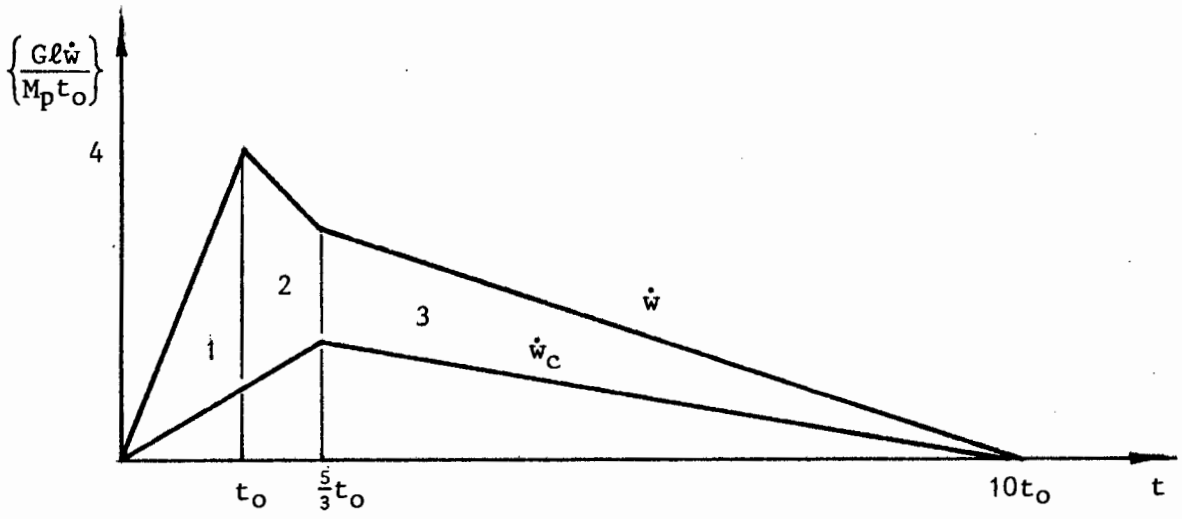

Fig. 2.7 : Velocity-Time Plot for Two Mass Cantilever

2.3 HOLONOMIC ANALYSIS OF THE TWO-MASS CANTILEVER

The problem will now be reconsidered using the holonomic material model described in detail in Section 1.5. We note first that during the loading phase, $0 \quad t \quad t_o$, the non-holonomic applies equally well for the holonomic case, since no unloading occurs. We must thus consider three ranges of the load P, as in the previous Section.

2.3.1 $P \leq \frac{M_p}{2\ell}$

As before, there will be no motion for this range of P.

2.3.2 $\frac{M_p}{2\ell} \leq P \leq \frac{3M_p}{\ell}$

The motion in this range of P will be exactly the same as in Section 2.2.2. The cantilever rotates as a rigid body about the support, and the hinge rotation rate has the same sign throughout the motion. For this condition, the holonomic beam and the non-holonomic beam behave identically throughout the motion.

2.3.3 $P \geq \frac{3M_p}{\ell}$

The motion of the cantilever, while the force P is acting (phase 1), is the same as for Section 2.2.3, i.e. there will be hinges at the support and centre mass. The equations of motion are given by equations (2.33) and (2.34). The same value of $P = 5M_p/\ell$ will be used as a specific example. The accelerations are thus given by equations (2.38) and (2.39) and are

$$\ddot{w}(t) = 4\left\{\frac{M_p}{G\ell}\right\}, \tag{2.62}$$

$$\ddot{w}_c(t) = \left\{\frac{M_p}{G\ell}\right\}. \tag{2.63}$$

The velocities and displacements are given by equations (2.40) and (2.41) and equations (2.42) and (2.43) respectively, i.e.

$$\dot{w}(t) = 4\left\{\frac{M_p}{G\ell}\right\}t \quad , \tag{2.64}$$

$$\dot{w}_c(t) = \left\{\frac{M_p}{G\ell}\right\}t \quad , \tag{2.65}$$

$$w(t) = 2\left\{\frac{M_p}{G\ell}\right\}t^2 \quad , \tag{2.66}$$

$$w_c(t) = 0.5\left\{\frac{M_p}{G\ell}\right\}t^2 \quad . \tag{2.67}$$

At time $t = t_o$ the velocities and displacements are

$$\dot{w}(t_o) = 4\left\{\frac{M_p}{G\ell}\right\}t_o \quad , \qquad w(t_o) = 2\left\{\frac{M_p}{G\ell}\right\}t_o^2 \quad , \tag{2.68}$$

$$\dot{w}_c(t_o) = \left\{\frac{M_p}{G\ell}\right\}t_o \quad , \qquad w_c(t_o) = 0.5\left\{\frac{M_p}{G\ell}\right\}t_o^2 \quad . \tag{2.69}$$

The second phase, with $P = 0$, now begins and the non-holonomic equations still apply since no unloading has yet occurred. The accelerations are given by equations (2.46) and (2.47);

$$\ddot{w}(t) = -\left\{\frac{M_p}{G\ell}\right\} \quad , \tag{2.70}$$

$$\ddot{w}_c(t) = \left\{\frac{M_p}{G\ell}\right\} \quad . \tag{2.71}$$

The velocities and displacements are given by equations (2.48) and (2.49) and equations (2.50) and (2.51) respectively;

$$\dot{w}(t) = \left\{\frac{M_p}{G\ell}\right\}(4t_o - t) \quad , \tag{2.72}$$

$$\dot{w}_c(t) = \left\{\frac{M_p}{G\ell}\right\}(t_o + t) \tag{2.73}$$

$$w(t) = \left\{\frac{M_p}{G\ell}\right\}\left(4t_o t - 0.5t^2 + 2t_o^2\right) , \tag{2.74}$$

$$w_c(t) = \left\{\frac{M_p}{G\ell}\right\}\left(t_o t + 0.5t^2 + 0.5t_o^2\right) . \tag{2.75}$$

In the non-holonomic case this phase ends when the centre hinge rotation rate becomes zero, but in the holonomic case the phase ends when the centre hinge rotation becomes zero, i.e. when the cantilever straightens out. Thus this phase ends when

$$w_c(t_1) = 0.5w(t_1) . \tag{2.76}$$

Thus, substituting equations (2.74) and (2.75) and $t = t_1$, into equation (2.76) we have

$$\left\{\frac{M_p}{G\ell}\right\}\left(t_o t_1 + 0.5t_1^2 + 0.5t_o^2\right) = 0.5\left\{\frac{M_p}{G\ell}\right\}\left(4t_o t_1 - 0.5t_1^2 + 2t_o^2\right) . \tag{2.77}$$

Dividing equation (2.77) by $M_p/G\ell$ and rearranging

$$0.75t_1^2 - t_o t_1 - 0.5t_o^2 = 0 .$$

Solving for t_1, we find only one possible root,

$$t_1 = 1.72t_o . \tag{2.78}$$

The velocities at the end of this phase (phase 2) are found by substituting equation (2.78) into equations (2.72) and (2.73);

$$\dot{w}(t_1) = \left\{\frac{M_p}{G\ell}\right\}\left(4t_o - 1.72t_o\right) = 2.28\left\{\frac{M_p}{G\ell}\right\}t_o , \tag{2.79}$$

$$\dot{w}_c(t_1) = \left\{\frac{M_p}{G\ell}\right\}\left(t_o + 1.72t_o\right) = 2.72\left\{\frac{M_p}{G\ell}\right\}t_o , \tag{2.80}$$

and the displacements are found by substituting equation (2.78) into equation (2.74) and the result into equation (2.76),

$$w(t_1) = \left\{\frac{M_p}{G\ell}\right\}\left(4t_o(1.72t_o) - 0.5(1.72t_o)^2 + 2t_o^2\right)$$

$$= 7.40\left\{\frac{M_p}{G\ell}\right\}t_o^2 , \tag{2.81}$$

$$w_c(t_1) = 0.5\left(7.40\left\{\frac{M_p}{G\ell}\right\}t_o^2\right)$$

$$= 3.70\left\{\frac{M_p}{G\ell}\right\}t_o^2 \ . \qquad (2.82)$$

At the end of phase 2, the following conditions hold;

$$\theta_c = 0 \ ,$$

$$\dot{\theta}_c \neq 0 \ ,$$

where θ_c and $\dot{\theta}_c$ are the centre hinge rotation and rotation rate. Rotation continues in phase 3, but with $\theta_c < 0$. For a holonomic material, the change in sign of θ_c implies change in sign of moment, hence the equations must be reformulated.

Consider body forces shown in Fig. 2.8. Writing the equations of motion for the two masses shown in Fig. 2.8 , we have

$$-F = G\ddot{w} \ , \qquad (2.83)$$

$$-F_c = G\ddot{w}_c \ . \qquad (2.84)$$

Moments about the support gives

$$F.2\ell + F_c.\ell = M_p \ , \qquad (2.85)$$

and moments to the right of the centre mass gives

$$F.\ell = -M_p \ . \qquad (2.86)$$

Rearranging equation (2.86) to solve for F , we obtain

$$F = -\frac{M_p}{\ell} \ . \qquad (2.87)$$

Substituting equation (2.87) into (2.85) to solve for F_c , we find

$$\left\{-\frac{M_p}{\ell}\right\}.2\ell + F_c.\ell = M_p \ ,$$

or

$$F_c = 3\left\{\frac{M_p}{\ell}\right\} \ . \qquad (2.88)$$

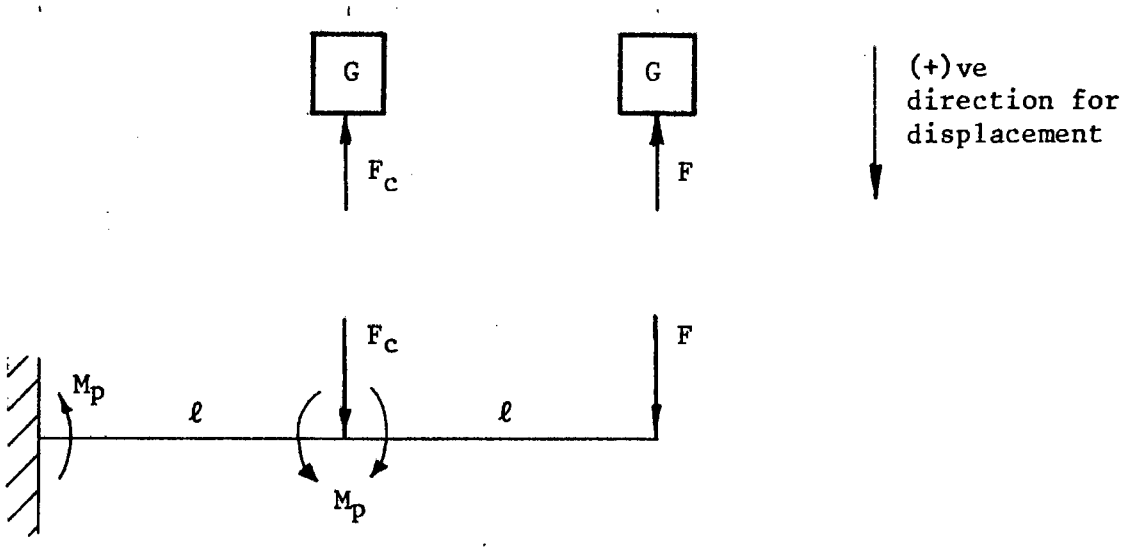

Fig. 2.8 : Body Force Representation

Substituting equations (2.87) and (2.88) into equations (2.83) and (2.84) respectively, we obtain the accelerations

$$\ddot{w} = \frac{M_p}{G\ell} , \tag{2.89}$$

$$\ddot{w}_c = -3\left\{\frac{M_p}{G\ell}\right\} . \tag{2.90}$$

The initial conditions for phase 3 are given by equations (2.79) and (2.80) and equations (2.81) and (2.82);

$$\dot{w}(0) = 2.28\left\{\frac{M_p}{G\ell}\right\}t_o , \qquad w(0) = 7.40\left\{\frac{M_p}{G\ell}\right\}t_o^2 , \tag{2.91}$$

$$\dot{w}_c(0) = 2.72\left\{\frac{M_p}{G\ell}\right\} t_o , \qquad w_c(0) = 3.70\left\{\frac{M_p}{G\ell}\right\}t_o^2 . \tag{2.92}$$

The velocities are

$$\dot{w}(t) = \frac{M_p}{G\ell}\left(2.28t_o + t\right) , \tag{2.93}$$

$$\dot{w}_c(t) = \frac{M_p}{G\ell}\left(2.72t_o - 3t\right) . \tag{2.94}$$

The displacements are

$$w(t) = \frac{M_p}{G\ell}\left(7.4t_o^2 + 2.28t_o t + 0.5t^2\right) , \tag{2.95}$$

$$w_c(t) = \frac{M_p}{G\ell}\left(3.7t_o^2 + 2.72t_o t - 1.5t^2\right) . \tag{2.96}$$

At the beginning of this phase (phase 3), $\theta_c = 0$. During the phase θ_c is negative and decreases to a certain point and then increases again until it is again equal to zero, when the phase ends. The hinge at the support remains positive throughout the phase and continues to increase in magnitude.

This phase thus ends when $\theta_c = 0$, when

$$w_c(t_2) = 0.5w(t_2) . \tag{2.97}$$

Thus substituting equations (2.95) and (2.96) and $t = t_2$ into

equation (2.97), we have

$$\left\{\frac{M_p}{G\ell}\right\}\left(3.7t_o^2+2.72t_ot_2-1.5t_2^2\right) = 0.5\left\{\frac{M_p}{G\ell}\right\}\left(7.4t_o^2+2.28t_ot_2+0.5t_2^2\right) . \qquad (2.98)$$

Dividing equation (2.98) by $M_p/G\ell$ and rearranging gives

$$1.75t_2^2 - 1.58t_ot_2 = 0 .$$

Solving for t_2, we find

$$t_2 = 0.0 \quad \text{or} \quad 0.90t_o .$$

The first root indicates the beginning of the phase and the other the end. We put

$$t = 0.90t_o . \qquad (2.99)$$

The velocities at time t_2 at the end of phase 3 are found by substituting equation (2.99) into equations (2.93) and (2.94);

$$\dot{w}(t_2) = \frac{M_p}{G\ell}\left(2.28t_o + (0.90t_o)\right)$$

$$= 3.18\left\{\frac{M_p}{G\ell}\right\}t_o . \qquad (2.100)$$

$$\dot{w}_c(t_2) = \frac{M_p}{G\ell}\left(2.72t_o - 3(0.90t_o)\right)$$

$$= 0.02\left\{\frac{M_p}{G\ell}\right\}t_o . \qquad (2.101)$$

The displacements at time t_2 are found by substituting equation (2.99) into equations (2.95) and (2.97);

$$w(t_2) = \left\{\frac{M_p}{G\ell}\right\}\left(7.4t_o^2 + 2.28t_o(0.90t_o) + 0.50(0.90t_o)^2\right)$$

$$= 9.86\left\{\frac{M_p}{G\ell}\right\}t_o \ , \qquad (2.102)$$

$$w_c(t_2) = 0.5\left(9.86\left\{\frac{M_p}{G\ell}\right\}t_o^2\right.$$

$$= 4.93\left\{\frac{M_p}{G\ell}\right\}t_o^2 \ . \qquad (2.103)$$

The centre hinge rotation θ_c , was positive in phases 1 and 2 and negative in phase 3. At the end of phase 3, $\theta_c = 0$ and in phase 4, θ_c will become positive again. The equations of motion will thus be the same for phases 2 and 4, provided that the support hinge rotation, θ , maintains the same sign.

For phase 4, the accelerations are given by equations (2.70) and (2.71), as in phase 2;

$$\ddot{w}(t) = -\left\{\frac{M_p}{G\ell}\right\} \ , \qquad (2.104)$$

$$\ddot{w}_c(t) = \left\{\frac{M_p}{G\ell}\right\} \ . \qquad (2.105)$$

The initial conditions for phase 4 are given by equation (2.100) and (2.101) and equations (2.102) and (2.103), as follows:

$$\dot{w}(0) = 3.18\left\{\frac{M_p}{G\ell}\right\}t_o \ , \qquad w(0) = 9.86\left\{\frac{M_p}{G\ell}\right\}t_o^2 \ , \qquad (2.106)$$

$$\dot{w}_c(0) = 0.02\left\{\frac{M_p}{G\ell}\right\}t_o \ , \qquad w_c(0) = 4.93\left\{\frac{M_p}{G\ell}\right\}t_o^2 \ . \qquad (2.107)$$

The equations for velocity are found by integrating the accelerations and using initial conditions to give

$$\dot{w}(t) = \frac{M_p}{G\ell}\left(3.18t_o - t\right) \ , \qquad (2.108)$$

$$\dot{w}_c(t) = \frac{M_p}{G\ell}\left(0.02t_o + t\right) \ . \qquad (2.109)$$

The equations for displacement are found by integrating the velocities and using the initial conditions to give

$$w(t) = \frac{M_p}{G\ell}\left(9.86t_o^2 + 3.18t_o t - 0.50t^2\right) , \tag{2.110}$$

$$w_c(t) = \frac{M_p}{G\ell}\ 4.93t_o^2 + 0.02t_o t + 0.50t^2) . \tag{2.111}$$

The phase ends, as each of these phases, when

$$w_c = 0.5w . \tag{2.112}$$

Substituting equations (2.110) and (2.111) (with $t = t_3$) into equation (2.112), we have

$$\left\{\frac{M_p}{G\ell}\right\}\left(4.93t_o^2+0.02t_o t_3+0.50t_3^2\right) = 0.5\left\{\frac{M_p}{G\ell}\right\}\left(9.86t_o^2+3.18t_o t_3-0.50t_3^2\right) . \tag{2.113}$$

Dividing equation (2.113) by $M_p/G\ell$ and rearranging, gives

$$0.75t_3^2 - 1.57t_o t_3 = 0 .$$

Solving for t_3, we have the non-trivial root

$$t_3 = 2.09t_o . \tag{2.114}$$

The velocities at time t_3 at the end of phase 4 are found by substituting equation (2.114) into equations (2.108) and (2.109),

$$\dot{w}(t_3) = \frac{M_p}{G\ell}\left(3.18t_o - (2.09t_o)\right)$$

$$= 1.09\left\{\frac{M_p}{G\ell}\right\}t_o , \tag{2.115}$$

$$\dot{w}_c(t_3) = \frac{M_p}{G\ell}\left(0.02t_o + (2.09t_o)\right)$$

$$= 2.11\left\{\frac{M_p}{G\ell}\right\}t_o , \tag{2.116}$$

and the displacements are found by substituting equation (2.114) into equations (2.110) and (2.112) ,

$$w(t_3) = \left\{\frac{M_p}{G\ell}\right\}\left(9.86t_o^2 + 3.18t_o(2.09t_o) - 0.5(2.09t_o)^2\right)$$

$$= 14.33\left\{\frac{M_p}{G\ell}\right\}t_o^2 \ , \qquad (2.117)$$

$$w_c(t_3) = 0.5\left(14.33\left\{\frac{M_p}{G\ell}\right\}t_o^2\right)$$

$$= 7.16\left\{\frac{M_p}{G\ell}\right\}t_o^2 \ . \qquad (2.118)$$

We can now see that the equations of phase 3 will again apply, with $\theta_c < 0$. We can thus anticipate the form of the solution. A velocity-time plot for the tip and centre mass velocity $\dot{w}$ and $\dot{w}_c$ is shown in Fig. 2.9 with each phase numbered. If we confine ourselves to the range $\theta > 0$, it can be seen from this plot that, after phase 2, the cantilever has an overall motion involving rotation about the support with a periodic oscillation superimposed. Thus phases 3, 5 and 7 and phases 4, 6 and 8 are identical. The increases and decreases in velocity are the same for these two sets of phases. The details of the response need only to be calculated up to the end of phase 4.

The values of $\dot{w}$ and $\dot{w}_c$ as calculated for phase 1 to 4, as well as the changes in velocity from phase to phase can be tabulated, and are shown in Table 2.1. Fig. 2.10 shows $\dot{w}$ and $\dot{w}_c$ plotted as a function of time.

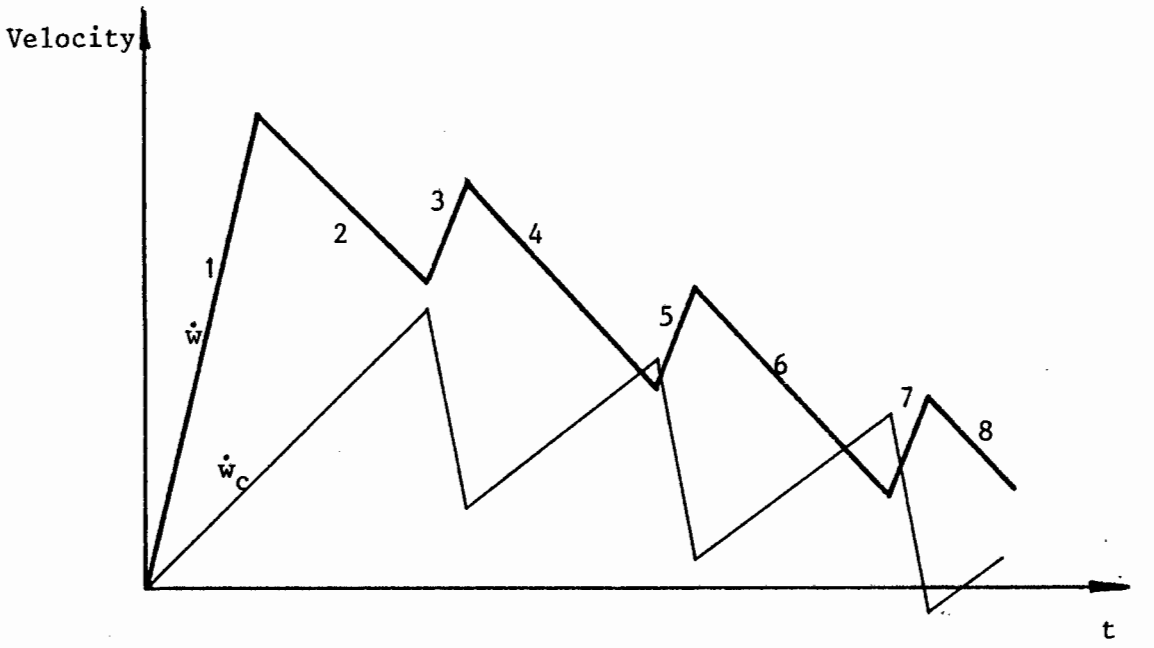

Fig. 2.9 : Velocity-Time Plot for Cantilever

Phase	$\dot{w}$	$\Delta\dot{w}$	$\dot{w}_c$	$\Delta\dot{w}_c$	Δt
	$0.00\left\{\frac{M_p}{G\ell}\right\}t_o$		$0.00\left\{\frac{M_p}{G\ell}\right\}t_o$		
1		$+4.00\left\{\frac{M_p}{G\ell}\right\}t_o$		$+1.00\left\{\frac{M_p}{G\ell}\right\}t_o$	$1.00(t_o)$
	4.00		1.00		
2		−1.72		+1.72	1.72
	2.28		2.72		
3		+0.90		−2.70	0.90
	3.18		0.02		
4		−2.09		+2.09	2.09
	1.09		2.11		
5		+0.90		−2.70	0.90
	1.99		−0.59		
6		−2.09		+2.09	2.09
	−0.10		+0.50		
7		+0.90		−2.70	0.90

TABLE 2.1

From the graphs in Fig. 2.10, it can be seen that the average tip and centre mass velocities become zero at time $t \cong 10t_o$. This is when the average downwards motion ends. The average motion will now be upwards; when the support hinge, θ , changes sign the equations of motion must be reformulated. The system, being conservative, will continue to oscillate with an overall motion about the support and a superimposed periodic motion of the two masses. The anticipated average tip velocity $\dot{w}_{ave}$ is shown in Fig. 2.10.

Fig. 2.10.

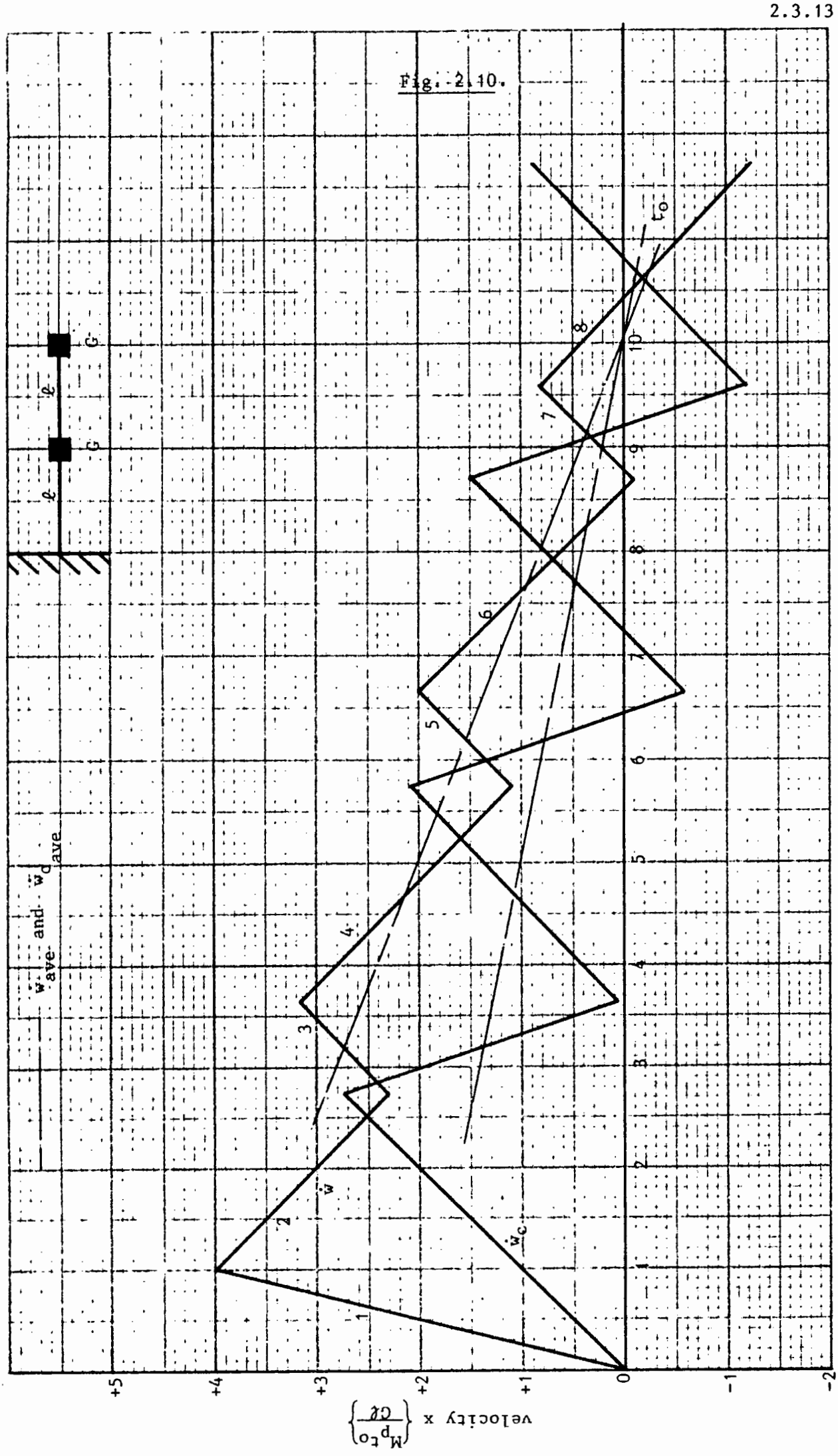
velocity x $\left\{\frac{M_p t_o}{GL}\right\}$
+5
+4
+3
+2
+1
0
-1
-2
$\dot{w}_c$
$\dot{w}$
$\dot{w}_{d\,ave}$ and $\dot{w}_{ave}$
t_o
G
G
L
L

2.4 THE EFFECT OF THE MASS RATIO ON HOLONOMIC ANALYSIS OF THE TWO MASS CANTILEVER

It is of interest to ascertain whether the behaviour of the holonomic two lump mass cantilever is sensitive to the ratio of the centre mass to the tip mass. For this purpose an analysis of the periodic behaviour of the two beams shown in Fig. 2.11(a) and 2.11(b) was carried out. The equations of motion for these beams are identical to those formulated in Section 2.3, except that the correct values of the masses must be substituted. The accelerating force P was chosen so that the tip velocity $\dot{w}$ is equal to $4(M_p/G\ell)t_o$ at time t_o. Thus for the case in Fig. 2.11(a), we put $P = 9(M_p/\ell)$ and for the case in Fig. 2.11(b) we put $P = 5(M_p/\ell)$.

In Section 2.3 a value of $5(M_p/\ell)$ was used for P. Plots of $\dot{w}$ and $\dot{w}_c$ as functions of time are shown in Figs. 2.12 and 2.13 for the cases in Fig. 2.11(a) and Fig. 2.11(b) respectively.

It can be seen that the results are essentially the same as the case treated in detail in Section 2.3. It appears as if the amplitude of the oscillation about the mean velocity is larger for the smaller mass.

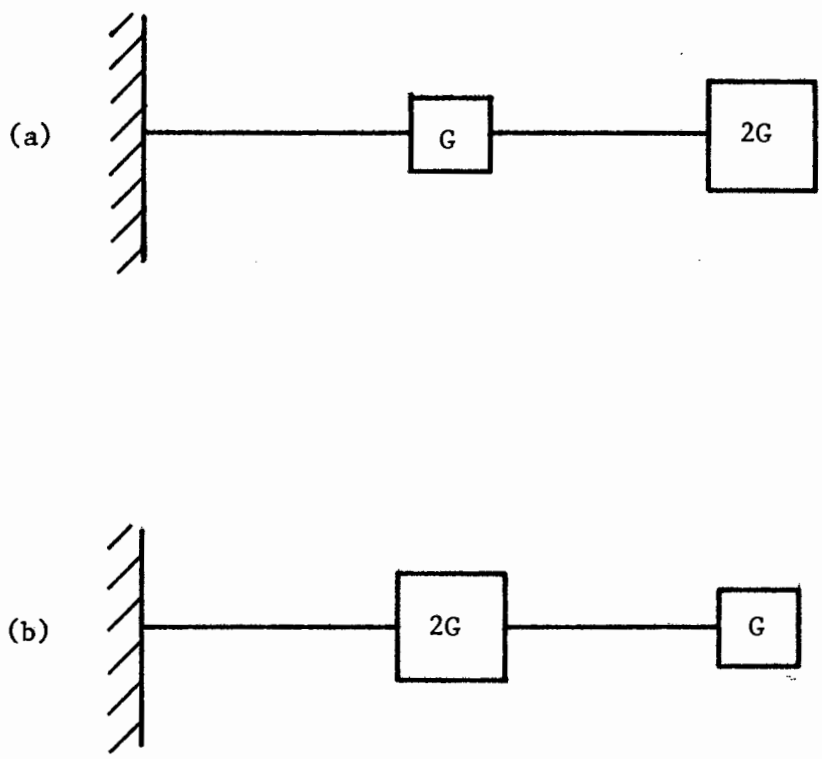

Fig. 2.11 : Two Mass Cantilever with Variable Mass Ratios

Fig. 2.12.

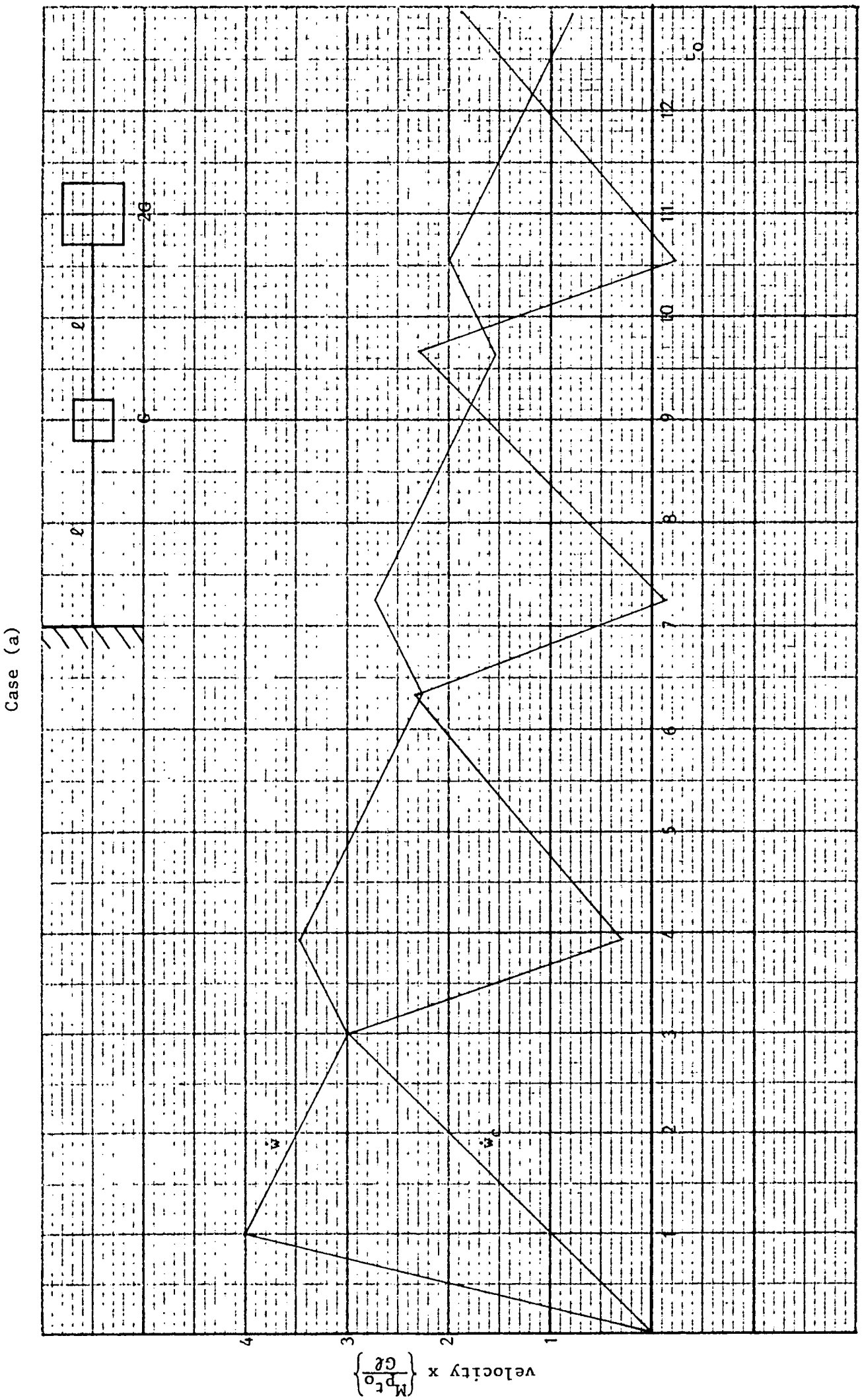

Fig. 2.13.

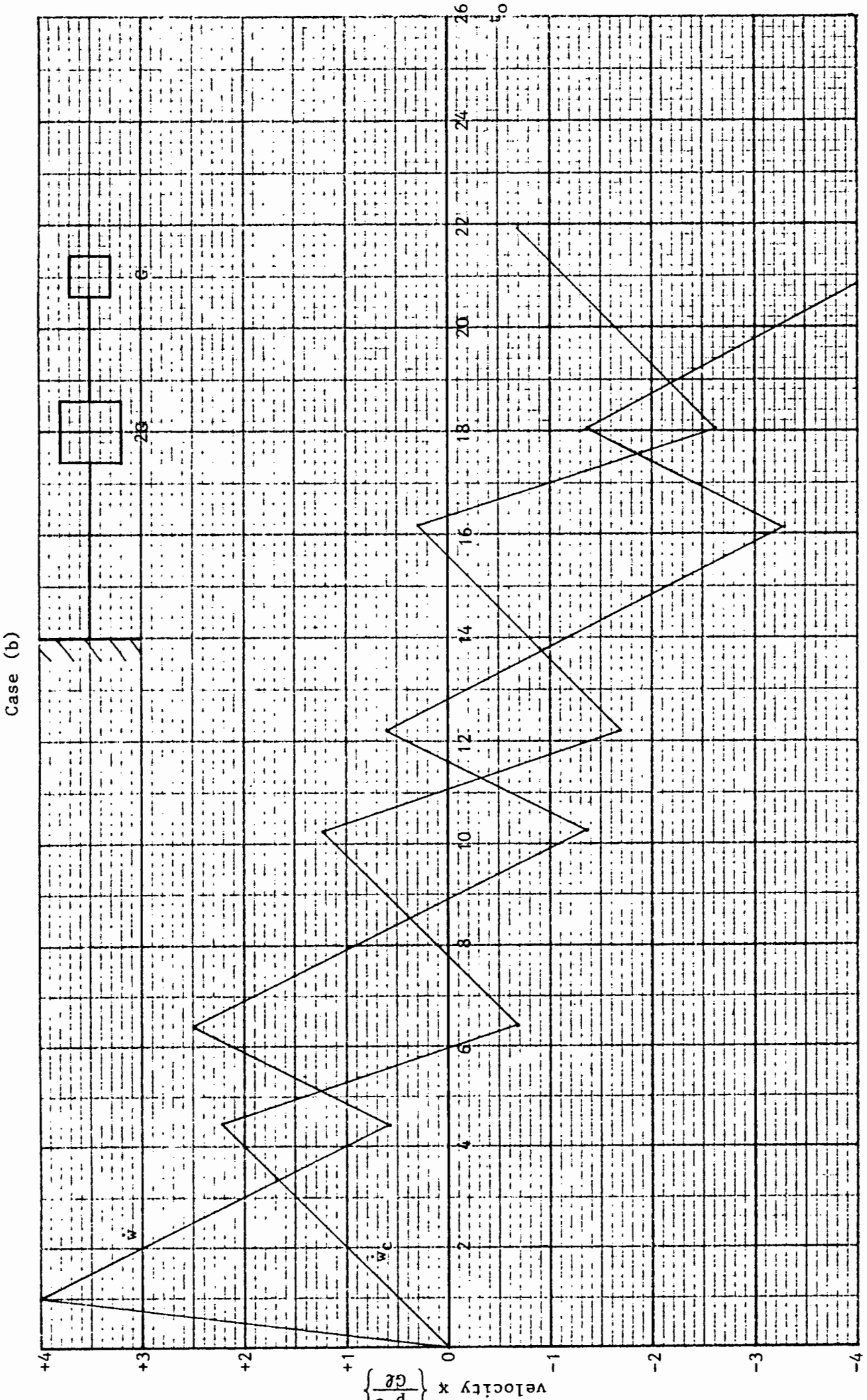
Case (b)
velocity x $\left\{\frac{M_p t_o}{GL}\right\}$
+4
+3
+2
+1
0
-1
-2
-3
-4
2
4
6
8
10
12
14
16
18
20
22
24
26
t_o
$\dot{w}$
$\dot{w}_c$
2B
6

2.5 HOLONOMIC ANALYSIS OF THE TWO MASS CANTILEVER USING A FIXED MODE APPROXIMATION

The response pattern for the two lump mass cantilever analysed in Section 2.3 will now be compared to a fixed mode approximation where the cantilever rotates about the support as a rigid body. An energy balance will be used to determine the initial velocities of the mode approximation.

The accelerating force P, applied at the tip of the cantilever and the displacement of the force during the interval $0 \leq t \leq t_o$ are found from equations (2.35) and (2.68);

$$P = 5\left\{\frac{M_p}{\ell}\right\} , \tag{2.119}$$

$$w(t_o) = 2\left\{\frac{M_p}{G\ell}\right\}t_o^2 . \tag{2.120}$$

The energy input E_T into the system is thus

$$E_T = P.w(t_o)$$

$$= 10\left\{\frac{M_p^{\ 2}}{G\ell^2}\right\}t_o^2 . \tag{2.121}$$

Assuming that the cantilever rotates about the support as a rigid body, we may put

$$w_c = \tfrac{1}{2}w , \tag{2.122}$$

and

$$\theta = \frac{w}{2\ell} , \tag{2.123}$$

where θ is the hinge rotation. Treating w as the single displacement parameter, an energy balance at time $t \geq t_o$ gives,

$$\tfrac{1}{2}G\dot{w}^2(t) + \tfrac{1}{2}G\dot{w}_c^2(t) + M_p\theta(t) = E_T ,$$

or

$$\frac{5}{8}G\dot{w}^2(t) + \frac{Mp}{2\ell}w(t) = 10\frac{Mp^2}{G\ell^2}t_o^2 \ . \qquad (2.124)$$

The displacement when $\dot{w} = 0$, which will be the maximum displacement w_m , is

$$w_m = 20\left\{\frac{Mp}{G\ell}\right\}t_o^2 \ . \qquad (2.125)$$

CHAPTER 3.

FIXED MODE CONDITIONS FOR THE CONTINUOUS CANTILEVER WITH TIP MASS

3.1 INTRODUCTION

Before beginning a detailed study of the response of a continuous mass cantilever to a pulse load on its tip, it is of interest to consider three mode motions of the holonomic cantilever. Mode motions are motions in which the shape of the displacement and velocity fields are fixed, or alternatively, motions in which the displacement function can be written as the product of separate functions of x and t. The formulation of the mode motions is comparatively straightforward, as there are no propagating discontinuities.

3.2 CANTILEVER ROTATING ABOUT SUPPORT AS RIGID BODY

The first mode motion has acceleration, velocity and displacement fields of the shape shown in Fig. 3.1. The acceleration at the tip of the cantilever is given by equation (1.49).

$$\ddot{w} = \frac{-\frac{M_P}{\ell}}{\left(G + \frac{1}{3}m\ell\right)} . \tag{3.1}$$

In dimensionless form this becomes

$$\ddot{\bar{w}} = \frac{-1}{\left(1 + \frac{1}{3}\beta\right)} , \tag{3.2}$$

where

$$\ddot{\bar{w}} = \frac{d^2\bar{w}}{d\tau^2} ,$$

$$\beta = \frac{m\ell}{G} ,$$

$$\bar{w} = \frac{w}{\ell} .$$

This case is very straightforward, and will not be discussed in detail.

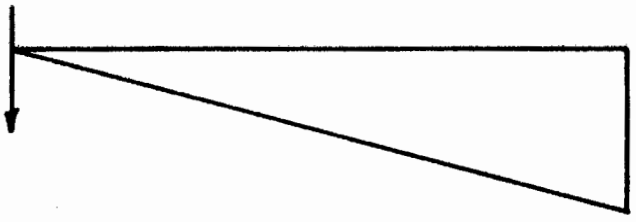

Fig. 3.1 : Velocity and Acceleration Fields

3.3 ACCELERATION PHASE WITH A HINGE IN CANTILEVER, WHICH IS A FIXED DISTANCE OF z FROM THE TIP .

Consider the cantilever subject to a fixed transverse load P at its tip, with zero initial displacement and velocity. As is known from the non-holonomic case, the motion will be in a fixed mode, with a displacement field of the form shown in Fig. 3.2. The velocity and acceleration fields are of the same shape.

For a given set of values of P , M_p , m , G , ℓ , there will be a unique hinge position characterised by z . The acceleration can be obtained by a moment balance between hinge and tip and by a linear momentum balance, since the shear force at the hinge will be zero. The moment balance gives

$$P = \frac{M_p}{z} + \left(G + \tfrac{1}{3}mz\right)\ddot{w} ,$$

or

$$\ddot{w} = \frac{P - \dfrac{M_p}{z}}{\left(G + \tfrac{1}{3}mz\right)} . \tag{3.3}$$

The linear momentum balance gives

$$P = G\ddot{w} + \tfrac{1}{2}mz\ddot{w} ,$$

or

$$\ddot{w} = \frac{P}{\left(G + \tfrac{1}{2}mz\right)} . \tag{3.4}$$

Eliminating $\ddot{w}$ from these equations, we get a quadratic equation for z ;

$$\tfrac{1}{6}\left\{\frac{Pm}{M_p}\right\}z^2 - \tfrac{1}{2}(m)z - G = 0 . \tag{3.5}$$

This equation yields two roots for z , only one of which is positive. This positive root gives the unique position of the hinge during acceleration. In dimensionless form equation (3.5) can be written as

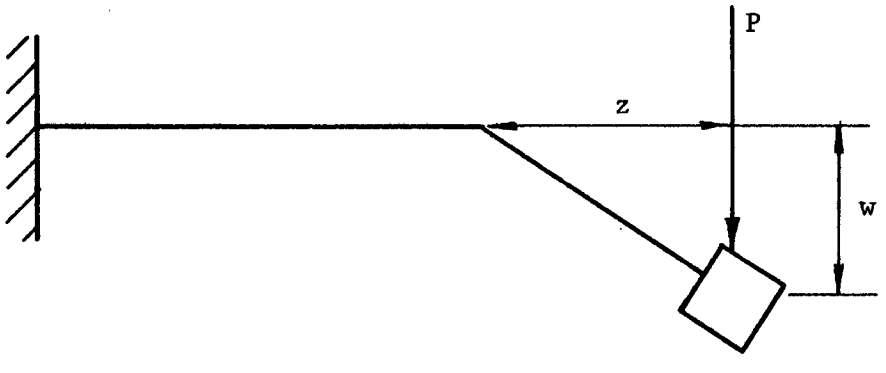

Fig. 3.2 : Acceleration Phase

$$\tfrac{1}{6}\alpha\bar{z}^2 - \tfrac{1}{2}\bar{z} - \tfrac{1}{\beta} = 0 \ , \tag{3.6}$$

where

$$\alpha = \frac{P\ell}{M_p} \ ,$$

$$\beta = \frac{m\ell}{G} \ ,$$

$$\bar{z} = \frac{z}{\ell} \ . \tag{3.7}$$

Putting equation (3.3) in dimensionless form, we have

$$\ddot{\bar{w}} = \frac{\alpha - \frac{1}{\bar{z}}}{\left(1 + \frac{1}{3}\beta\bar{z}\right)} \ , \tag{3.8}$$

where

$$\tau = \sqrt{\frac{M_p}{G\ell^2}} \, . \, t \ .$$

$$\ddot{\bar{w}} = \frac{d^2\bar{w}}{d\tau^2}$$

3.4 MODE MOTIONS WITH TWO HINGES IN THE CANTILEVER, ONE AT THE SUPPORT AND THE OTHER A DISTANCE OF z FROM THE TIP

Again, from non-holonomic behaviour, we may anticipate the existence of higher modes of free motion. A second mode, with two hinges, can be expected. We consider the displaced shape shown in Fig. 3.4. There are three displacement variables, the tip and centre hinge accelerations, $\ddot{w}$ and $\ddot{v}$ respectively, and the position of the centre hinge, z, from the tip. There are three dynamic conditions; we set the sum of moments about the support hinge equal to zero, the sum of moments about the centre hinge equal to zero and the shear force at the centre hinge equal to zero. The zero shear force at the centre hinge is a consequence of the minimum bending moment at the hinge. The bending moment diagram is shown in Fig. 3.3. The velocity and acceleration fields also have the shape shown in Fig. 3.4.
The sum of moments about the support gives

$$- M_p + \tfrac{1}{2}m\ddot{v}(\ell-z)\tfrac{2}{3}(\ell-z) + \tfrac{1}{2}m\ddot{v}z(\ell-\tfrac{2}{3}z) - \tfrac{1}{2}m\ddot{w}z(\ell-\tfrac{1}{3}z) - G\ddot{w}\ell = 0 ,$$

or

$$- M_p + \tfrac{1}{3}m\ddot{v}\ell(\ell-\tfrac{1}{2}z) - \tfrac{1}{2}m\ddot{w}z(\ell-\tfrac{1}{3}z) - G\ddot{w}\ell = 0 . \qquad (3.9)$$

In dimensionless form, this equation becomes

$$- 1 + \tfrac{1}{3}\beta\ddot{\bar{v}}(1-\tfrac{1}{2}\bar{z}) - \tfrac{1}{2}\beta\ddot{\bar{w}}(\bar{z}-\tfrac{1}{3}\bar{z}^2) - \ddot{\bar{w}} = 0 , \qquad (3.10)$$

where

$$\ddot{\bar{w}} = \frac{d^2\bar{w}}{d\tau^2} , \quad \bar{w} = \frac{w}{\ell} , \quad \beta = \frac{m\ell}{G} ,$$

$$\ddot{\bar{v}} = \frac{d^2\bar{v}}{d\tau^2} , \quad \bar{v} = \frac{v}{\ell} , \quad \bar{z} = \frac{z}{\ell} .$$

The sum of moments to the right of the centre hinge gives

$$M_p + \tfrac{1}{6}m\ddot{v}z^2 - \tfrac{1}{3}m\ddot{w}z^2 - G\ddot{w}z = 0 , \qquad (3.11)$$

which becomes, in dimensionless form,

$$1 + \tfrac{1}{6}\beta\ddot{\bar{v}}\bar{z}^2 - \tfrac{1}{3}\beta\ddot{\bar{w}}\bar{z}^2 - \ddot{\bar{w}} = 0 . \qquad (3.12)$$

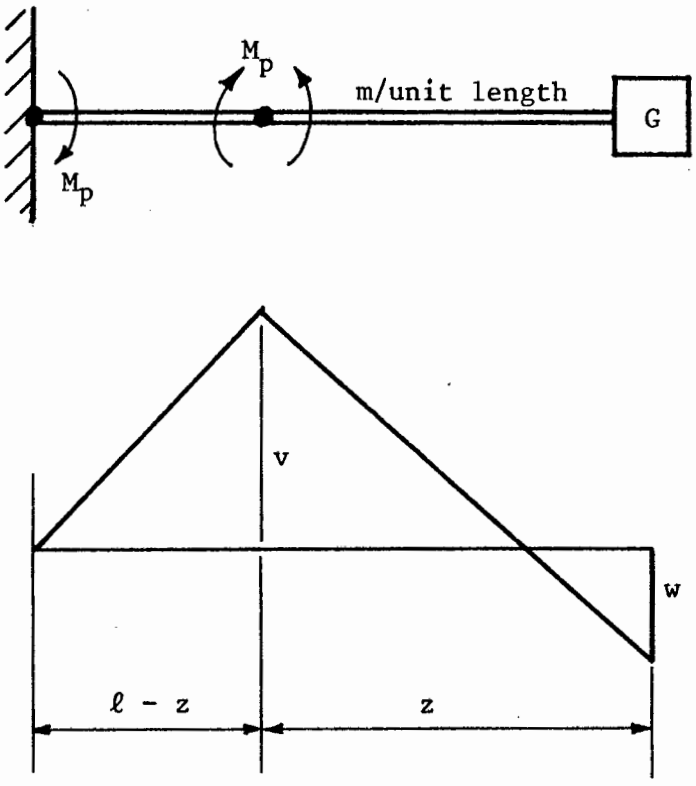

Fig. 3.3 : Displaced Shape and Dimensions of Cantilever

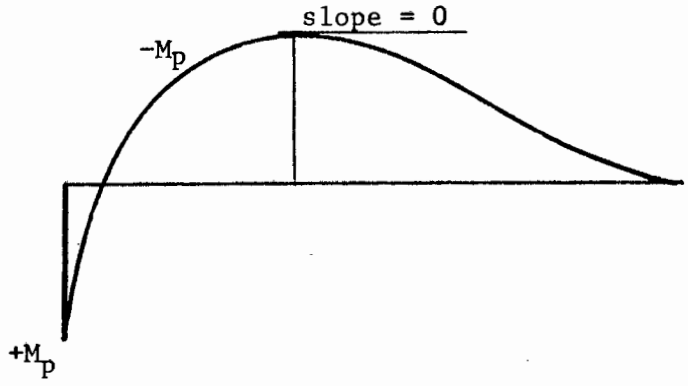

Fig. 3.4 : Bending Moment Diagram

The sum of forces to the right of the centre hinge gives

$$\tfrac{1}{2}m\ddot{v}z = \tfrac{1}{2}m\ddot{w}z + G\ddot{w} \ . \tag{3.13}$$

In dimensionless form this is

$$\tfrac{1}{2}\beta\ddot{\bar{v}}\bar{z} = \tfrac{1}{2}\beta\ddot{\bar{w}}\bar{z} + \ddot{\bar{w}} \ . \tag{3.14}$$

Solving the three simultaneous equations (3.10), (3.12) and (3.14) for the variables $\ddot{\bar{w}}$, $\ddot{\bar{v}}$ and $\bar{z}$, we find

$$\ddot{\bar{w}} = \frac{1}{\left(\frac{1}{6}\beta\bar{z}^2 - \frac{1}{3}\bar{z} + 1\right)} \ , \tag{3.15}$$

$$\ddot{\bar{v}} = w + 2\left\{\frac{\ddot{\bar{w}}}{\beta\bar{z}}\right\} \ , \tag{3.16}$$

$$\bar{z} = \frac{(7 - \beta) + \sqrt{4(\beta - 7)^2 - 32(1 - 2\beta)}}{2(1 - 2\beta)} \ . \tag{3.17}$$

Fig. 3.5 shows $\ddot{\bar{w}}$, $\ddot{\bar{v}}$ and $\bar{z}$ plotted against β. We see from this plot that $0{,}298 \leqq \bar{z} \leqq 0{,}500$.

Fig. 3.5.

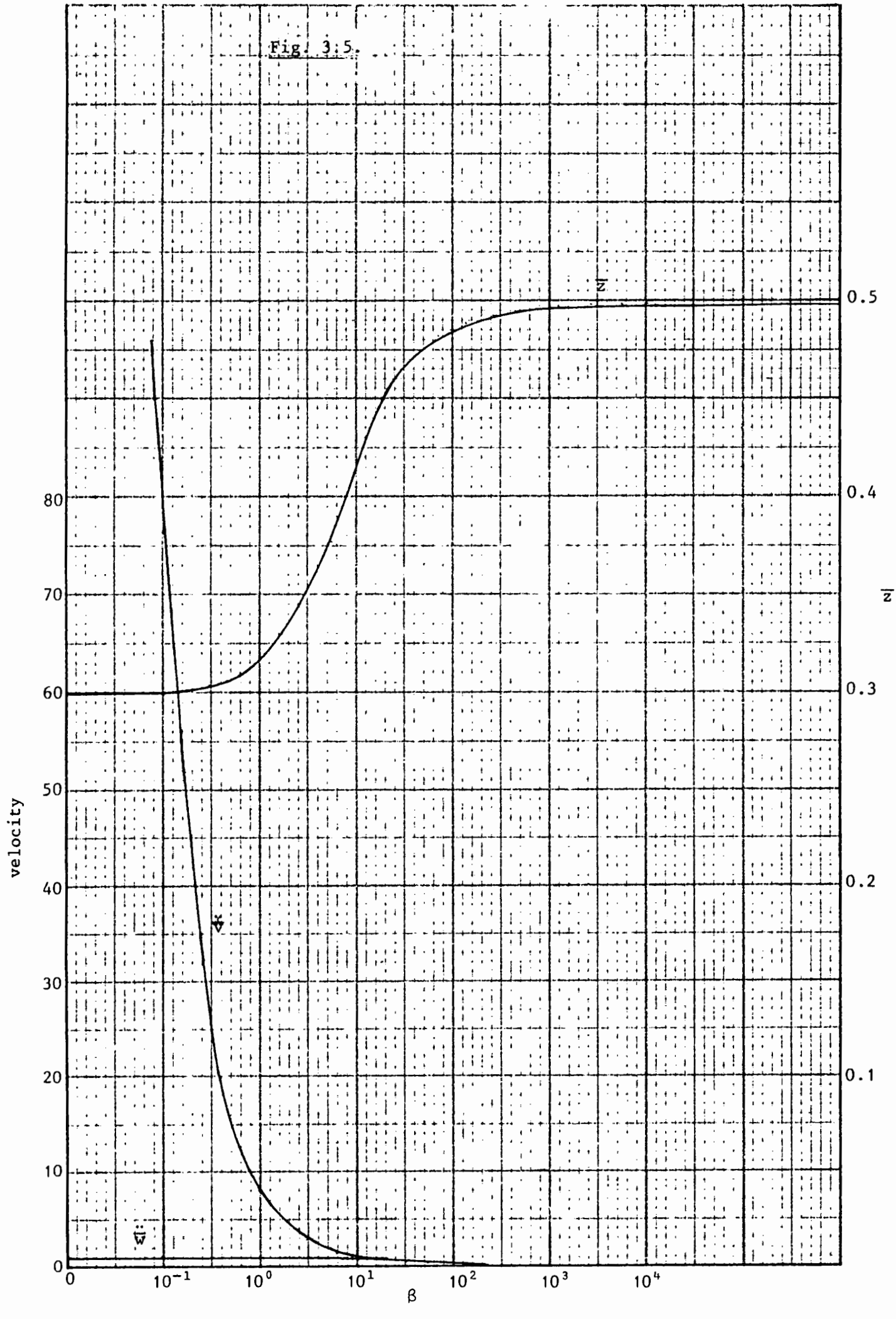
velocity
80
70
60
50
40
30
20
10
0
0
10^{-1}
10^{0}
10^{1}
10^{2}
10^{3}
10^{4}
β
$\bar{w}$
$\bar{u}$
$\bar{N}$
0.5
0.4
0.3
0.2
0.1
$\bar{z}$

CHAPTER 4.

HOLONOMIC ANALYSIS OF CONTINUOUS CANTILEVER WITH TIP MASS

4.1 INTRODUCTION

We now consider the response of a holonomic cantilever to a fixed load P applied at the tip over the time interval $0 \leq t \leq t_o$. As before, the span of the cantilever is ℓ, the mass per unit length m, the tip mass is G, and the plastic moment M_p. The motion can again be divided into a number of phases, the form of which can be anticipated from our earlier studies. The first phase is a fixed mode motion, as described in Section 3.3, over the time interval $0 \leq t \leq t_o$. The second phase is a motion rather similar to that found in Parkes's analysis, in which there is one travelling hinge. The second phase ends, however, when a hinge forms at the support, and the third phase involves two hinges, one of which is moving.

The formulation of the equations of motion for the second and third phases of motion will be accompanied by the use of Lagrange's equations. A study of the propagating rotation discontinuity in the holonomic beam will also be necessary. The equations of motion for the second and third phases of motion were solved numerically, and details of these computations will be given.

4.2 THE FIRST PHASE

During the first phase the cantilever is subjected to a constant force P acting on the tip mass for the period $0 \leq t \leq t_o$. The motion is a fixed mode, as discussed in Section 3.3, and the displaced shape is shown in Fig. 4.1. The hinge forms at a distance z_o from the tip. The acceleration is given by equation (3.3) in Section 3.3 and is

$$\ddot{w} = \frac{P - \frac{M_p}{z_o}}{\left(G + \frac{1}{3}mz_o\right)} . \tag{4.1}$$

In dimensionless form this becomes

$$\ddot{\bar{w}} = \frac{\left(\alpha - \frac{1}{\bar{z}_o}\right)}{\left(1 + \frac{1}{3}\beta\bar{z}_o\right)} , \tag{4.2}$$

where

$$\alpha = \frac{P\ell}{M_p} ,$$

$$\beta = \frac{m\ell}{G} ,$$

$$\bar{z}_o = \frac{z_o}{\ell} ,$$

$$\bar{w} = \frac{w}{\ell}$$

$$\tau = \sqrt{\frac{M_p}{G\ell^2}} \cdot t \tag{4.3}$$

The distance between the hinge and tip, $\bar{z}_o$, is found by rearranging equation (3.6) to give

$$\alpha\beta\bar{z}_o^2 - 3\beta\bar{z}_o - 6 = 0 . \tag{4.4}$$

Solving for z_o, we have the only positive root

$$\bar{z}_o = \frac{3\beta + \sqrt{9\beta^2 + 24\alpha\beta}}{2\alpha\beta} . \tag{4.5}$$

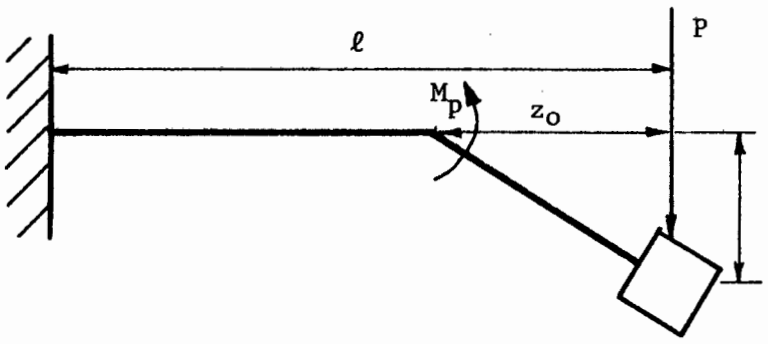

Fig. 4.1 : Acceleration Phase

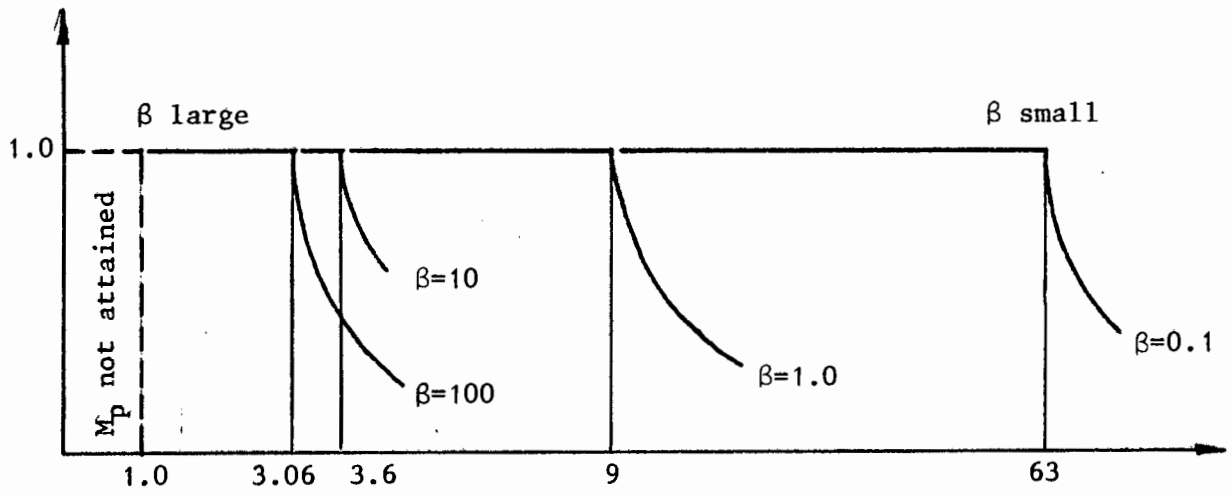

Fig. 4.2

The relation between α , β and z_o is shown is shown diagrammatically in Fig. 4.2. In this diagram, $\bar{z}_o = 1.0$ indicates that a hinge forms at the support. For a specific value of β , there are three distinct regions of α values. Consider $\beta = 1.0$, for example. If $0 < \alpha < 1.0$, M_p will not be attained and there will be no motion. For $1.0 < \alpha \leq 9.0$, $\bar{z}_o = 1$, i.e. the hinge is at the support and there will be a fixed mode motion for $t > t_o$. If however $\alpha > 9.0$, we will have $0 < \bar{z}_o \leq 1.0$, and there will be a moving hinge in phases 2 and 3.

Fig. 4.2 also shows that if β is small, α must be very large for a moving hinge to occur in phase 2. For very large β values, and $\bar{z}_o = 1.0$, $\alpha \to 3$. Thus if $\alpha < 3$, there will be fixed mode motion for the complete response for all β .

During phase 1 the bending moment diagram for the cantilever is given by Fig. 4.3.

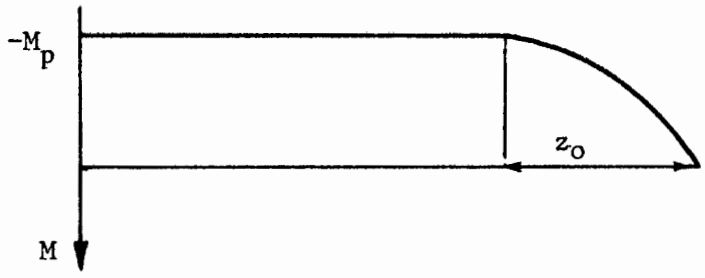

Fig. 4.3 : Bending Moment Diagram

4.3 THE SECOND PHASE

Consider the displacement field in Fig. 4.4. This is the same shape as that considered in the previous Section; however, we now have $P = 0$ and we anticipate that the hinge will move, i.e. $z = z(t)$. The displacement variables will be w and θ_c, the tip deflection and hinge rotation respectively. The displacement of the cantilever between the hinge and tip will be given by

$$\begin{aligned} u(z,t) &= w\left(1 - \frac{x}{z}\right) , \\ &= w - \theta_c x , \end{aligned} \tag{4.6}$$

where

$$z = \frac{w}{\theta_c} .$$

Thus the displacement for the whole cantilever can be written as

$$\begin{aligned} u &= w - \theta_c x , && 0 \leqq x \leqq z , \\ &= 0 , && z \leqq x \leqq \ell . \end{aligned} \tag{4.7}$$

The velocity is given by

$$\begin{aligned} \dot{u} &= \dot{w} - \dot{\theta}_c x , && 0 \leqq x \leqq z , \\ &= 0 , && z \leqq x \leqq \ell . \end{aligned} \tag{4.8}$$

From equation (4.8) it can be seen that there is a discontinuity or jump in the velocity field at $x = z$, shown in Fig. 4.5. The velocity at $x = z$,

$$\dot{u} = \dot{w} - \dot{\theta}_c z ,$$

can be equal to zero only if

$$\dot{z} = \frac{1}{\theta_c}\left(\dot{w} - z\dot{\theta}_c\right) = 0 .$$

This would imply that the cantilever is deforming in a fixed mode, i.e. there is no moving hinge.

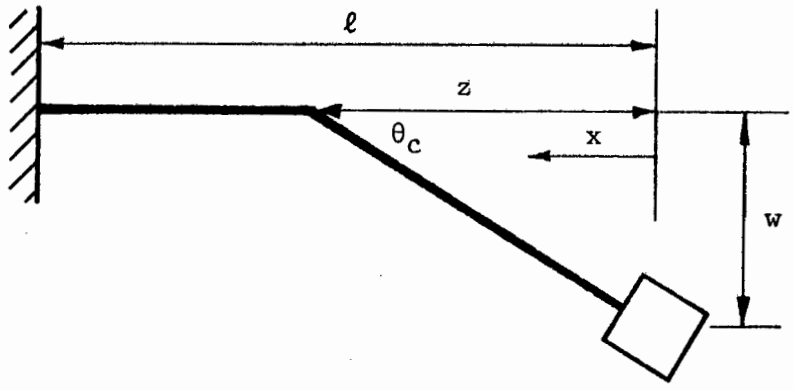

Fig. 4.4 : Displaced Shape of Cantilever

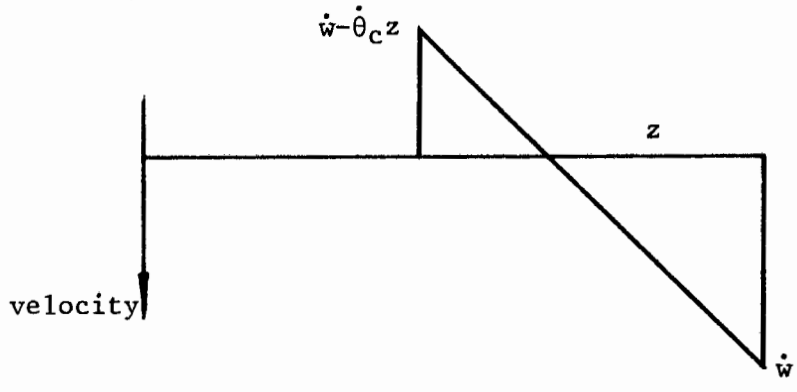

Fig. 4.5 : Velocity Field

The velocity discontinuity moving along the cantilever is equivalent to a shock front travelling through a medium. Consider Fig. 4.6 which shows the discontinuity which is travelling from right to left along the beam.

Shear strain is assumed to be negligible, and hence we may put

$$\phi = \frac{\partial u}{\partial x} \tag{4.9}$$

where ϕ is the rotation of the cross-section at any point. Rotating inertia is also ignored.

In the interval of time dt the shock moves from $z(t)$ to $z(t + dt)$, passing through an element of length dx. Conservation of linear moment for the element dx requires that

$$\left(S^+ - S^-\right)dt + mdx\left\{\frac{\partial u^+}{\partial t} - \frac{\partial u^-}{\partial t}\right\} = 0 , \tag{4.10}$$

or, where $[\,]$ denotes $(\,)^+ - (\,)^-$ and $\dot{z}dt = dx$,

$$[S] + m\dot{z}\left[\frac{\partial u}{\partial t}\right] = 0 . \tag{4.11}$$

Continuity of the displacement $u(z)$ requires that

$$\left[\frac{\partial u}{\partial t}\right] + \dot{z}\left[\frac{\partial u}{\partial x}\right] = 0 . \tag{4.12}$$

Substituting this into equation (4.11) gives

$$[S] = m\dot{z}^2\left[\frac{\partial u}{\partial x}\right] , \tag{4.13}$$

which can be written

$$[S] = m\dot{z}^2\,\theta_c \quad . \tag{4.14}$$

There will thus be a jump in S at the moving hinge.

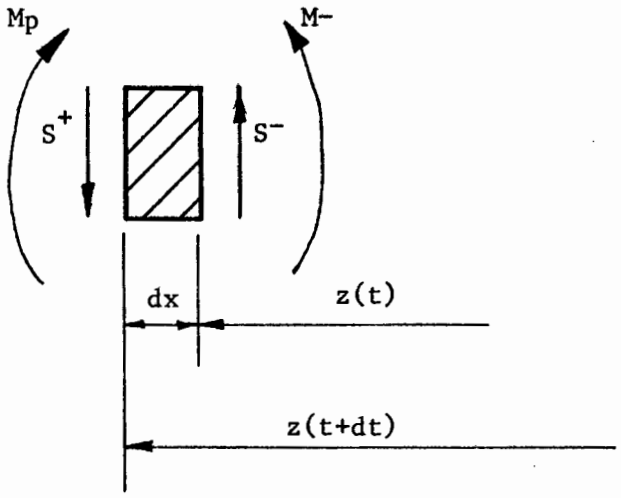

Fig. 4.6 : Shear Force Discontinuity

The equations of motion for the displaced configuration shown in Fig. 4.4 will be obtained using Lagrange's equations. With displacement variables w and θ_c, these equations are

$$\frac{d}{dt}\left\{\frac{\partial L}{\partial \dot{w}}\right\} - \frac{\partial L}{\partial w} = 0 \ , \tag{4.15}$$

$$\frac{d}{dt}\left\{\frac{\partial L}{\partial \dot{\theta}_c}\right\} - \frac{\partial L}{\partial \theta_c} = 0 \ , \tag{4.16}$$

where

$$L = K - V \ . \tag{4.17}$$

K denotes the kinetic energy of the beam and V the potential energy.

The kinetic energy is given by

$$K = \int_0^z \tfrac{1}{2} m \dot{u}^2 dx + \tfrac{1}{2} G \dot{u}^2 \ . \tag{4.18}$$

Using equation (4.6), this becomes

$$\begin{aligned} K &= \int_0^z \tfrac{1}{2} m \left(\dot{w} - \dot{\theta}_c x\right)^2 dx + \tfrac{1}{2} G \dot{w}^2 \\ &= \tfrac{1}{6} \frac{m}{\dot{\theta}_c}\left\{\dot{w}^3 - \left(\dot{w} - \dot{\theta}_c z\right)^3\right\} + \tfrac{1}{2} G \dot{w}^2 \ . \end{aligned} \tag{4.19}$$

The potential energy is the energy stored in the hinge and is given by

$$V = M_p \theta_c \ . \tag{4.20}$$

Using equation (4.17), equation (4.15) becomes

$$\frac{d}{dt}\left\{\frac{\partial K}{\partial \dot{w}}\right\} - \frac{d}{dt}\left\{\frac{\partial V}{\partial \dot{w}}\right\} - \frac{\partial K}{\partial w} + \frac{\partial V}{\partial w} = 0 \ , \tag{4.21}$$

and similarly equation (4.16) becomes

$$\frac{d}{dt}\left\{\frac{\partial K}{\partial \dot{\theta}_c}\right\} - \frac{d}{dt}\left\{\frac{\partial V}{\partial \dot{\theta}_c}\right\} - \frac{\partial K}{\partial \theta_c} + \frac{\partial V}{\partial \theta_c} = 0 \ . \tag{4.22}$$

Substituting the expressions for K and V , we can evaluate the derivatives required in equation (4.21).

$$\frac{d}{dt}\left\{\frac{\partial K}{\partial \dot{w}}\right\} = m\ddot{w}z - \tfrac{1}{2}m\ddot{\theta}_c z^2 + G\ddot{w} - m\theta_c\dot{z}^2 \ , \tag{4.23}$$

where

$$z = \frac{w}{\theta_c} \ ,$$

$$\dot{z} = \frac{1}{\theta_c}\left(\dot{w} - \dot{\theta}_c z\right) \ ,$$

$$\frac{\partial K}{\partial w} = \tfrac{1}{2}m\theta_c\dot{z}^2 \ , \tag{4.24}$$

$$\frac{d}{dt}\left\{\frac{\partial V}{\partial \dot{w}}\right\} = \frac{\partial V}{\partial w} = 0 \ . \tag{4.25}$$

Thus, substituting into equation (4.21), we find

$$\frac{d}{dt}\left\{\frac{\partial L}{\partial \dot{w}}\right\} - \frac{\partial L}{\partial w} = \left(mz + G\right)\ddot{w} - \tfrac{1}{2}mz^2\ddot{\theta}_c + \tfrac{1}{2}m\theta_c\dot{z}^2 = 0 \ . \tag{4.26}$$

Similarly, substituting the expressions for K and V , we can evaluate the derivatives required in equation (4.22).

$$\frac{d}{dt}\left\{\frac{\partial K}{\partial \dot{\theta}_c}\right\} = \tfrac{1}{3}m\ddot{\theta}_c z^3 - \tfrac{1}{2}m\ddot{w}z^2 - mz\theta_c\dot{z}^2 \ , \tag{4.27}$$

$$\frac{\partial K}{\partial \theta_c} = -\tfrac{1}{2}mz\theta_c\dot{z}^2 \ , \tag{4.28}$$

$$\frac{d}{dt}\left\{\frac{\partial V}{\partial \dot{\theta}}\right\} = 0 \ , \tag{4.29}$$

$$\frac{\partial V}{\partial \theta_c} = +M_p \ . \tag{4.30}$$

Thus, substituting into equation (4.22), we find

$$\frac{d}{dt}\left\{\frac{\partial L}{\partial \dot{\theta}_c}\right\} - \frac{\partial}{\partial \theta_c} = \tfrac{1}{3}m\ddot{\theta}_c z^3 - \tfrac{1}{2}m\ddot{w}z^2 - \tfrac{1}{2}mz\theta_c\dot{z}^2 + M_p = 0 \ . \tag{4.31}$$

The holonomic model is a model of a reversible elastic material, and hence the equations of motion must also lead to conservation of energy. This provides a means of checking the equations. The total energy in the system is given by

$$\begin{aligned} E_T &= K + V \\ &= \tfrac{1}{6}\frac{m}{\dot\theta_c}\left\{\dot w^3 - \left(\dot w - \dot\theta_c z\right)^3\right\} + \tfrac{1}{2}G\dot w^2 + M_p\theta_c \ , \\ &= \tfrac{1}{2}m\dot w^2 z - \tfrac{1}{2}m\dot w\dot\theta_c z^2 + \tfrac{1}{6}m\dot\theta_c^2 z^3 + \tfrac{1}{2}G\dot w^2 + M_p\theta_c \ . \end{aligned} \tag{4.32}$$

The rate of change of energy is

$$\begin{aligned} \frac{dE_T}{dt} &= mz\ddot w\dot w + \tfrac{1}{2}m\dot w^2\dot z - \tfrac{1}{2}m\ddot w\dot\theta_c z^2 - \tfrac{1}{2}m\dot w\ddot\theta_c z^2 \\ &\quad - \tfrac{1}{2}m\dot w\dot\theta_c\cdot 2z\dot z + \tfrac{1}{6}m2\dot\theta_c\ddot\theta_c z^3 + \tfrac{1}{6}m\dot\theta_c^2\cdot 3z^2\dot z + \tfrac{1}{2}G\dot w\cdot 2\ddot w + M_p\dot\theta_c \ , \\ &= \tfrac{1}{2}m\left(\dot w - \dot\theta_c z\right)^2\dot z + \left\{mz\ddot w - \tfrac{1}{2}mz^2\ddot\theta_c + G\ddot w\right\}\dot w \\ &\quad + \left\{\tfrac{1}{3}m\ddot\theta_c z^3 - \tfrac{1}{2}m\ddot w z^2 + M_p\right\}\dot\theta_c \ . \end{aligned} \tag{4.33}$$

Equations (4.26) and (4.31) are now substituted into equation (4.33) to give

$$\begin{aligned} &= \tfrac{1}{2}m\left(\dot w - \dot\theta_c z\right)^2\dot z + \left\{-\tfrac{1}{2}m\theta_c\dot z^2\right\}\dot w + \left\{+\tfrac{1}{2}mz\theta_c\dot z^2\right\}\dot\theta_c \ , \\ &= \tfrac{1}{2}m\theta_c^2\dot z^3 - \tfrac{1}{2}m\theta_c^2\dot z^3 \ , \\ &= 0 \ , \end{aligned}$$

where

$$\dot z = \frac{1}{\theta_c}\left(\dot w - \dot\theta_c z\right) \ .$$

It follows then that the energy is constant, as we expect for this freely moving system.

Referring back to equation (4.14), the shear force diagram of the cantilever will have a positive jump at the moving hinge of magnitude given by equation (4.14).

The shear force at the support, as shown in the freebody diagram in Fig. 4.7, will be given by the rate of change in linear momentum. The linear momentum L_M of the cantilever is

$$L_M = \int_0^{\ell} m\dot{u}dx + G\dot{u} ,$$

$$= \int_0^{z} m\left(\dot{w} - \dot{\theta}_c x\right)dx + G\dot{w} ,$$

$$= (mz + G)\dot{w} - \tfrac{1}{2}m\dot{\theta}_c z^2 \quad . \tag{4.34}$$

Thus

$$\frac{dL_M}{dt} = (mz + G)\ddot{w} + m\dot{z}\dot{w} - \tfrac{1}{2}m\ddot{\theta}_c z^2 - m\dot{\theta}_c z\dot{z} ,$$

$$= (mz + G)\ddot{w} - \tfrac{1}{2}mz^2\ddot{\theta}_c + m\theta_c\dot{z}^2 . \tag{4.35}$$

Substituting equation (4.26) into (4.35) gives

$$\frac{dL_M}{dt} = \tfrac{1}{2}m\theta_c\dot{z}^2 . \tag{4.36}$$

This is half of the value given by equation (4.14). The shear force diagram will thus be as shown in Fig. 4.8. The $\frac{1}{2}m\theta_c\dot{z}^2$ term can also be seen in equations (4.26) and (4.31).

Equations (4.26) and (4.31) must now be solved for the two unknowns, $\ddot{w}$ and $\ddot{\theta}_c$. This is done by rearranging the equations as follows -

$$mz + G\ddot{w} - \tfrac{1}{2}mz^2\ddot{\theta}_c = -\tfrac{1}{2}m\theta_c\dot{z}^2 ,$$

$$-\tfrac{1}{2}mz^2\ddot{w} + \tfrac{1}{3}mz^3\ddot{\theta}_c = +\tfrac{1}{2}m\theta_c z\dot{z}^2 - M_p . \tag{4.37}$$

The solution is

$$\ddot{w} = \frac{mz\theta_c\dot{z}^2 - 6M_p}{z(mz + 4G)} , \tag{4.38}$$

$$\ddot{\theta} = \frac{mz\theta_c\dot{z}^2\left(\frac{1}{4}mz + \frac{1}{2}G\right) - M_p(mz + G)}{\frac{1}{3}mz^3\left(\frac{1}{4}mz + G\right)} . \tag{4.39}$$

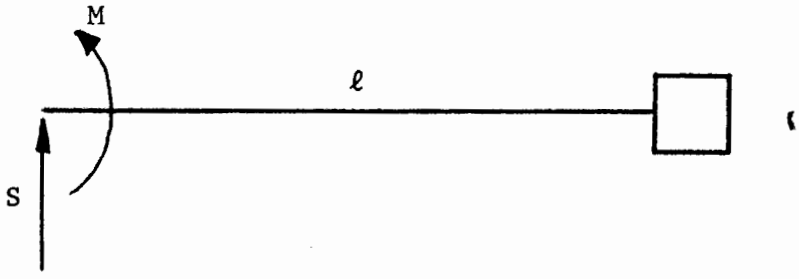

Fig. 4.7 : Free Body Diagram

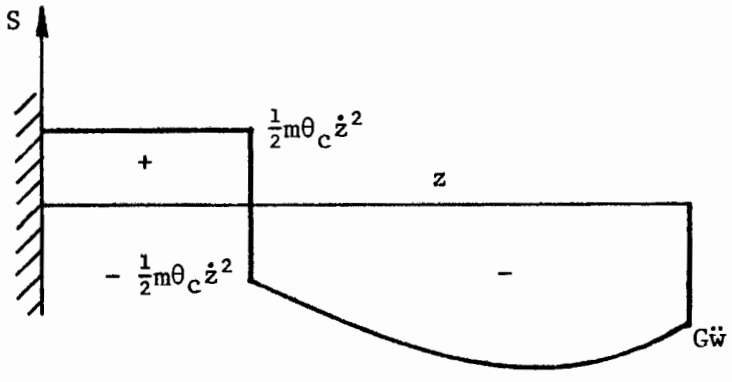

Fig. 4.8 : Shear Force Diagram

In dimensionless form, these equations are

$$\ddot{\bar{w}} = \frac{\beta\bar{z}\theta_c\dot{\bar{z}}^2 - 6}{\bar{z}\,(\beta\bar{z} + 4)}\,, \tag{4.40}$$

$$\ddot{\theta}_c = \frac{\frac{1}{2}\beta\bar{z}\theta_c\dot{\bar{z}}^2\left(\frac{1}{2}\beta\bar{z} + 1\right) - \left(\beta\bar{z} + 1\right)}{\frac{1}{3}\beta\bar{z}^3\left(\frac{1}{4}\beta + 1\right)}\,, \tag{4.41}$$

where

$$\beta = \frac{m\ell}{G}\,,$$

$$\bar{z} = \frac{z}{\ell}\,,$$

$$\bar{\theta}_c = \theta_c\,,$$

$$\tau = \sqrt{\frac{M_p}{G\ell^2}}.t\,,$$

$$\bar{w} = \frac{w}{\ell}\,. \tag{4.42}$$

The bending moment diagram is shown in Fig. 4.9. Its shape can be deduced from the acceleration diagram (Fig.4.10) and the shear force diagram (Fig. 4.8). In the rigid region the moment increases from $-M_p$ at the moving hinge to a value

$$-M_p + \tfrac{1}{2}m\theta_c\dot{z}^2(\ell - z)$$

at the support. Evidently, when

$$\tfrac{1}{2}m\theta_c\dot{z}^2(\ell - z) = 2M_p \tag{4.43}$$

a second hinge may form at the support, and the equations of motion derived from phase two are no longer valid.

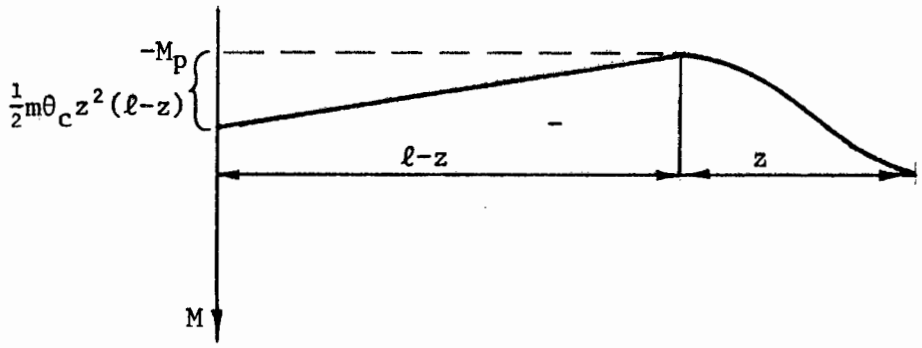

Fig. 4.9 : Bending Moment Diagram

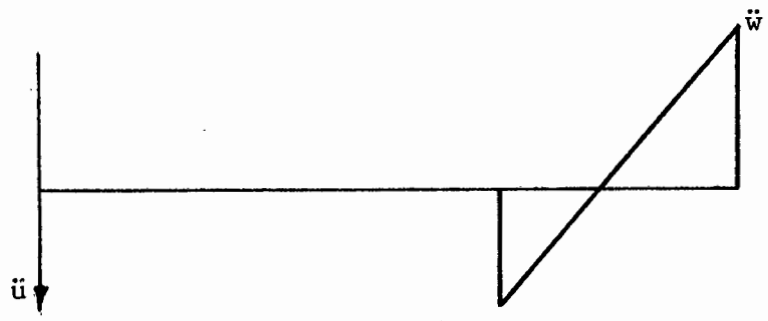

Fig. 4.10 : Acceleration Field

4.4 THE THIRD PHASE

At the end of phase two an additional hinge forms at the support; the rotation of this hinge will be denoted by θ . In the third phase we assume that there will be a fixed hinge at the support and a moving hinge in the beam. The displaced shape is shown in Fig. 4.11. We choose as the displacement variables the tip displacement w and the hinge rotations θ , θ_c . The distance, z , between the centre hinge θ_c and the tip, is given by

$$z = \left\{\frac{w - \theta\ell}{\theta_c}\right\} \tag{4.44}$$

and the centre hinge velocity, $\dot{z}$, is given by

$$\dot{z} = \frac{1}{\theta_c}\left(\dot{w} - \dot{\theta}\ell - \dot{\theta}_c z\right) . \tag{4.45}$$

The transverse displacement of the cantilever, referring to Fig. is given by

$$\begin{aligned} u(x,t) &= \left(\theta + \theta_c\right)(\ell - x) - \left\{\left(\theta + \theta_c\right)\ell - w\right\} , \\ &= w - \left(\theta + \theta_c\right) \qquad 0 \leqq x \leqq z \\ u(x,t) &= \theta(\ell - x) \qquad z \leqq x \leqq \ell . \end{aligned} \tag{4.46}$$

The velocity is given by

$$\begin{aligned} \dot{u}(x,t) &= \dot{w} - \left(\dot{\theta} + \dot{\theta}_c\right)x \qquad 0 \leqq x \leqq z \\ &= \dot{\theta}(\ell - x) \qquad z \leqq x \leqq \ell . \end{aligned} \tag{4.47}$$

The equations of motion for this phase will be obtained, as in phase two, by using Lagrange's equations;

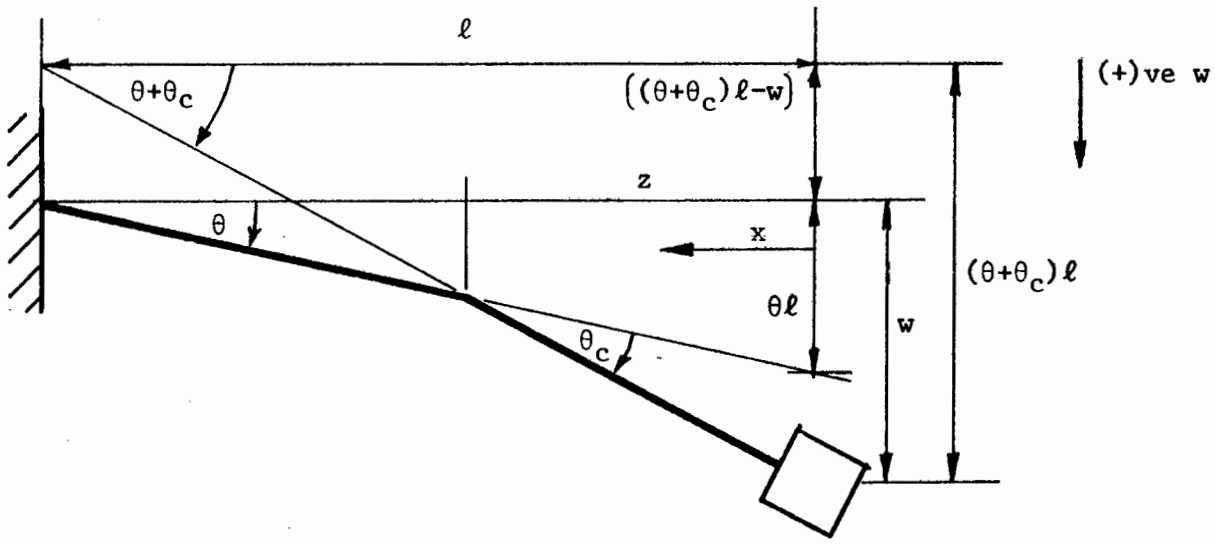

Fig. 4.11 : Displaced Shape of Cantilever

$$\frac{d}{dt}\left\{\frac{\partial L}{\partial \dot{\theta}}\right\} - \frac{\partial L}{\partial \theta} = 0 \quad , \tag{4.48}$$

$$\frac{d}{dt}\left\{\frac{\partial L}{\partial \dot{\theta}_c}\right\} - \frac{\partial L}{\partial \theta_c} = 0 \quad , \tag{4.49}$$

$$\frac{d}{dt}\left\{\frac{\partial L}{\partial \dot{w}}\right\} - \frac{\partial L}{\partial w} = 0 \quad , \tag{4.50}$$

where

$$L = K - V \quad . \tag{4.51}$$

The kinetic energy of the cantilever is given by

$$K = \int_0^{\ell} \tfrac{1}{2} m \dot{u}^2 dx + \tfrac{1}{2} G \dot{u}^2 \quad . \tag{4.52}$$

Substituting equation (4.51), we have

$$K = \int_0^z \tfrac{1}{2} m \left\{\dot{w} - (\dot{\theta} + \dot{\theta}_c)x\right\}^2 dx + \int_z^{\ell} \tfrac{1}{2} m \left\{\dot{\theta}(\ell - x)\right\}^2 dx + \tfrac{1}{2} G \dot{w}^2 \quad ,$$

$$= \tfrac{1}{2} m z \dot{w}^2 - \tfrac{1}{2} m z^2 (\dot{\theta}+\dot{\theta}_c)\dot{w} + \tfrac{1}{6} m z^3 (\dot{\theta}+\dot{\theta}_c)^2 + \tfrac{1}{6} m (\ell - z)^3 \dot{\theta}^2 + \tfrac{1}{2} G \dot{w}^2 \quad . \tag{4.53}$$

The potential energy of the cantilever is given by

$$V = M_p|\theta| + M_p|\theta_c| \quad , \tag{4.54}$$

as θ and θ_c can have positive or negative values.

Equation (4.53) and (4.54) are now substituted into equation (4.48),

$$\frac{d}{dt}\left\{\frac{\partial K}{\partial \dot{\theta}}\right\} = -\tfrac{1}{2} m (2z\dot{z}\dot{w} + z^2 \ddot{w}) + m z^2 \dot{z}(\dot{\theta}+\dot{\theta}_c) + \tfrac{1}{3} m z^3 (\ddot{\theta}+\ddot{\theta}_c) + \tfrac{1}{3} m \ddot{\theta} (\ell - z)^3 + m \dot{\theta} (\ell - z)^2 (-\dot{z}) \tag{4.55}$$

$$\frac{\partial K}{\partial \theta} = \tfrac{1}{2} m \dot{w}^2 \left\{-\frac{\ell}{\theta_c}\right\} - m z \left\{-\frac{\ell}{\theta_c}\right\}(\dot{\theta}+\dot{\theta}_c) + \tfrac{1}{2} m (\dot{\theta}+\dot{\theta}_c)^2 z^2 \left\{-\frac{\ell}{\theta_c}\right\} + \tfrac{1}{2} m \dot{\theta}^2 (\ell - z)^2 \frac{\ell}{\theta_c}$$

$$= -\tfrac{1}{2} m \frac{\ell}{\theta_c} \left\{\dot{w} - (\dot{\theta} + \dot{\theta}_c) z\right\}^2 + \tfrac{1}{2} m \theta^2 (\ell - z)^2 \frac{\ell}{\theta_c} \tag{4.56}$$

$$\frac{\partial V}{\partial \theta} = M_p \operatorname{sgm} \theta \tag{4.57}$$

where sgmθ denotes the following

$$\text{sgm}\theta = +1 \quad \text{for} \quad \theta > 0$$

and

$$\text{sgm}\theta = -1 \quad \text{for} \quad \theta < 0 .$$

$$\frac{d}{dt}\frac{\partial V}{\partial \dot{\theta}} = 0 . \tag{4.58}$$

Hence

$$\frac{d}{dt}\left\{\frac{\partial L}{\partial \dot{\theta}}\right\} - \frac{\partial L}{\partial \theta} = -\tfrac{1}{2}mz^2\ddot{w} + \tfrac{1}{3}mz^3\left(\ddot{\theta} + \ddot{\theta}_c\right) + \tfrac{1}{3}m(\ell - z)^3\ddot{\theta} + M_p\text{sgm}\theta$$
$$+ \left\{mz^2\left(\dot{\theta} + \dot{\theta}_c\right) - mz\dot{w} - m(\ell - z)^2\dot{\theta}\right\}\dot{z} + \tfrac{1}{2}m\frac{\ell}{\theta_c}\left\{\dot{w} - \left(\dot{\theta} + \dot{\theta}_c\right)z\right\}^2$$
$$- \tfrac{1}{2}m\frac{\ell}{\theta_c}(\ell - z)^2\dot{\theta}^2 = 0 . \tag{4.59}$$

Similarly equation (4.53) and (4.54) are substituted into equation (4.49)

$$\frac{d}{dt}\left\{\frac{\partial K}{\partial \dot{\theta}_c}\right\} = -\tfrac{1}{2}m\left(2z\dot{z}\dot{w} + z^2\ddot{w}\right) + mz^2\dot{z}\left(\dot{\theta} + \dot{\theta}_c\right) + \tfrac{1}{3}mz^3\left(\ddot{\theta} + \ddot{\theta}_c\right) \tag{4.60}$$

$$\frac{\partial K}{\partial \theta_c} = \tfrac{1}{2}m\dot{w}^2\left\{\frac{-z}{\theta_c}\right\} - mz\left\{\frac{-z}{\theta_c}\right\}\left(\theta+\theta_c\right)\dot{w} + \tfrac{1}{2}m\left(\dot{\theta}+\dot{\theta}_c\right)^2z^2\left\{\frac{-z}{\theta_c}\right\} + \tfrac{1}{2}m\dot{\theta}^2(\ell-z)^2\left\{\frac{z}{\theta_c}\right\}$$

$$\frac{\partial V}{\partial \theta_c} = M_p\text{sgm} \tag{4.61}$$

$$\frac{d}{dt}\left\{\frac{\partial V}{\partial \dot{\theta}_c}\right\} = 0 . \tag{4.62}$$

Hence

$$\frac{d}{dt}\left\{\frac{\partial L}{\partial \dot{\theta}_c}\right\} - \frac{\partial}{\partial \theta_c} = -mz\dot{z}\dot{w} - \tfrac{1}{2}mz^2\ddot{w} + mz^2\left(\dot{\theta}+\dot{\theta}_c\right)\dot{z} + \tfrac{1}{3}mz^3\left(\ddot{\theta}+\ddot{\theta}_c\right) + M_p\text{sgm}\theta_c$$
$$+ \tfrac{1}{2}m\left\{\frac{z}{\theta_c}\right\}\left\{\dot{w} - \left(\dot{\theta} + \dot{\theta}_c\right)z\right\}^2 - \tfrac{1}{2}m\dot{\theta}^2(\ell - z)^2\left\{\frac{z}{\theta_c}\right\} = 0 . \tag{4.63}$$

Similarly equations (4.53) and (4.54) are substituted into equation (4.50)

$$\frac{d}{dt}\left\{\frac{\partial K}{\partial \dot{w}}\right\} = m(\ddot{w}z + \dot{w}\dot{z}) - m\dot{z}\dot{z}\left(\dot{\theta} + \dot{\theta}_c\right) - \tfrac{1}{2}mz^2\left(\ddot{\theta} + \ddot{\theta}_c\right) + G\ddot{w} \tag{4.64}$$

$$\frac{\partial K}{\partial w} = \tfrac{1}{2}m\left\{\frac{1}{\theta_c}\right\}\left\{\dot{w} - \left(\dot{\theta} + \dot{\theta}_c\right)z\right\}^2 - \tfrac{1}{2}m\left\{\frac{1}{\theta_c}\right\}(\ell - z)^2\dot{\theta}^2 \tag{4.65}$$

$$\frac{d}{dt}\left\{\frac{\partial V}{\partial \dot{w}}\right\} = 0 \tag{4.66}$$

$$\frac{\partial V}{\partial w} = 0 \, . \tag{4.67}$$

Hence

$$\frac{d}{dt}\left\{\frac{\partial L}{\partial \dot{w}}\right\} - \frac{\partial L}{\partial w} = (mz + G)\ddot{w} - \tfrac{1}{2}mz^2\left(\ddot{\theta} + \ddot{\theta}_c\right) + m\dot{w}\dot{z} - mz\left(\dot{\theta} + \dot{\theta}_c\right)\dot{z}$$

$$- \tfrac{1}{2}m\left\{\frac{1}{\theta_c}\right\}\left\{\dot{w} - \left(\dot{\theta} + \dot{\theta}_c\right)z\right\}^2 + \tfrac{1}{2}m\left\{\frac{1}{\theta_c}\right\}(\ell - z)^2\dot{\theta}^2 = 0 \, . \tag{4.66}$$

As in Section 4.3, the equations of motion for phase three are checked by verifying conservation of energy. The total energy in the system using equations (4.53) and (4.54) is given by

$$E_T = K + V$$

$$= \tfrac{1}{2}mz\dot{w}^2 - \tfrac{1}{2}mz^2\dot{w}\left(\dot{\theta} + \dot{\theta}_c\right) + \tfrac{1}{6}mz^3\left(\dot{\theta} + \dot{\theta}_c\right)^2 + \tfrac{1}{6}m(\ell - z)^3\dot{\theta}^2$$

$$+ \tfrac{1}{2}G\dot{w}^2 + M_p\left\{|\theta| + |\theta_c|\right\} \, . \tag{4.67}$$

The rate of change of energy is

$$\frac{dE_T}{dt} = \left\{\tfrac{1}{3}m(\ell - z)^3\ddot{\theta} - \tfrac{1}{2}mz^2\ddot{w} + \tfrac{1}{3}mz^3\left(\ddot{\theta} + \ddot{\theta}_c\right) + Mpsgm\theta\right\}\dot{\theta}$$

$$+ \left\{\tfrac{1}{3}mz^3\left(\ddot{\theta} + \ddot{\theta}_c\right) - \tfrac{1}{2}mz^2\ddot{w} + M_psgm\theta_c\right\}\dot{\theta}_c$$

$$+ \left\{(G + mz)\ddot{w} - \tfrac{1}{2}mz^2\left(\ddot{\theta} + \ddot{\theta}_c\right)\right\}\dot{w}$$

$$+ \left\{-m\left\{\dot{w} - \left(\dot{\theta} + \dot{\theta}_c\right)z\right\}^2 - \tfrac{1}{2}m(\ell - z)^2\dot{\theta}^2\right\}\dot{z} \tag{4.68}$$

Substituting equations (4.59), (4.63) and (4.66) into (4.68) we have

$$\frac{dE_T}{dt} = \left\{\left\{mz\left(\dot{z}_2\right) + m(\ell-z)^2\dot{\theta}\right\}\dot{z} + -m\frac{\ell}{\theta_c}\left\{(\ell-z)^2\dot{\theta}^2 - \left(\dot{z}_2\right)^2\right\}\right\}\dot{\theta}$$

$$+ \left\{mz\left(\dot{z}_2\right)\dot{z} + \tfrac{1}{2}m\frac{z}{\theta_c}\left\{(\ell-z)^2\dot{\theta}^2-\left(\dot{z}_2\right)^2\right\}\right\}\dot{\theta}_c+\left\{\tfrac{1}{2}m\frac{1}{\theta_c}\left\{\left(\dot{z}_2\right)^2-(\ell-z)^2\dot{\theta}^2\right\}-m\dot{z}\left(\dot{z}_2\right)\right\}\dot{w}$$

$$+ \left\{\tfrac{1}{2}m\left\{\left(\dot{z}_2\right)^2 - (\ell-z)^2\dot{\theta}^2\right\}\right\}\dot{z}$$

$$= m\dot{z}\left\{(\ell-z)^2\dot{\theta}^2-\left(\dot{z}_2\right)^2\right\} + \tfrac{1}{2}m\dot{z}\left\{\left(\dot{z}_2\right)^2-(\ell-z)^2\dot{\theta}^2\right\} + \tfrac{1}{2}m\dot{z}\left\{\left(\dot{z}_2\right)^2-(\ell-z)^2\dot{\theta}^2\right\} ,$$

and hence

$$\frac{dE_T}{dt} = 0 , \tag{4.69}$$

where

$$\dot{z} = \frac{1}{\theta_c}\left\{\dot{w} - \dot{\theta}\ell - \dot{\theta}_c z\right\} , \tag{4.70}$$

$$\dot{z}_2 = \left\{\dot{w} - \left(\dot{\theta} + \dot{\theta}_c\right)z\right\} . \tag{4.71}$$

It follows that the energy in phase three is constant.

The equations of motion must now be solved for the accelerations $\ddot{\theta}$, $\ddot{\theta}_c$ and $\ddot{w}$. Rearranging equations (4.59), (4.63) and (4.66), we have

$$\tfrac{1}{3}m\left\{z^3 + (\ell-z)^3\right\}\ddot{\theta} + \tfrac{1}{3}mz^3\ddot{\theta}_c - \tfrac{1}{2}mz^2\ddot{w} = - M_p sgm\theta$$

$$- \left\{mz^2\left(\dot{\theta}+\dot{\theta}_c\right)-mz\dot{w}-m(\ell-z)^2\dot{\theta}\right\}\dot{z} - \tfrac{1}{2}m\left\{\frac{\ell}{\theta_c}\right\}\left\{\dot{w}-\left(\dot{\theta}+\dot{\theta}_c\right)z\right\}^2 + \tfrac{1}{2}m\frac{\ell}{\theta_c}(\ell-z)^2\dot{\theta}^2 , \tag{4.72}$$

$$\tfrac{1}{3}mz^3\ddot{\theta} + \tfrac{1}{3}mz^3\ddot{\theta}_c - \tfrac{1}{2}mz^2\ddot{w} = \left\{mz\dot{w} - mz^2\left(\dot{\theta} + \dot{\theta}_c\right)\right\}\dot{z} - M_p sgm\theta$$

$$- \tfrac{1}{2}m\frac{z}{\theta_c}\left\{\dot{w} - \left(\dot{\theta} + \dot{\theta}_c\right)z\right\}^2 + \tfrac{1}{2}m\frac{z}{\theta_c}(\ell - z)^2\dot{\theta}^2 , \tag{4.73}$$

$$- \tfrac{1}{2}mz^2\ddot{\theta} - \tfrac{1}{2}mz^2\ddot{\theta}_c + (mz + G)\ddot{w} = - m\left\{\dot{w} - z\left(\dot{\theta} + \dot{\theta}_c\right)\right\}\dot{z}$$

$$+ \tfrac{1}{2}m\left\{\frac{1}{\theta_c}\right\}\left\{\dot{w} - \left(\dot{\theta} + \dot{\theta}_c\right)z\right\}^2 - \tfrac{1}{2}m\left\{\frac{1}{\theta_c}\right\}(\ell - z)^2\dot{\theta}^2 . \tag{4.74}$$

Solving these equations, we find

$$\ddot{\theta} = \frac{(E + CG - HB)}{A} \quad , \tag{4.75}$$

$$\ddot{\theta}_c = \frac{\left\{F - \frac{BE}{A} - GC\left(\frac{B}{A} - 1\right)\right\}}{B\left(1 - \frac{B}{A}\right)} = H \quad , \tag{4.76}$$

$$\ddot{w} = \frac{\left\{P + \frac{CF}{B} - 2\frac{CE}{A}\right\}}{\left\{D - \frac{C^2}{B}\right\}} = G \quad , \tag{4.77}$$

where

$$A = \tfrac{1}{3}m\left(z^3 + (\ell - z)^3\right) \quad ,$$

$$B = \tfrac{1}{3}mz^3 \quad ,$$

$$C = \tfrac{1}{2}mz^2 \quad ,$$

$$D = mz + G \quad ,$$

$$E = - M_p sgm\theta + \left(mz\{\dot{z}_2\} + m(\ell-z)^2\dot{\theta}\right)\dot{z} + \tfrac{1}{2}m\frac{\ell}{\theta_c}\left((\ell-z)^2\dot{\theta}^2 - \{\dot{z}_2\}^2\right) \quad ,$$

$$F = - M_p sgm\theta_c + mz\{\dot{z}_2\}\dot{z} + \tfrac{1}{2}m\frac{z}{\theta_c}\left((\ell-z)^2\dot{\theta}^2 - \{\dot{z}_2\}^2\right) \quad ,$$

$$P = \tfrac{1}{2}m\frac{1}{\theta_c}\left(\{\dot{z}_2\}^2 - (\ell-z)^2\dot{\theta}^2\right) - m\left(\dot{z}_2\right)\dot{z} \quad ,$$

$$\dot{z}_2 = \left(\dot{w} - \{\dot{\theta} + \dot{\theta}_c\}z\right) \quad ,$$

$$\dot{z} = \frac{1}{\theta_c}\left(\dot{w} - \dot{\theta}\ell - \dot{\theta}_c z\right) \quad ,$$

$$z = \frac{1}{\theta_c}\left(w - \theta\ell\right) \quad . \tag{4.78}$$

Equation (4.75) can be simplified by substituting for H, i.e.

$$\ddot{\theta} = \frac{\left[E + CG - B\left\{\frac{F - \frac{BE}{A} - GC\left(\frac{B}{A} - 1\right)}{B\left(1 - \frac{B}{A}\right)}\right\}\right]}{A}$$

$$= \left\{\frac{E - F}{A - B}\right\} \quad . \tag{4.79}$$

Equation (4.76) is rearranged to give

$$\ddot{\theta}_c = \frac{\frac{A(F - E)}{(A - B)} + E + GC}{B} . \tag{4.80}$$

Equations (4.78), (4.79) and (4.77) together with equations (4.78) are now put in dimensionless form. Equations (4.78) become

$$\begin{aligned}
\bar{A} &= \tfrac{1}{3}\left(\bar{z}^3 + (1 - \bar{z})^3\right) , \\
\bar{B} &= \tfrac{1}{3}\bar{z}^3 , \\
\bar{C} &= \tfrac{1}{2}\bar{z}^2 , \\
\bar{D} &= \frac{1}{\beta} + \bar{z} , \\
\bar{E} &= -\mathrm{sgm}\theta + \beta\left(\bar{z}\{\dot{\bar{z}}_2\} + (1-\bar{z})^2\dot{\bar{\theta}}\right)\dot{\bar{z}} + \tfrac{1}{2}\beta\frac{1}{\bar{\theta}_c}\left((1-\bar{z})^2\dot{\bar{\theta}}^2 - \{\dot{\bar{z}}_2\}^2\right) , \\
\bar{F} &= -\mathrm{sgm}\theta_c + \beta\bar{z}\{\dot{\bar{z}}_2\}\dot{\bar{z}} + \tfrac{1}{2}\beta\frac{\bar{z}}{\bar{\theta}_c}\left((1-\bar{z})^2\dot{\bar{\theta}}^2 - \{\dot{z}_2\}^2\right) , \\
\bar{P} &= \tfrac{1}{2}\beta\frac{1}{\bar{\theta}_c}\left(\{\dot{\bar{z}}_2\}^2 - (1-\bar{z})^2\dot{\bar{\theta}}^2\right) - \beta\{\dot{\bar{z}}_2\}\dot{\bar{z}} , \\
\dot{\bar{z}}_2 &= \left(\dot{\bar{w}} - \{\dot{\bar{\theta}} + \dot{\bar{\theta}}_c\}\bar{z}\right) , \\
\dot{\bar{z}} &= \frac{1}{\bar{\theta}_c}\left(\dot{\bar{w}} - \dot{\bar{\theta}} - \dot{\bar{\theta}}_c\bar{z}\right) , \\
\bar{z} &= \frac{1}{\bar{\theta}_c}\left(\bar{w} - \bar{\theta}\right) .
\end{aligned} \tag{4.81}$$

Equations (4.78), (4.79) and (4.77), can then be written as

$$\ddot{\bar{\theta}} = \frac{\left(\bar{E} - \bar{F}\right)}{\beta\left(\bar{A} - \bar{B}\right)} , \tag{4.82}$$

$$\ddot{\bar{\theta}}_c = \frac{\frac{\bar{A}\left(\bar{F} - \bar{E}\right)}{\left(\bar{A} - \bar{B}\right)} + \bar{E} + G\bar{C}}{\beta\bar{B}} , \tag{4.83}$$

$$\ddot{\bar{w}} = \frac{\bar{P} + \frac{\bar{C}\,\bar{F}}{\bar{B}} - 2\frac{\bar{C}\,\bar{E}}{\bar{A}}}{\beta\left\{\bar{D} - \frac{\bar{C}^2}{\bar{B}}\right\}} , \tag{4.84}$$

where

$$\bar{z} = \frac{z}{\ell} \quad ,$$

$$\bar{w} = \frac{w}{\ell} \quad ,$$

$$\beta = \frac{m\ell}{G} \quad ,$$

$$\tau = \sqrt{\frac{M_p}{G\ell^2}} \cdot t \quad . \tag{4.85}$$

For $w > 0$, we consider two displacement configurations; the first is shown in Fig. 4.12, with the associated shear force and bending moment diagram, while the second is shown in Fig. 4.13.

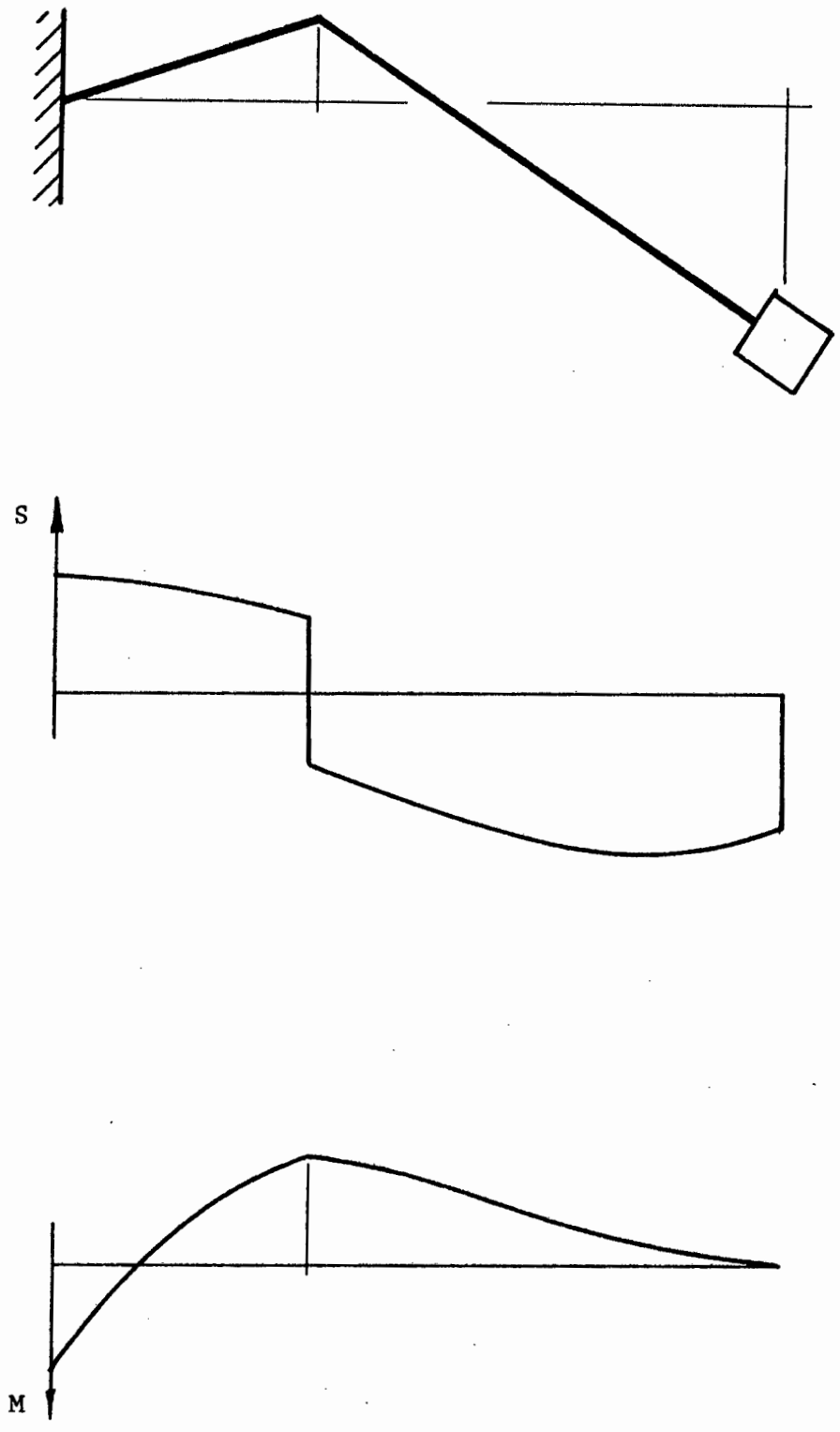

Fig. 4.12 : Displaced Configuration with Associated Shear Force and Bending Moment Diagrams

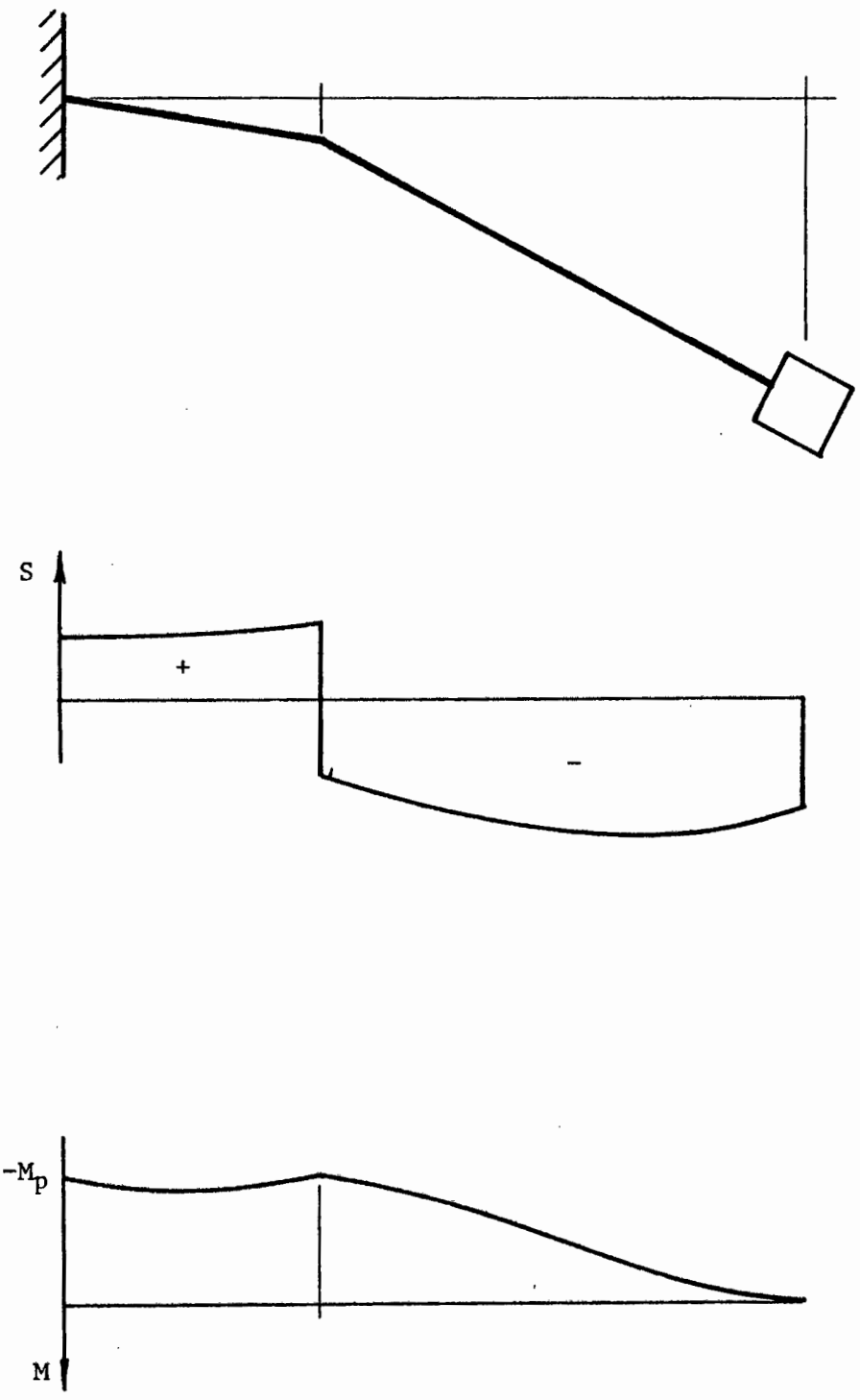

Fig. 4.13 : Displaced Configuration with Associated Shear Force and Bending Moment Diagrams

4.5 NUMERICAL ANALYSIS

In each of the phases for which we have formulated the equations of motion, the acceleration parameters which we denote by $\ddot{u}_i$, are given as functions of the velocity parameters $\dot{u}_i$ and the displacements u_i . Hence

$$\ddot{u}_i = \ddot{u}_i (\dot{u}_1 , u_1 , \dot{u}_2 , u_2 , \dot{u}_3 , u_3 , ...) . \tag{4.86}$$

These relations are written as first order equations by introducing

$$v_i = \dot{u}_i ,$$

and putting

$$\dot{v}_i = \dot{u}_i (\dot{u}_1 , u_1 , \dot{u}_2 , u_2 , ...) . \tag{4.87}$$

Numerical integration on the two sets of equations ,

$$\dot{u}_i = v_i , \tag{4.88}$$

$$\dot{v}_i = \ddot{u}_i (v , u , v , u , ...) , \tag{4.89}$$

can now be carried out. The equations are integrated using a fourth order six stage Runge-Kutta method (Lambert, 1973). The integration is done in two stages;

$$v_i^{t+h} = v_i^t + \frac{h}{6}\left\{k_1 + 4k_3 + k_4\right\} \tag{4.90}$$

where

$$\begin{aligned}
k_1 &= \ddot{u}_i \left\{v_1^t , u_1^t , v_2^t , u_2^t , ...\right\} \\
k_2 &= \ddot{u}_i \left\{v_1^t + \tfrac{1}{2}hk_1 , u_1^t + \tfrac{1}{2}hk , v_2^t + \tfrac{1}{2}hk_1 , ...\right\} \\
k_3 &= \ddot{u}_i \left\{v_1^t + \tfrac{1}{4}hk_1 + \tfrac{1}{4}hk_2 , u_1^t + \tfrac{1}{4}hk_1 + \tfrac{1}{4}hk_2 , v_2^t + \tfrac{1}{4}hk_1 + \tfrac{1}{4}hk_2 , ...\right\} \\
k_4 &= \ddot{u}_i \left\{v_1^t - hk_2 + 2hk_3 , u_1^t - hk_2 + 2hk_3 , v_2^t - .....\right\} \\
k_5 &= \ddot{u}_i \left\{v_1^t + \frac{h}{27}(7k_1+10k_2+k_4) , u_1^t + \frac{h}{27}(7k_1+10k_2+k_4) , v_2^t + ...\right\} \\
k_6 &= \ddot{u}_i \left\{v_1^t + \frac{h}{625}(28k_1-125k_2+546k_3+54k_4-378k_5) , u_1^t + \frac{h}{625}(...) , v_2^t ...\right\}
\end{aligned} \tag{4.91}$$

and

$$u_i^{t+h} = u_i^t + \frac{h}{6}\left\{k_1 + 4k_3 + k_4\right\} \tag{4.92}$$

where

$$\begin{aligned}
k_1 &= v_i^t \\
k_2 &= v_i^t + \tfrac{1}{2}hk_1 \\
k_3 &= v_i^t + \tfrac{1}{4}hk_1 + hk_2 \\
k_4 &= v_i^t - hk_2 + hk_3 \\
k_5 &= v_i^t + \frac{h}{27}\left\{7k_1 + 10k_2 + k_4\right\} \\
k_6 &= v_i^t + \frac{h}{625}\left\{28k_1 - 125k_2 + 546k_3 + 54k_4 - 378k_5\right\}
\end{aligned} \tag{4.93}$$

The estimate for the associated truncation error is

$$T_i^{t+h} = \frac{h}{336}\left\{-42k_1 - 224k_3 - 21k_4 + 162k_5 + 125k_6\right\} \tag{4.94}$$

Equations (4.40) and (4.41) and equations (4.82), (4.83) and (4.84) derived for phases two and three respectively are substituted into equation (4.91), along with values for v_1^t , u_1^t , v_2^t , u_2^t , ...

Considerable difficulty was encountered in carrying out the numerical integration of phase three. The difficulties may have either a physical or a mathematical origin, and this will be discussed in more detail shortly. However, care was taken to avoid conventional instabilities in the numerical integration process. The time step h was kept extremely small; it was set at the practical lower limit of 10^{-12} dimensionless units dictated by the fifteen significant figures available on the University of Cape Town Univac computer working in double precision. The equations were rearranged to avoid ill-conditioning. Nevertheless, a check on the total energy at each time step showed that the energy was not remaining constant, and hence that some inaccuracy was introduced.

An implicit Runge-Kutta routine, which iterates down to a predetermined error bound at each step, was tried, but with worse results. Predictor-Corrector methods were not considered, as they need at least four starting values which have to be generated using a Runge-Kutta or similar method. Another disadvantage is the fixed time step length; Runge-Kutta methods have the advantage that the time step length h can be increased or decreased depending on the error term (4.94). This can save a great deal of computation time.

As the integration progressed, the system lost or gained up to half its original energy, despite the precautions taken in the numerical analysis. In order to show results and to reveal the apparent sources of difficulty, it was decided to adjust the centre hinge rotation θ_c at each time step in such a way as to maintain the energy constant.

A number of examples were run on the computer and a typical case will be given as illustration. The calculation was carried out in terms of dimensionless values, which were obtained using the curves in Fig. 4.2;

$$\begin{aligned} \alpha &= 63 \quad , \\ \beta &= 1.0 \quad , \\ \bar{z}_o &= 0.1 \quad , \\ \bar{E}_T &= 18.90 \quad . \end{aligned} \tag{4.95}$$

Each of the three phases of motion must be considered separately.

Phase one comprises an acceleration in a fixed mode with a hinge, $\bar{\theta}_c$, at $\bar{z}_o$ from tip. The shape of the response curves are known and the end of phase values are calculated by hand using equation (4.2);

$$\begin{aligned} \bar{\theta}_c &= 3.0 \quad , \\ \dot{\bar{\theta}}_c &= 60.0 \quad , \\ \bar{w} &= 0.3 \quad , \\ \dot{\bar{w}} &= 6.0 \quad . \end{aligned} \tag{4.96}$$

The bending moment is constant from the hinge to the support and is equal to $-M_p$.

The response curves for phases two and three are obtained using the computer. The initial values for phase two are given by equation (4.96). The hinge $\overline{\theta}_c$ starts moving towards the support and the phase ends when the bending moment at the support reaches a value of $+M_p$. This happens when (cf. equation 4.43)

$$\tfrac{1}{2}m\theta_c\dot{z}^2(\ell - z) = 2M_p$$

where $\tfrac{1}{2}m\theta_c\dot{z}^2$ is the shear force at the hinge. A second hinge, $\overline{\theta}$, now forms at the support to initiate phase three. The hinge $\overline{\theta}_c$ moves from $\bar{z} = 0.100$ to $\bar{z} = 0.124$ during phase two and the displacements and velocities at the end of the phase are

$$\begin{aligned} \overline{\theta}_c &= 8.54 \ , \\ \dot{\overline{\theta}}_c &= 31.05 \ , \\ \bar{w} &= 1.06 \ , \\ \dot{\bar{w}} &= 5.83 \ . \end{aligned} \tag{4.97}$$

Phase three is a free motion phase with a periodic oscillation and a moving hinge $\overline{\theta}_c$. The initial conditions for this phase are given by equation (4.97) together with the additional conditions

$$\begin{aligned} \overline{\theta} &= 0.00 \ , \\ \dot{\overline{\theta}} &= 0.00 \ . \end{aligned} \tag{4.98}$$

Equations (4.82), (4.83) and (4.84) are dependent upon the sign of $\overline{\theta}$ and have to be changed whenever θ changes sign.

The numerical integration was terminated when the solution became unstable. The approaching instability can be quite clearly seen in the plots of $\dot{z}(t)$, in Fig. 4.14, and $\dot{\bar{v}}(t)$, the transverse velocity at the moving hinge, in Fig. 4.15. The tip velocity $\dot{\bar{w}}(t)$, also shown in Fig. 4.15, behaves quite smoothly.

The pattern in phase three can thus be seen to be made up of an oscillation of the central hinge imposed on a more or less monotonic overall motion involving a rotation above the fixed end and a decrease

on tip velocity. This accords with the pattern of behaviour found in the two mass approximation in Chapter 2, and can be anticipated. What is not anticipated, however, is the increasing frequency and amplitude of the superimposed oscillatory motion, leading finally to a breakdown of the numerical integration procedure.

Purely numerical problems, as opposed to physical sources of instability, cannot be totally eliminated as the origin of the breakdown of the equations. However, considerable care was taken with these equations, and Figs. 4.14 and 4.15 are the results of an integration involving a number of time steps lying between 10^6 and 10^7. It must also be considered that the source of the difficulty is physical, and that a more detailed analytical study of the problem is required.

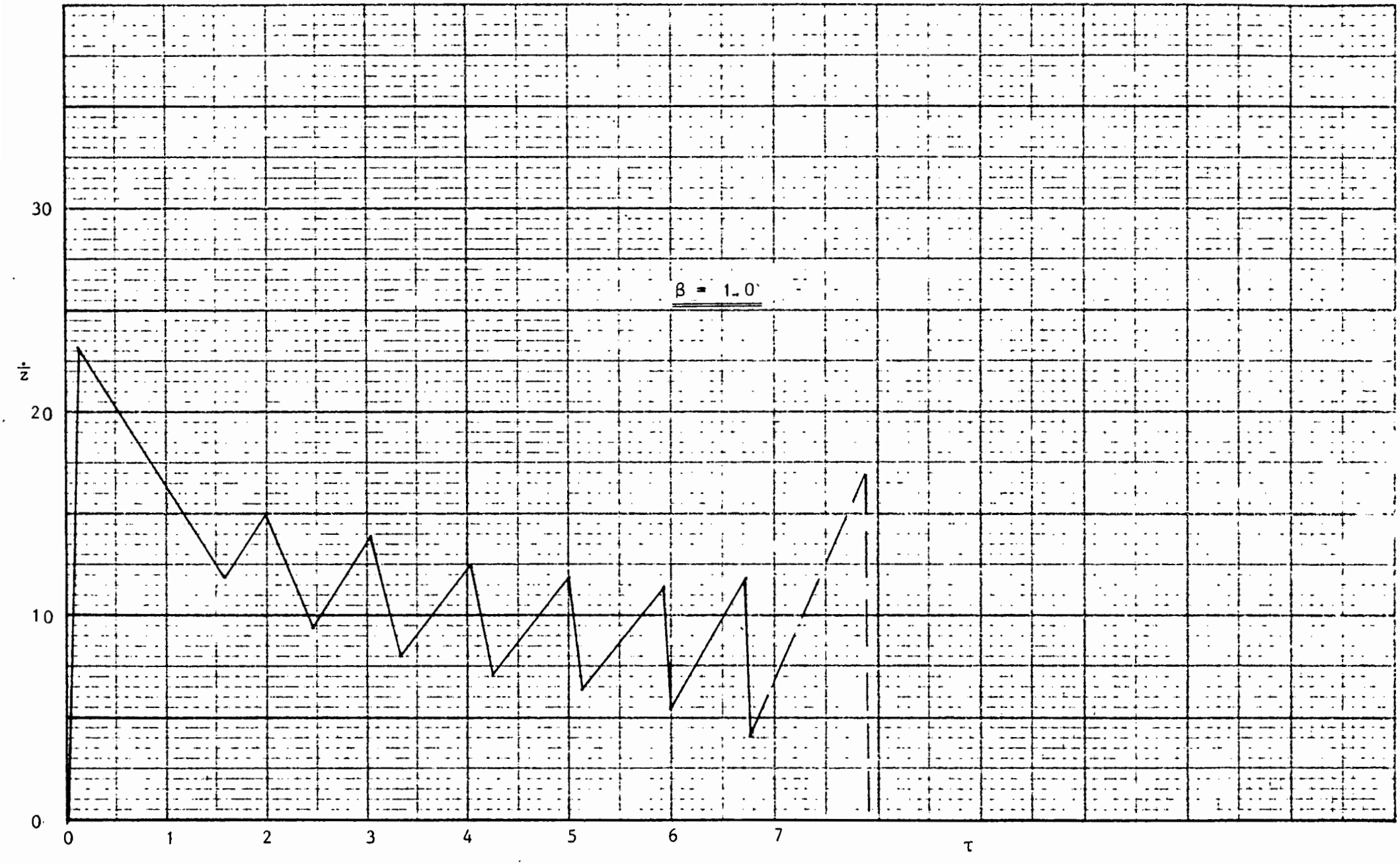

Fig. 4.14.

Fig. 4.15.

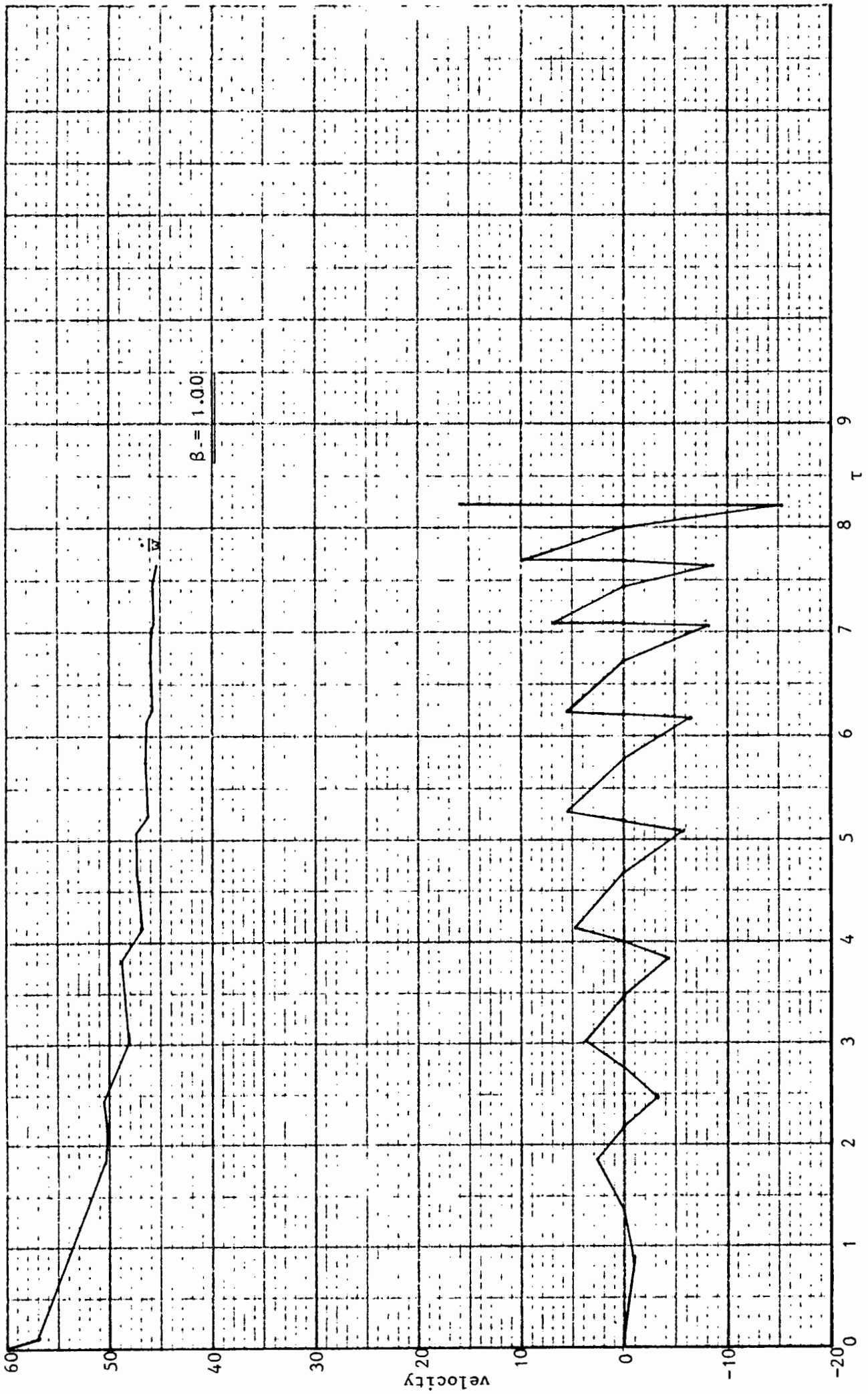

CHAPTER 5.

CONCLUSIONS

In the sequence of arguments set out in Chapter 1, we have been led in this thesis to the study of a holonomic rigid-plastic structure subjected to dynamic loading in order to assess whether such a material model could be useful in producing approximate solutions to more realistic problems. To the knowledge of the writer, dymanic analysis with this material model has not been previously attempted, and the study has thus involved aspects of behaviour which are fundamentally different from non-holonomic dynamic behaviour.

The analysis of a two mass model was carried out successfully, and this would seem to indicate that more complex lump mass models can, in principle, also be handled. In the case of a continuous mass distribution, however, several new factors appeared. A travelling hinge in the holonomic case introduced new kinds of discontinuities, particularly the jump in shear force which is markedly different from the non-holonomic case. The instability in the equations discussed in the previous chapter may well be simply our inability to handle the equations; however, we have shown a distinct and steady increase in the frequency of the oscillation which leads finally to the breakdown, and this could also indicate a physical factor leading to instability.

It must be concluded, then, that our understanding of the analysis of the holonomic version of Parkes's problem is not complete. From a purely fundamental point of view, there would seem to be merit in continuing this study in order to resolve the problems encountered, and to fully understand the holonomic analysis of dynamically loaded rigid-plastic structures. It is very clear, however, that holonomic behaviour is far more complicated than non-holonomic behaviour, and we can assert quite categorically that the introduction of deformation theory in dynamic problems of this type will not lead to a simplification or an easy approximate method of solution.

6.1 BIBLIOGRAPHY

R. Courant & D. Hilbert, *Methods of Mathematical Physics*, Vol. 1, Interscience, 1953.

E.W. Parkes, "The Permanent Deformation of a Cantilever Struck Transversely at its Tip", *Proc. Roy. Soc.*, London, 228 (Series A), 462, 1954.

J.D. Lambert, *Computational Methods in Ordinary Differential Equations*, John Wiley and Sons, 1973.

M. Taya & T. Mura, "Dynamic Plastic Behaviour of Structures under Impact Loading investigated by the Extended Hamilton's Principle", *Int. J. Solids & Structures*, 10, 197, 1974.

J.B. Martin, "Extremal Principles and Convergence in Plastic Structural Dynamics", Lecture series on *Dynamics of Plastic Structures*, CISM, Udine, September, 1979.

P.S. Symonds, "Approximation Techniques for Impulsively Loaded Plastic Structures", Lecture series on *Dynamics of Plastic Structures*, CISM, Udine, September, 1979.

7.1 APPENDIX

COURSE	YEAR	CREDITS
AM316 : Analysis of Dynamical Systems	1978	5
CE500 : Advanced Soil Mechanics	1978	5
CE502 : Low Cost Sanitation	1978	5
CE529 : Field Theory & Groundwater Flow ...	1979	5
Thesis		20
TOTAL		40

UNIVERSITY OF CAPE TOWN

UNIVERSITY EXAMINATION : OCTOBER 1978

AM316 : Analysis of Dynamical Systems

Time : 3 hours

Attempt no more than SIX questions :

1. Consider the pair of equations

$$\frac{dx}{dt} = f_1(x,y) \quad , \quad \frac{dy}{dt} = f_2(x,y)$$

and prove that if $\frac{\partial f_1}{\partial x} + \frac{\partial f_2}{\partial y}$ has the same sign in a region R then the pair of equations cannot have a closed path in R .

The pair of equations

$$\frac{dx}{dt} = 1 - xy$$

$$\frac{dy}{dt} = x - y^3$$

describe, in dimensionless form, a process for producing product y from material x . Find the critical points of the system and determine their type. Test whether there is a limit cycle in the positive quadrant and without drawing a detailed phase-plane diagram discuss the main characteristics of the trajectories in this quadrant.

(20)

2.(a) Consider the differential equation

$$\frac{dx}{dt} = t + x^2 \qquad x(0) = 0$$

and show that the equation satisfies the conditions for Picard's iteration procedure. Calculate the first three terms in the Picard iteration process. Determine an upper bound on the error in using the first two terms to estimate x on the interval $0 \leq t \leq 0,2$. Obtain an estimate for $x(0,2)$ using the first two terms in the iteration procedure and give an estimate of the bound on the error.

2.(b) on Page 2.

University of Cape Town, University Examination, October 1978
AM316 : Analysis of Dynamical Systems (continued):

2.(b) Prove that the solution to a differential equation

$$\frac{dx}{dt} = f(x,t) \qquad x(0) = 0$$

obtained by the Picard procedure is unique.

(20)

3.(a) Define the exponential of a matrix and show formally that the set of equations

$$\dot{X} = AX \qquad X_o = X(0)$$

where $X = (X_1, X_2, \ldots, X_n)$ and A is $n \times n$ matrix, has a solution

$$X(t) = e^{A(t-t_o)} X_o \quad ,$$

and use the result to find expressions for X_1 and X_2 in terms of $X_1(0)$ and $X_2(0)$ if

$$A = \begin{pmatrix} 0 & -K \\ K & 0 \end{pmatrix}$$

Calculate only two terms in each of the series.

(b) If you are given

$$A = \begin{pmatrix} 2 & -2 & 0 \\ -2 & 1 & 1 \\ 0 & 1 & 3 \end{pmatrix}$$

describe a method of investigating the stability of the equations which arise from substituting this form of A into $\dot{X} = AX$. Do not go into details of the calculation.

(17)

University of Cape Town, University Examination, October 1978
AM316 : Analysis of Dynamical Systems (continued):

4.(a) Given the equations

$$\frac{dr}{dt} = r(r-1)(r-2) \quad , \quad \frac{d\theta}{dt} = 1 \ ,$$

in radial coordinates, determine the positions and senses of the limit cycles. Illustrate them on a phase plane diagram.

(b) A particular van der Pol equation can be written in the form

$$\dot{x} = y - 2(\frac{x^3}{3} - x)$$

$$\dot{y} = - x \ .$$

Use the Liapunov function $V(x,y) = x^2 + y^2$ to show that the origin is asymptotically unstable for the disc $x^2 + y^2 \leq 3$. Further use the Levinson-Smith theorem to show that a stable limit cycle exists.

(18)

5. Use $\nabla v = (ax, by)$ where a , b are indetermined coefficients to start the gradient method of constructing a Liapunov function to establish the stability of the origin in the system

$$\dot{x} = - y + \varepsilon x(x^2 + y^2 - 1)$$

$$\dot{y} = x + \varepsilon y(x^2 + y^2 - 1)$$

where $\varepsilon = +1$ or -1 . Use the Liapunov function to discuss the stability of the origin $(0, 0)$ and to determine the invariant sets positive limiting sets, negative limiting sets for each of the two cases.

(20)

University of Cape Town, University Examination, October 1978
AM316 : Analysis of Dynamical Systems (continued):

6. Use the example of the motion of a particle constrained to move under gravity on a smooth circle, radius a, which rotates with an angular velocity Ω about a vertical axis, to explain "Poincares rules" for stability and bifurcation points. Define

$\lambda = \frac{g}{a^2}$ and consider the cases $0 < \lambda < 1$, $\lambda = 0$

(20)

7.(a) Given the n^{th} order linear differential equation

$$P(D)\ x(t) = 0$$

show that the null solution is asymptotically stable if and only if P has zeros with negative real parts.

(b) Find the values of "a" for which

$$\frac{d^4x}{dt^4} + a\frac{d^3x}{dt^3} + 3\frac{d^2x}{dt^2} + 2\frac{dx}{dt} + x = 0$$

is stable.

(18)

UNIVERSITY OF CAPE TOWN

DEPARTMENT OF CIVIL ENGINEERING

FINAL EXAMINATION DECEMBER 1978

COURSE CE 500 - ADVANCED SOIL MECHANICS

MINIMUM REQUIREMENTS FOR COURSE :

Part A - This written examination (Time: 3 hours 20 minutes)
Part B - A short project. (Draft Mini-regulations for Foundation Design)
Part C - A longer project (On approved subject of candidate's choice)

PART A - Written Examination

WORK IN S.I.UNITS. A choice of questions is permitted . Attempt as many questions as you wish, but note that full marks for this paper will correspond to 100 marks. The marks, and an approximate guide to the time which might be required for each question, are indicated after each question.
WHEN ANSWERING A QUESTION, PROVIDE THE FORMULA WHICH IS BEING USED; STATE THE SOURCE (WITH AUTHOR) OF ANY METHOD OR OF ANY QUOTATION AND PROVIDE ANY SKETCHES WHICH ARE NECESSARY FOR A READER TO UNDERSTAND YOUR ANSWER.

IF VALUES MUST BE ASSUMED FOR CALCULATIONS, STATE YOUR ASSUMED VALUES. LIST ANY IMPORTANT ASSUMPTIONS OF CONCEPT USED IN YOUR ANSWER.

MARKS WILL BE ALLOCATED TO THE LOGICAL LAYOUT OF YOUR ANSWERS.

FOR CALCULATIONS : Assume specific weight of water = 10 kN/m^3.

CONVERSIONS : The following approximations can be used for converting other units to the SI units :
(Note that kg is not acceptable as a weight unit in S.I. units, but in certain old references the weight of a kilogram mass was used as a weight unit).

APPROXIMATIONS : ONLY FOR THE APPROXIMATE CONVERSION OF EXISTING VALUES IN TABLES

Atmosphere $\approx$ 1 $kg(wt)/cm^2$ $\approx$ 1 ton/ft^2 (107 kN/m^2) $\approx$ 100 kN/m^2
$\approx$ 33 ft of water $\approx$ 10 m of water $\approx$ 100 kPa
$\approx$ 15 lb/in^2 $\approx$ 1 bar $\approx$ 2,2 kip/ft^2 $\approx$ 2200 lb/ft^2

1 foot	$\approx$ 0,305 m	1 inch	= 0,0254 m
1 kN	$\approx$ 224,8 pounds	1 kip	= 1000 pounds
1 m	$\approx$ 3,281 ft	1 kg(wt)	$\approx$ 2,2 pounds
1 m	$\approx$ 1,094 yards	1 kg(wt)	$\approx$ 10 newtons (approximately)

USE SI UNITS IN YOUR CALCULATIONS

Marks per question:

Q1	20 marks	Q5	15 marks
Q2	32 marks	Q6	30 marks
Q3	20 marks	Q7	20 marks
Q4	25 marks	Q8	20 marks.

Question 1.

Figure 1 shows a non-circular trial slip surface which has been drawn through a rockfill dam with a clay core.

The factor of safety F_s for this slip surface must be found for the partial pool case shown in Figure 1. In this particular example, the calculations may be simplified by assuming that $c = 75\ kN/m^2$ and $\phi = 0$ for the clay core. Because a $\phi = 0$ analysis is being made within the clay core, it will not be necessary to calculate the pore water pressures within the clay core.

The angle of internal friction for the compacted cohesionless rockfill is $\phi' = 43°$, except at the interface with the horizontal rock base where the value of ϕ' is $37°$.

Note that the zones AB, CD and EF are in the compacted rockfill ($\phi' = 43°$, $c = 0$). The portion BC is within the clay core. The portion DE is along an interface between the rockfill and the rock sub-base ($\phi' = 37°$, $c = 0$).

(20 marks, 40 minutes)

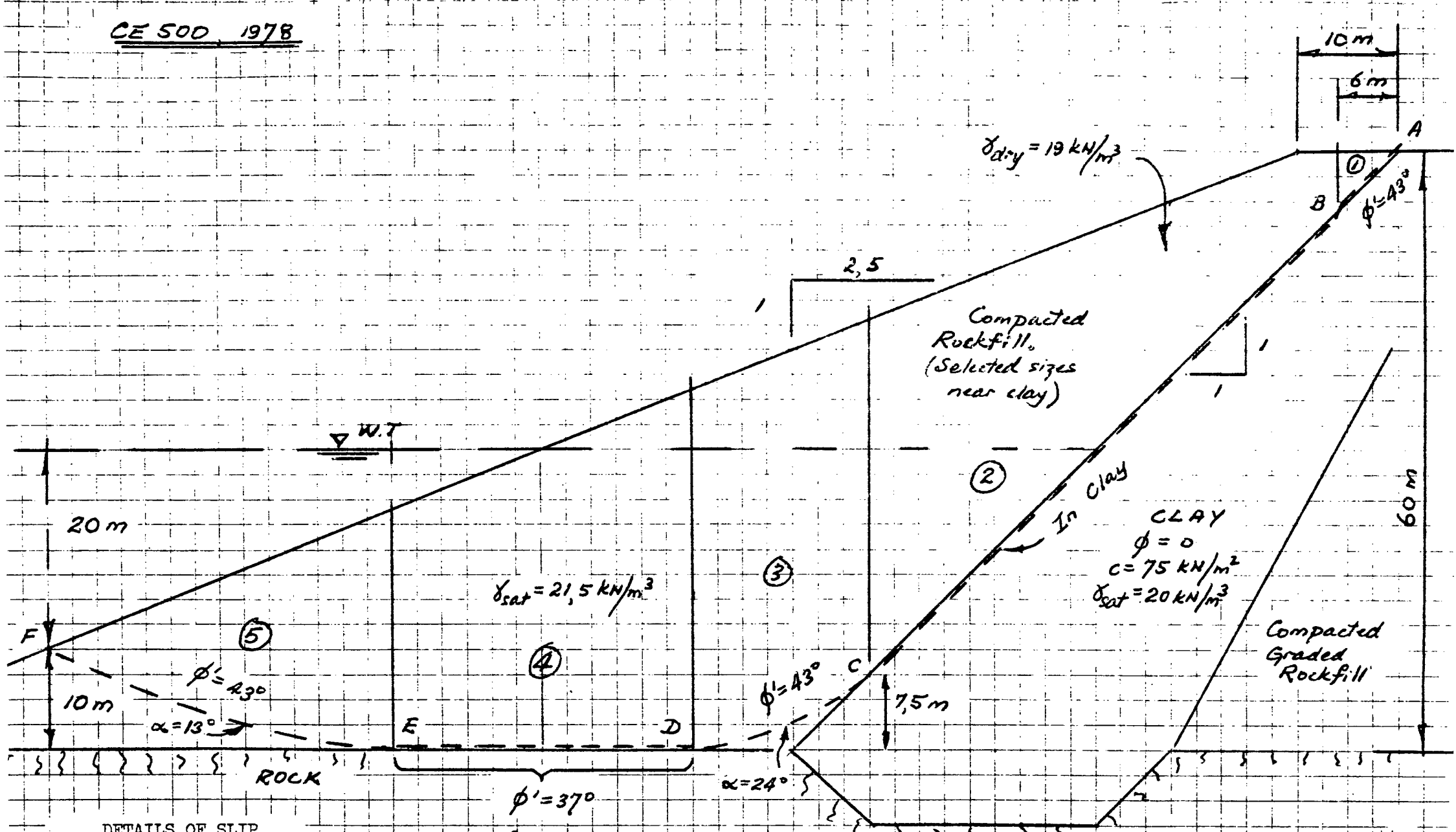

DETAILS OF SLIP

AB in rockfill	$\phi' = 43°$	
BC in clay	$\phi = 0$, $c = 75\ kN/m^2$	
CD in rockfill	$\phi' = 43°$	
DE rock interface	$\phi' = 37°$	
EF in rockfill	$\phi' = 43°$	

FIGURE 1

Non-circular slip surface.

Question 2.

Two identical beams XY and YZ are hinged together at the point Y and are attached to an elastic foundation supporting medium, as shown in Figure 2.

Each beam has a constant EI value throughout its length. The ends X and Z of the beams are free to deflect up or down with the supporting medium.

The value of $\frac{kh^4}{EI}$ for the system is 3,0.; where k is the coefficient of subgrade reaction, and h is the nodal distance (See Fig.2).

a) Consider the load system and the nodal points shown in Figure 2. Using finite difference approximations, derive a suitable set of equations from which the deflections at the nodes may be calculated.

Tabulate this set of equations in such a manner that the deflections at the seven nodes in Figure 2 are the only unknowns in the equations.

For this part of the question, the solution of the tabulated equations is not required.

(15 marks, 30 minutes)

b) By some simple direct method [other than by solving the equations in part (a) above], estimate the anticipated average settlement of the foundation system shown in Figure 2. Express your answer in terms of units of qh^4/EI.

(5 marks, 10 minutes)

c) Use the concept of symmetry and reduce the number of equations and unknowns in part (a). Hence solve these equations by approximate methods or by direct methods to estimate the maximum and minimum settlements. (It is suggested that this portion be left to near the end of the examination).

(12 marks, 25 minutes)

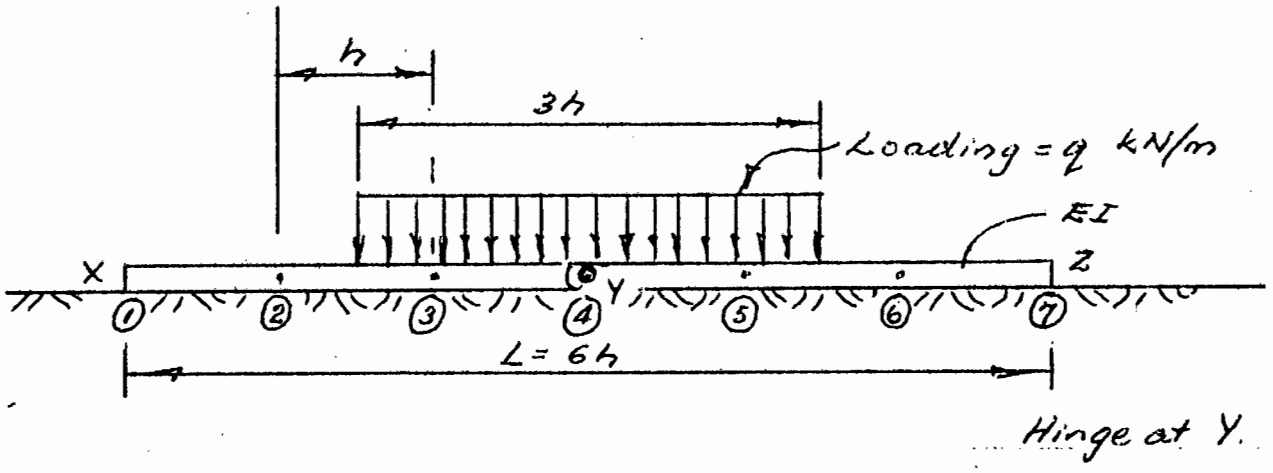

Figure 2

Question 3.

In this question, use the notation and sign conventions used by W.D. Means (i.e. in his book 'Stress and Strain', Springer 1976, p 130 - 180).

a) A geological deposit is homogeneously deformed from the undeformed shape shown in Figure 3a(i) to the deformed shape shown in the section in Figure 3a(ii)

Fig 3a(i) Undeformed Shape

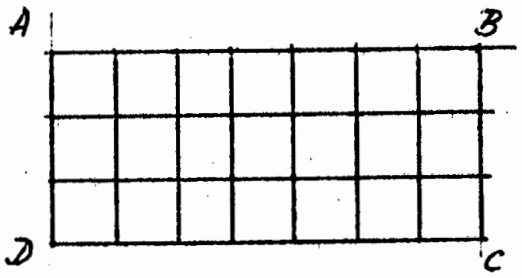

Fig 3a(ii) Deformed Shape.

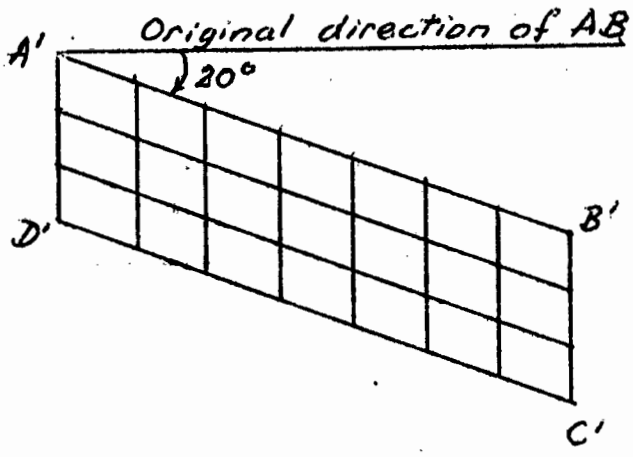

The original length of line AB (which was originally horizontal) has increased by 20 percent to the length A'B'. The original length AD has decreased by 15 percent to its new length A'D'. A'D' and AD are both vertical.

Calculate for each set (i.e. AB, AD) of the original grid lines:

i) The elongation ε
ii) The stretch S
iii) The quadratic elongation λ
iv) The natural strain $\bar{\varepsilon}$
v) The angular shear ψ
vi) The shear strain γ

3 b) On page 146 of his book, W.D. Means states:

Simple shear "is a deformation involving a non-zero strain component and a non-zero rotational component. It consists of a biaxial strain plus a rotation of the λ_1 and λ_3 axes about the λ_2 axis of unchanged length, such that one of the circular sections has the same orientation before and after deformation".

With the aid of sketches explain the above statement, and in particular describe what is meant by 'non-zero strain component', 'non-zero rotational component', 'λ_1 and λ_3 axes', and 'circular sections'.

c) The Mohr Circle for Stress is a graphical representation of the following equations:

$$\sigma_n = \tfrac{1}{2}(\sigma_1 + \sigma_2) + \tfrac{1}{2}(\sigma_1 - \sigma_2) \cos 2\theta \qquad (1)$$

and

$$\sigma_t = \tfrac{1}{2}(\sigma_1 - \sigma_2) \sin 2\theta \qquad (2)$$

Whereas the Mohr Circle for Infinitesimal Strain is based on the following equations:

$$\varepsilon = \tfrac{1}{2}(\varepsilon_1 + \varepsilon_2) + \tfrac{1}{2}(\varepsilon_1 - \varepsilon_2) \cos 2\theta \qquad (3)$$

and

$$\frac{\gamma}{2} = \tfrac{1}{2}(\varepsilon_1 - \varepsilon_2) \sin 2\theta \qquad (4)$$

However the Mohr Circle for Finite Strain is a graphical analogy of the following equations:

$$\lambda' = \tfrac{1}{2}(\lambda_1' + \lambda_2') + \tfrac{1}{2}(\lambda_1' - \lambda_2') \cos 2\theta' \qquad (5)$$

and

$$\gamma' = -\tfrac{1}{2}(\lambda_1' - \lambda_2') \sin 2\theta' \qquad (6)$$

With the aid of sketches and formulae, briefly, define the symbols used in the equations (3), (4), (5) and (6) above.

3 d) Figure 3d(i) shows portion of an undeformed section of a cylindrical gravel pile surrounded laterally by a soft compressible soil. This portion of the pile eventually shortens under vertical applied loading, and its diameter is increased as shown in Figure 3d(ii).

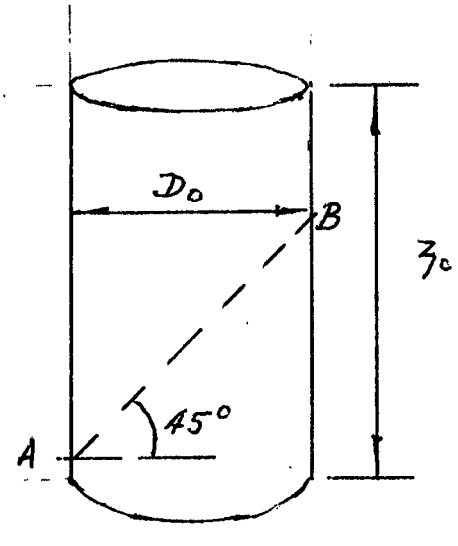

Fig 3 d(i)
Undeformed Portion of Gravel Pile

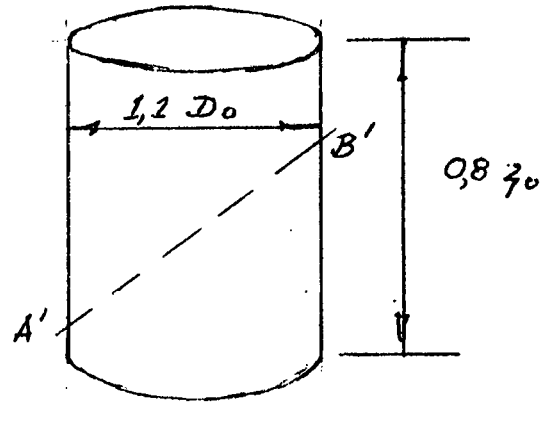

Fig 3 d(ii)
Deformed Portion of Gravel Pile.

(i) Has the gravel material in the pile shown compressive or dilatant behaviour during the above deformation process ?

(ii) Construct a Mohr Circle for Finite Strain for the above problem. Hence determine the elongation ε and the shear strain γ which has occurred along the line AB which was originally at 45° to the horizontal. For the line AB, this shear strain γ corresponds to an angular shear ψ. Draw a sketch to show the meaning of ψ in this case (for the line AB or A'B').

(20 marks, 40 minutes)

Question 4.

A continuous uniform elastic beam DE is supported by the footings A, B and C as shown in Figure 4(a). Two equal static vertical loads W_1 and W_2 are applied to the beam DE at the points F and G.

It is known that the settlement of the footings are nonlinear functions of the loads applied to the footings. Typical load settlement curves for the footings are shown in Figure 4(a).

a) Estimate the final settlements (cm) of the footings A, B and C. An iterative, or other method may be used. For your guidance, the following deflection formulae may be useful:

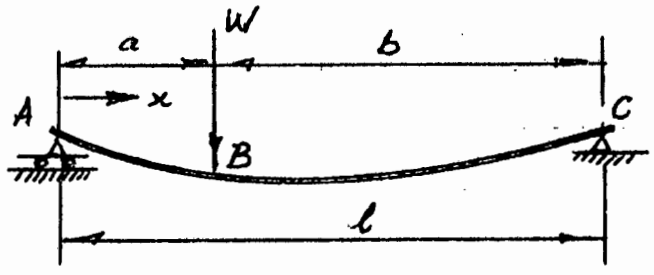

Deflections

$$(\text{A to B}); \quad y = -\frac{Wbx}{6EI\ell}\left[2\ell(\ell - x) - b^2 - (\ell - x)^2\right]$$

$$(\text{B to C}); \quad y = -\frac{Wa(\ell-x)}{6EI\ell}\left[2\ell b - b^2 - (\ell - x)^2\right]$$

(15 marks, 30 minutes)

b) Hence draw a flow chart for a suggested method of deflection analysis for problems of the type shown in Figure 4(a) for the general case in which the static loads, W_1 and W_2 might not be equal, and might be at other positions on the beam.

(10 marks, 20 minutes)

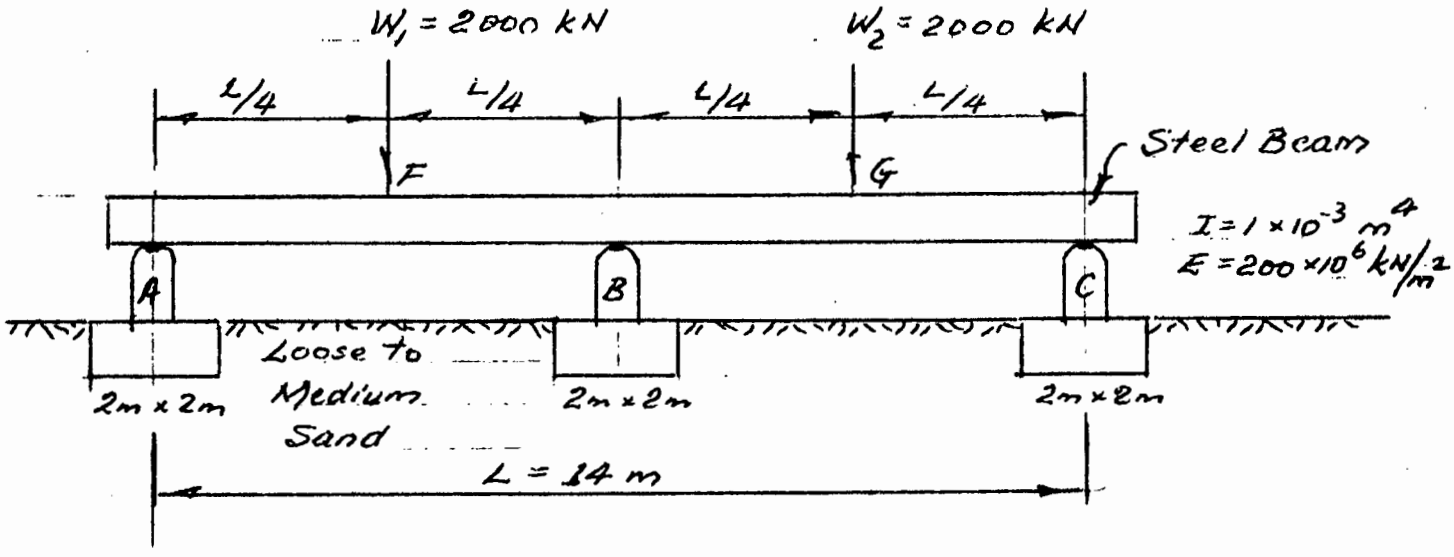

For footings A, B and C :-

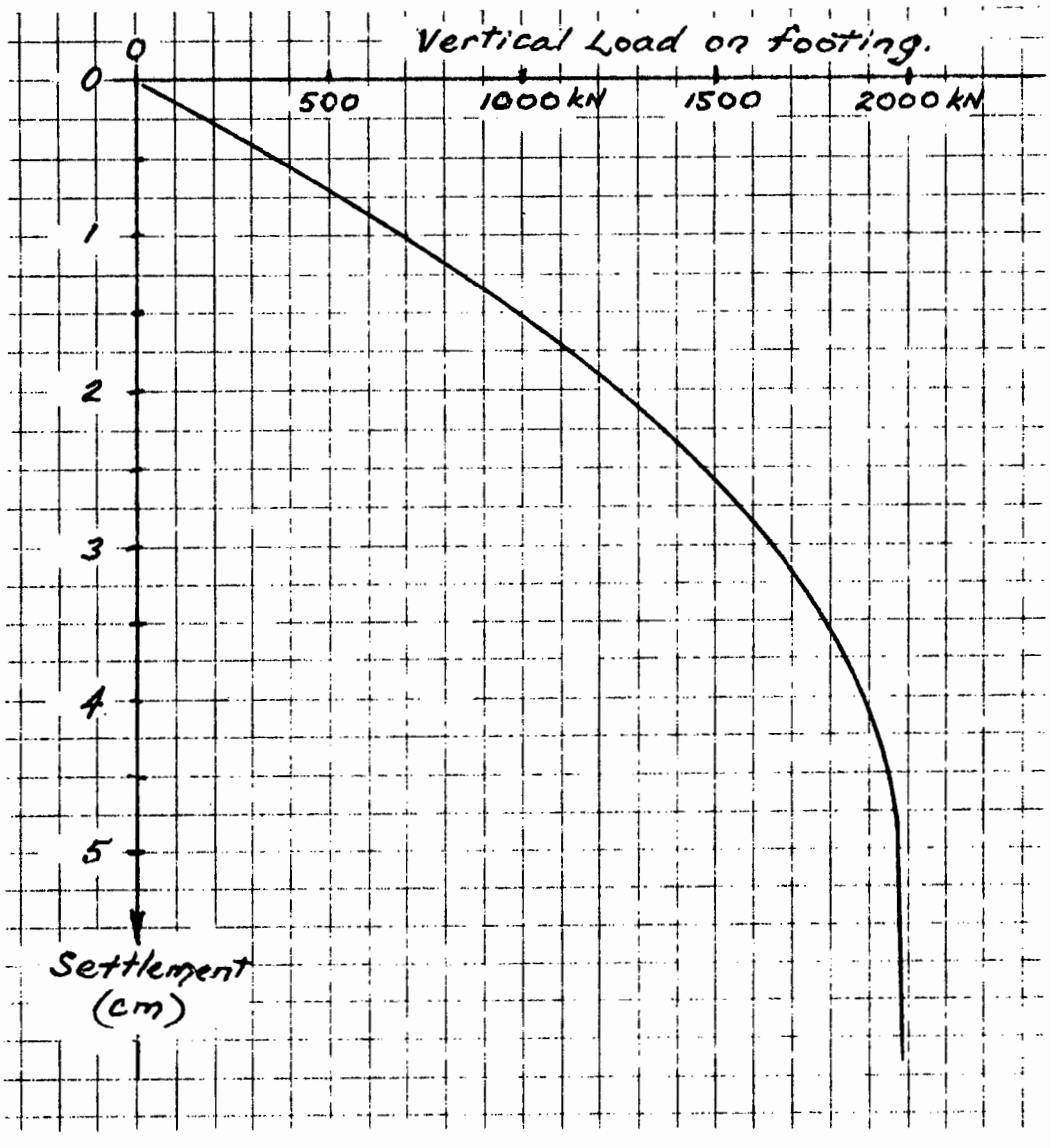

Figure 4(a)

QUESTION 5

Two vertical column loads V_A = 600 kN and V_B = 900 kN are to be carried by a strap footing (i.e. a cantilever or pumphandle footing).

The plan sections of the column are each 0,5 m x 0,5 m. Unfortunately the property boundary line must coincide with the outer surface of the column A, and all footings must be constructed within the property. (See Figure 5).

The allowable soil pressure is 100 kN/m^3 for both footings. The strap beam must not bear on the soil surface.

a) Determine suitable plan dimensions for the two footings.

b) Plot the shear force and bending moment diagrams for the region between the centres of the two columns (i.e. in the strap beam.).

(15 marks , 30 minutes)

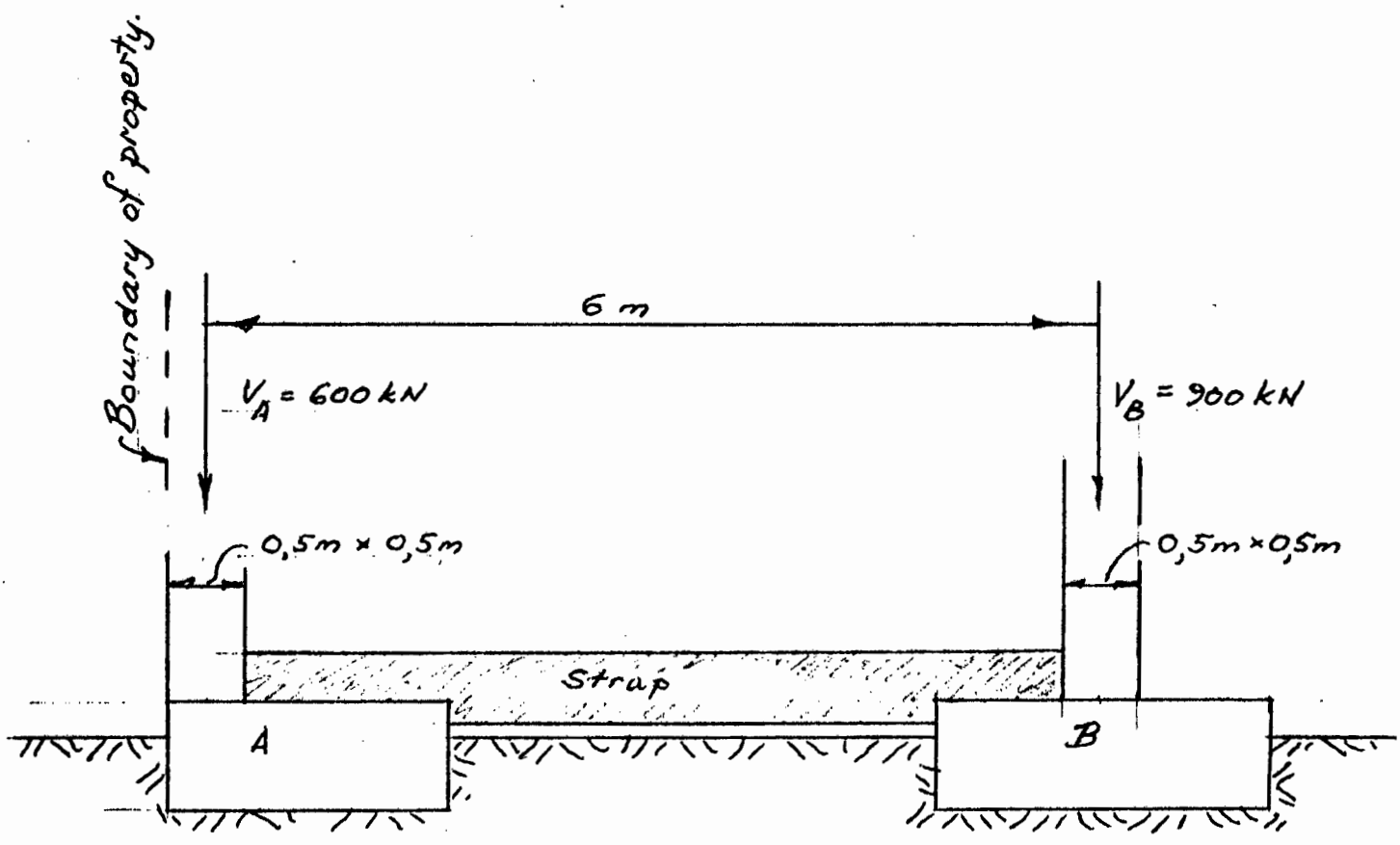

FIGURE 5 . The soil may be assumed to be very compressible when compared with the rigidity of the foundation structure.

QUESTION 6

a) In yourown words, and with the aid of sketches briefly explain (in two pages) the concept of 'unordered principal stress space' and in particular introduce the concept of 'failure surfaces i.e. failure envelopes' by discussing the results of different types of tests.

b) A cohesionless granular material has a maximum failure value of internal friction angle of $\phi' = 39^{o}$

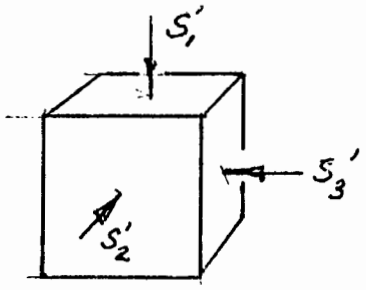

An element of this material is subjected to the principal effective stresses S_1', S_2' and S_3'.

It is known that

$S_2' = 200\ kN/m^2$ (compressive)

$S_3' = 100\ kN/m^2$ (compressive)

Find all the compressive or tensile values of S_1'. which are required to cause shear failure in the above element using :

i) the Mohr-Coulomb theory
ii) the Extended Tresca theory
iii) the Extended von Mises theory

c) In his lecture at the Roscoe Memorial Symposium, Prof. Bishop seems to have reservations about the validity of the strict definition of critical state as used by the Cambridge workers.

Briefly state the reasons for, and the nature of, Bishop's reservations. (Quote page numbers and sources where necessary).

d) In Figure 1,4(a) on page 10 of the above paper by Bishop it is often desirable to measure distances from the central point O'.

Prove that the displacement from O' to any point X on Figure 1,4(a) is

$\frac{1}{\sqrt{3}}[(S_1 - S_2)^2 + (S_2 - S_3)^2 + (S_3 - S_1)^2]^{\frac{1}{2}}$ where (S_1, S_2, S_3) are the principal stress co-ordinates of the stress point X.

(30 marks, 60 minutes)

QUESTION 7

In Geotechnique (September 1977), Dr V.F.B de Mello presented a paper entitled 'Reflections on design decisions of practical significance to embankment dams'.

Using your own words, list the most significant aspects and findings in his paper (quote page numbers and Figure numbers where necessary).

(20 marks, 40 minutes)

QUESTION 8

Briefly (2 to 3 pages) describe how finite difference equations may be used to find the deflected shape and the bending moments, shear forces, and twisting moments in a raft foundation which has the following plan view :

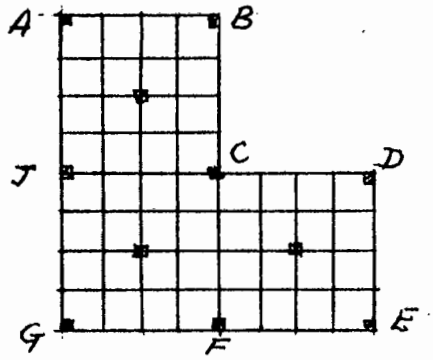

Raft foundation carries applied column loads at positions shown.

PLAN VIEW

If possible provide your answer in flow chart form, or list the various steps. Provide the necessary formulae, and quote your references.

(20 marks, 40 minutes)

UNIVERSITY OF CAPE TOWN

DEPARTMENT OF CIVIL ENGINEERING

DECEMBER EXAMINATION 1978

CE 502 - LOW COST SANITATION

Do All Questions

QUESTION 1

a. Discuss the biochemical and feacal bacterial degradation kinetics in facultative ponds, with particular reference to wind, temperature and radiation effects and the influence of raw and anaerobic pretreated influents.

b. Discuss the design of a septic tank-french drain disposal system for waste waters from individual houses.

QUESTION 2

Write an essay on the problems associated with the provision of water supply and an acceptable form of sanitation for low cost housing areas. The discussion should include a comparison of the different forms of sanitation that have been used in Africa.

QUESTION 3

Discuss the approach you would take and the factors to be considered when investigating sub-soil conditions for a low cost high density housing project.

/2....

QUESTION 4

Design an oxidation pond system to treat the effluent from a low cost housing township in the lowveld of the Transvaal.

Present population	10 000
Estimated future population	15 000
Sanitation provision	Regular waterborne flush system to sewers
Estimated waste flow/capita/day	50 - 90ℓ
Estimated BOD_5 contribution per capita/day	0,04 kg

The pond system is to consist of (a) a grit channel
(b) Open anaerobic lagoons
(c) Primary, secondary and tertiary facultative ponds.

Design the system making your own estimates of the factors required in the design. Provision to minimize odours from the anaerobic lagoon is to be built into the design.

QUESTION 5

a. List the conditions that must be satisfied for data to be normal distributed.

b. Under what conditions do you expect data to be log-normal distributed ? Illustrate with at least 3 examples giving your evaluation of the causes in each case.

c. Give the various measures of central tendency of a distribution and discuss their efficiency.

A random sample of 20 apples was taken from all the apples picked from a single tree, listed below in ranked arbitrary mass units.

11, 14, 15, 18, 18, 20, 20, 22, 22, 22,
26, 26, 27, 30, 30, 32, 36, 38, 40, 70

If you would wish to compare this tree's production with another, what measure of central tendency would you select ? If you would wish to determine the average mass of the apples of this tree would you use the same measure ? Determine with the aid of graphical statistics the answers to your selected measures.

/3....

QUESTION 5 (continued)

d. The following two sets of data were obtained on the concentration of E.coli in the effluent from a facultative oxidation pond during the winter and summer season respectively.

Winter : < 300, 400, 17 000, 12 000, 2500,
1000, 700, > 20 000, 6000, 3500,
2500, 1400, 9000, 7000, 1400,
> 20 000, 4000.

Summer : 440, 800, 1000, 1260, 1600,
1800, 2400, 2800, 4000, 6000.

Test using graphical statistical techniques if the selected statistical mean values of these two distributions are significantly different at 96% level of significance.

UNIVERSITY OF CAPE TOWN

DEPARTMENT OF CIVIL ENGINEERING

UNIVERSITY EXAMINATION - DECEMBER 1979

CE 529 - Field Theory and Groundwater Flow

Requirements for Course

Part A Tutorials were set

Part B This written examination ATTEMPT ALL QUESTIONS

Three days will be allocated to this examination. Candidates may have access to any written reference material, and should quote the name, source and date of any reference material used for answering each question.

Before starting this written examination, candidates are requested to sign the following declaration:

As a candidate for the above examination, I hereby agree that I will not discuss the contents of this examination nor my answers with any other present candidate or previous candidate for the examination in CE 529, and I shall not seek the help of any other professional persons who might be able to solve these problems.

Signed: ..... Date: .....

Print Name: .....

Part C A short project

General

Use S.I. units. Show the main intermediate answers in your calculations. When answering a question, provide the formula which is being used; state the author and source of any method or of any quotation and provide any sketches which are necessary for a reader to understand your answer. If values must be assumed for calculations, state your assumed values. List any important assumptions of concept used in your answer. Marks will be allocated for the logical layout of your answers.

Question 1.

The section through the dam in Figure 1 illustrates a nonhomogeneous section which consists of two soils which are each isotropic. The coefficients of permeability are such that $k_2 = 5k_1$. The value of k_1 is 10^{-3} cm/s.

A trench which consists of graded filter zones is located under the toe of the slope. Filter cloth exists between the fine soil and the graded filter stones. This trench is well drained, and is aerated from the atmosphere.

Draw a flownet for seepage through the nonhomogeneous dam section.(To larger scale).

Hence estimate the seepage rate Q of water into the trench (m^3 per day per metre into the paper). Also estimate the pore water pressure i.e. (kN/m^2) at the point X.

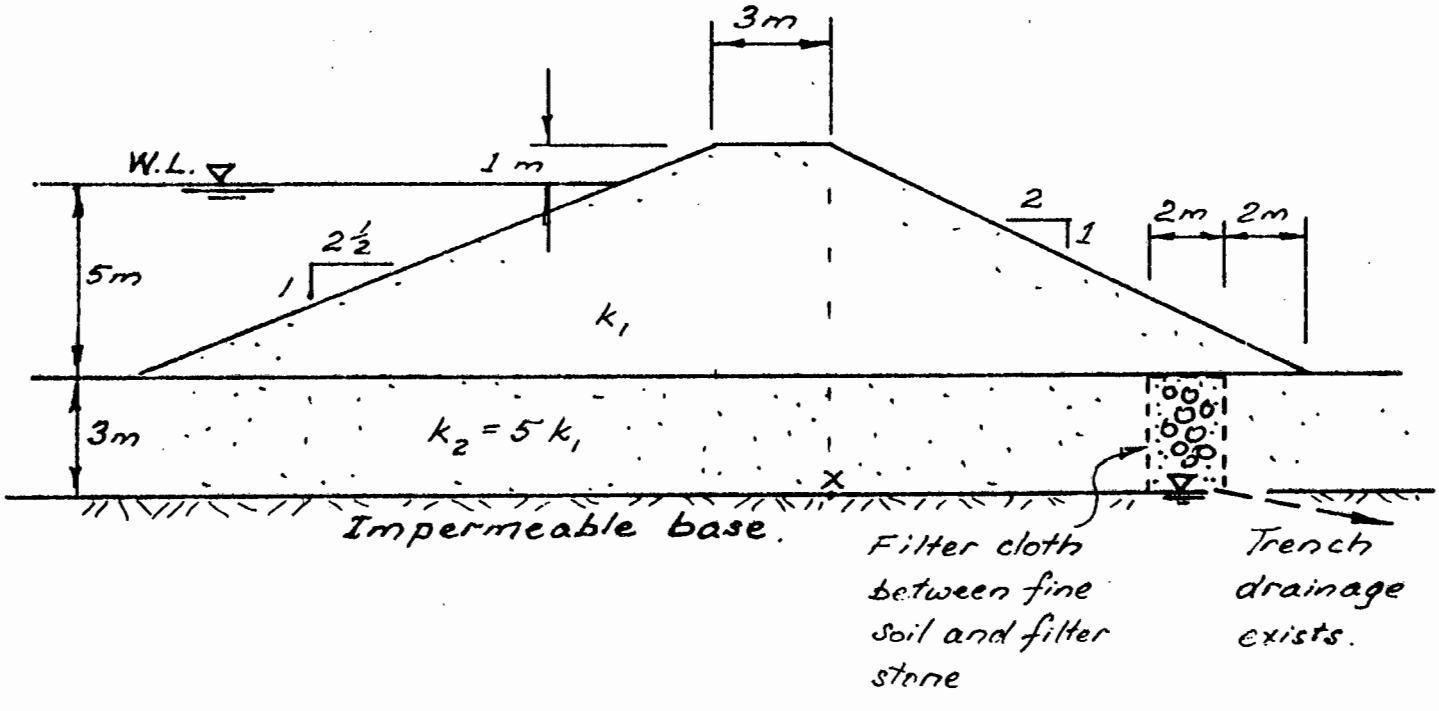

Figure 1

Question 2.

A flownet AKCB must be drawn to a large scale by the candidate such that a parabolic phreatic surface AK passes through the points A and K (see Figure 2). Point C may then be located so that flownet principles are satisfied in the region of C and K. Make sure the flowlines are smooth curves.

Now draw a velocity hodograph for your flownet. Describe any significant features which are noticed on this velocity hodograph. (Tabulate the vector components used to plot your velocity hodograph).

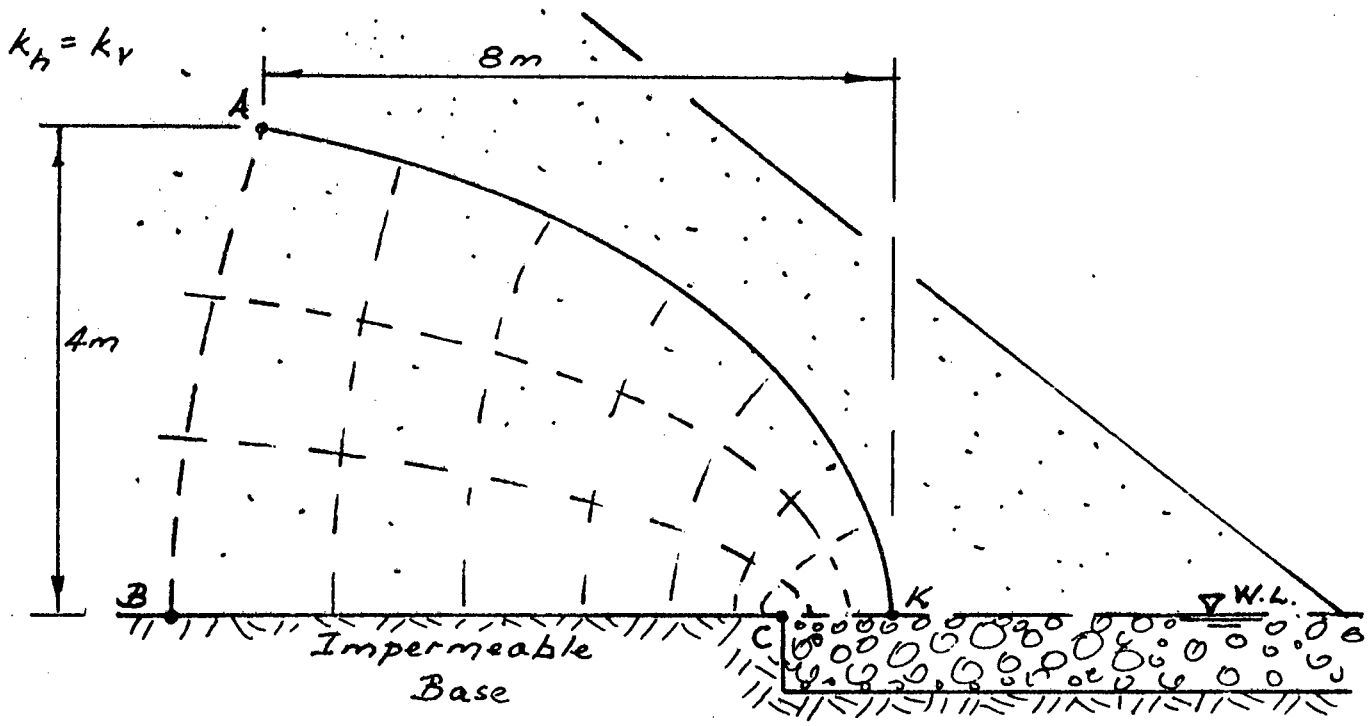

FIGURE 2

Question 3.

a.

Seepage flow occurs in a horizontally bedded confined aquifer. The aquifer is saturated and of constant thickness D = 2 m and has a uniform coefficient of permeability $k = 10^{-4}$ m/s.

The piezometric level h of the water in the aquifer varies across the two-dimensional horizontal x-y field according to the equation:

$$h = 3 + 0{,}1x + 0{,}2y + 0{,}02xy$$

This value of h is measured upwards in metres from the underside of the level aquifer.

i) Calculate the magnitude and direction of the vector Grad h at the point x = 4, y = 5. Provide a sketch to show the direction and magnitude of Grad h.

ii) Also draw the contours of h in the region of x = 4, y = 5, and from these contours estimate the direction of seepage at the point x = 4, y = 5, and the value of the hydraulic gradient at this point.

b.

Assume that a vector field $\mathbf{v}$ can be expressed in the form

$$\mathbf{v} = v_x\mathbf{i} + v_y\mathbf{j} = [4 - (y - 2)^2 - y]\mathbf{i} + 0\,\mathbf{j}$$

where

y is the vertical height in metres above a horizontal datum plane

i) Use the determinant formula to calculate the value of curl $\mathbf{v}$ at a height of y = 1 metre

ii) Consider a square element ABCD of side $\Delta\ell$ as shown in Figure 3b. The centre of the square is one metre above the datum plane

Figure 3b

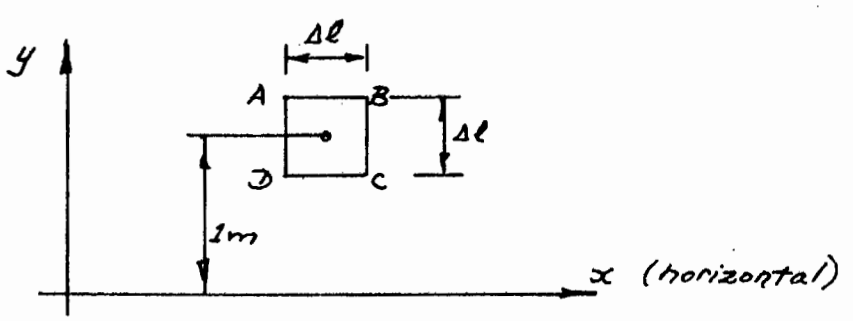

Calculate the circulation which exists around ABCD if $\Delta\ell$ = 0,5 metre. Tabulate your calculations. Hence estimate curl $\mathbf{v}$ at the centre of the element ABCD

What is the value of the angular velocity at the centre of ABCD?

iii) How does Stoke's theorem relate circulation and curl values ?

Question 4

Figure 4 illustrates a vertical section through a permeable system which consists of uniform isotropic sand placed in an impermeable container. The system is two metres wide normal to the plane of the paper.

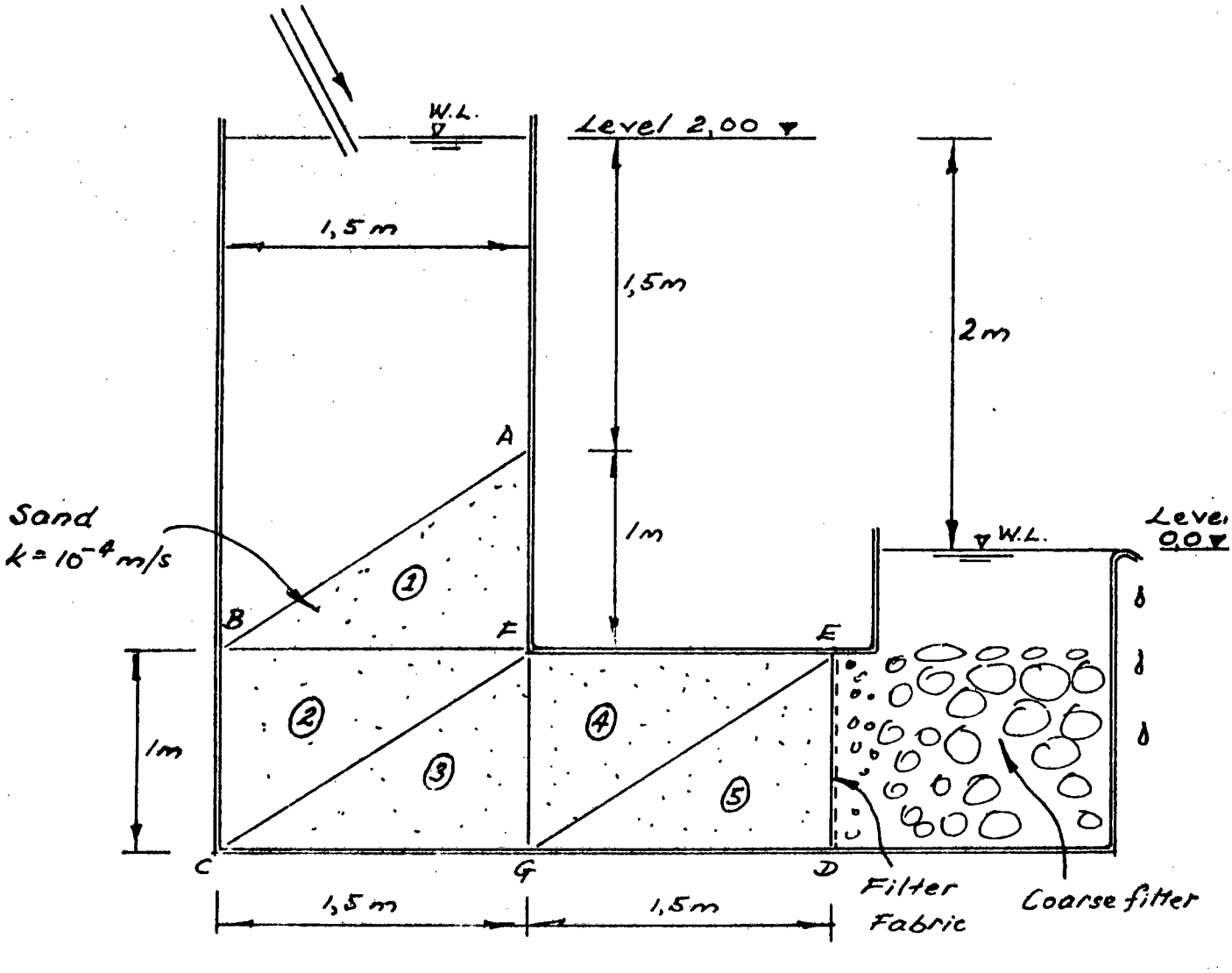

FIGURE 4

The piezometric level for surface AB can be assumed to be 2 units whereas the piezometric level for surface ED is zero.

a) Divide the seepage field into the five triangular elements shown in Figure 4. Using the finite element method, derive the necessary simultaneous equations so that the piezometric levels h at the nodes A,B,C,D,E,F and G can be calculated. Do not solve these simultaneous equations; merely present the equations with their numerical coefficients.

b) Also derive an equation from which it will be possible to calculate the total seepage rate Q (m^3/s) through the system.

Question 5.

In a two dimensional stress field, the body forces are constant and act vertically downwards due to gravity. i.e. $F_y = -20\ kN/m^3$, and $F_x = 0$. Tensile stresses will be regarded as positive.

However certain additional applied stresses act on the body so that the Airy stress function is

$$\phi = 2x^3y + y^3 \quad (x \text{ and } y \text{ are measured in metres}).$$

a. Check that this expression for ϕ satisfies the corresponding biharmonic differential equation for ϕ.

b. Consider the rectangular field ABCD shown in Figure 5.

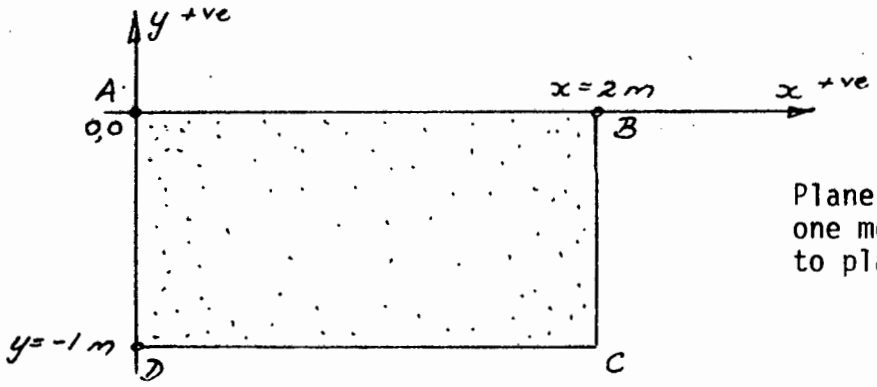

Figure 5

Derive expressions for σ_x, σ_y and τ_{xy} along the four different edges AB, BC, CD and AD

c. Hence draw the distributions of σ_x, σ_y and τ_{xy} along the edges AB, BC, CD and AD

d. Consider a few different points within the field ABCD and on the boundary of ABCD. Draw Mohr circles in order to estimate the directions of the principal stresses σ_1 and σ_2 at these points. Hence provide an approximate sketch showing the directions of the principal stress trajectories across the field ABCD.

Question 6.

The complex number $z = x + iy$ is a function of the complex number $w = \phi + i\psi$ via the expression $z = w^3$

The integer values of ϕ and ψ in the w plane form a square grid as shown in Figure 6a.

Determine the shapes of the two sets of curves ϕ = constant and ψ = constant (respectively) in the z plane by determining these lines for ϕ = -2, -1, 0, 1, 2, and ψ = -2, -1, 0, 1, 2.

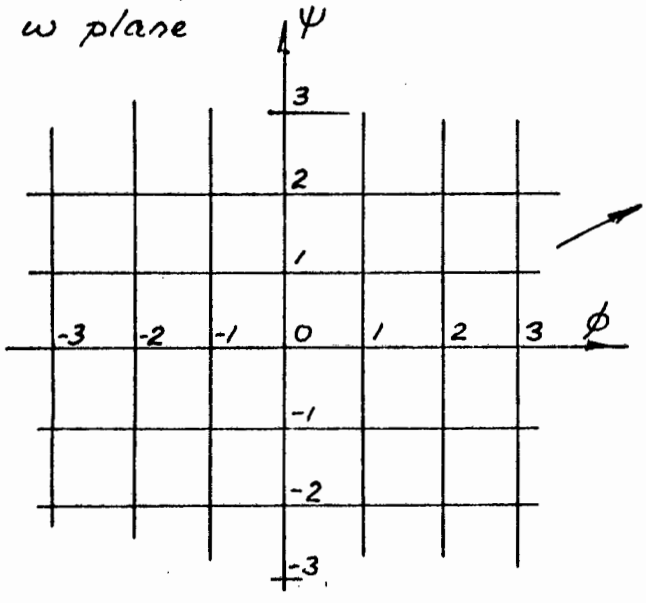

Figure 6a

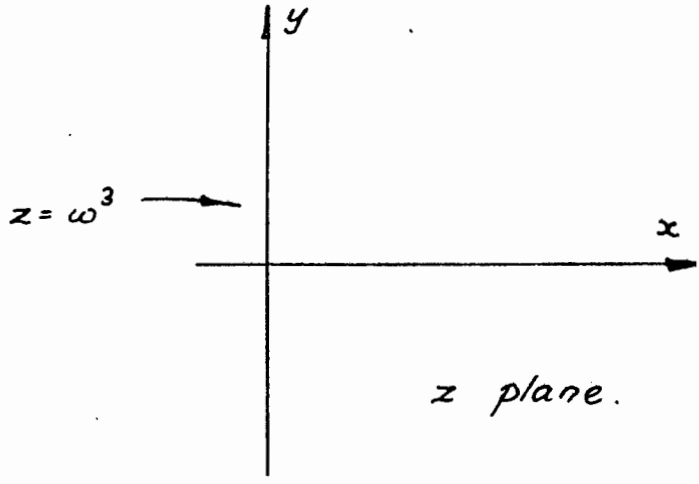

Figure 6b

Question 7. (Attempt either Part A or Part B but not both)

PART A

i) With the aid of a sketch define the concept of a storage coefficient S of an aquifer (i.e. as used by Raudkivi and Callander, or by Todd and others). Explain the units of S.

ii) Also define the transmissivity T of an aquifer. Explain the units of T. (Use S.I. units)

iii) Draw a descriptive flow chart which includes steps in the field method and in the calculations (including formulae and diagrams) for the Theis method for determining the values of S and T for an aquifer. The given formulae must be for SI units.

OR

PART B

i) What is an isotropic point in a photoelastic analysis ?

ii) Draw examples of typical isoclinics in the region of positive or negative isotropic points. Hence draw the directions of the principal stresses (i.e. isostatics) in the region of your two chosen isotropic points.

iii) Assume that you have been given the pattern of isochromatics, and the pattern of the full set of isoclinics for a stressed two-dimensional photoelastic model. You have also been given the fringe constant for the material of the nodel. Draw a descriptive flow chart which explains the main steps and calculations in the process for finding the stress values on the boundary of the model, and the complete stress condition at any point within the model. Explain how the principal stress trajectories can be obtained for this model.